IEEE Access
Multidisciplinary : Rapid Review : Open Access Journal

Received 25 September 2023, accepted 9 October 2023, date of publication 13 October 2023, date of current version 24 October 2023.

Digital Object Identifier 10.1109/ACCESS.2023.3324419

TOPICAL REVIEW

Critical Review on Torque Ripple Sources and Mitigation Control Strategies of BLDC Motors in Electric Vehicle Applications

N. PRABHU[1], R. THIRUMALAIVASAN[1], (Senior Member, IEEE), AND BRAGADESHWARAN ASHOK[2]

[1]School of Electrical Engineering, Vellore Institute of Technology, Vellore, Tamil Nadu 632014, India
[2]School of Mechanical Engineering, Vellore Institute of Technology, Vellore, Tamil Nadu 632014, India

Corresponding authors: R. Thirumalaivasan (thirumalai22@gmail.com) and Bragadeshwaran Ashok (ashokmts@gmail.com)

This research is supported by the Royal Academy of Engineering, United Kingdom under the scheme of Distinguished International Associates (Grant No: DIA-2022-150 & ESMN 2123/2/93), and the authors extend their appreciation to the Vellore Institute of Technology, Vellore, for this research work.

ABSTRACT In recent years, electric vehicles (EVs) have attracted a lot of attention and are rapidly growing trends today due to their ability to compete with and overtake fossil fuel-powered vehicles among all electrified transportation tools. The primary focus of EV evolution is on improving the driving range and optimizing energy consumption, both of which are essential demands achieved through improved and developing motor performance. The brushless direct current (BLDC) motor is one of the most superior choices for dynamic applications in EVs, providing the highest power density and capability of any motor. BLDCs are gaining popularity in EVs not only for their high performance in speed and position controls but also for meeting the requirements of smooth torque maintenance with torque ripple mitigation. This paper provides an overview of various advanced control strategies, such as field-oriented control (FOC), direct torque control (DTC), intelligent control (IC), controlling input voltage (CIV), current shaping techniques (CST), model predictive control (MPC), and sliding mode control (SMC). These strategies are used to regulate the torque ripples produced in BLDC motors, aiming to achieve energy-efficient EV performance for various applications. Additionally, it describes a cloud-based control system coupled with electric motor drives to address challenges in predicting current vehicle conditions for improved power distribution between the motor and battery systems. Furthermore, recent concerns and difficulties in advancing torque ripple mitigation control strategies are highlighted, with comparisons and discussions for future EV research. Finally, an evaluative study on BLDC motor drive in EVs with different control strategies reveals its significance and potential outcomes.

INDEX TERMS Brushless direct current (BLDC) motor, cloud-based torque control, control structural architecture, electric vehicles (EVs), various control strategies for torque ripple mitigation.

I. INTRODUCTION

Electric Vehicles (EVs) have made significant contributions to the development and global challenges of modern society by addressing environmental protection and energy savings in daily life [1], [2]. They are capable of efficiently and effectively addressing global challenges through the electrification of vehicular technology, which includes efficient motors, electronic motor controllers, advances in power electronics, and numerous distinct control techniques. Even though EVs offer simplicity for cheaper maintenance, high reliability to reduce component breakdowns, very low electricity costs, more comfort without vibration, increased efficiency, and accessibility compared to other vehicles [3], [4].

The improvement of driving range and power management in EVs is driven by motors that have high power density, high instantaneous power, rapid torque response, robustness, and high efficiency over a wide speed range. Today, there

The associate editor coordinating the review of this manuscript and approving it for publication was Wonhee Kim.

are many different types of electric motors available for evaluating EV performance, including the permanent magnet synchronous motor (PMSM), brushless direct current motor (BLDC), induction motor (IM), switched reluctance motor (SRM), and DC series motor [5]. However, BLDC motors are now more attractive and the most frequently used for EV applications due to their greater benefits when compared to all other motors. These benefits include high reliability, high starting torque, high efficiency, a wide range of speed regulation with high torque, and dynamic response [6], [7].

In addition, BLDC motors operate based on rotor position sensing to obtain the optimal voltage applied to the motor for improved performance, using low-resolution sensors or sensorless control [8]. Sensor-based schemes are used to determine the motor's rotation location with respect to the motor stator stationary plane, while sensorless schemes use back-electromotive force (EMF) estimation and a flux function to operate the motor with synchronous phase currents through the motor controller [9], [10].

One of the most important control modules in EVs is the motor controller, which is responsible for driving safety performance, has a significant impact on drive system efficiency and is involved in the vehicle's design comfort. Motor controllers in BLDC motors are used to operate and regulate the speed, torque, and position of the motor, allowing it to start, stop, and rotate quickly at high torque with variable input voltages. In this controller technology, motor-controlled parameters are used to ensure proper energy flow to the motor in an EV, including commutation current waves, pulse-width modulation (PWM) processes, current ripples, total harmonic distortion (THD), and electromagnetic torque. Developing a motor controller to regulate rotating systems is a challenging task accomplished using advanced power electronics components such as insulated gate bipolar junction transistor (IGBT)-based converters. Converters are employed to regulate the motor torque and improve the steady-state period of the rotor speed of BLDC motors by properly triggering pulses from the PWM vector component and obtaining the optimal voltage more quickly. Here, the PWM duty ratio is calculated using current commutation techniques in switching between phases to energize the stator windings and drive the motor to rotate properly, improving the BLDC motor's performance in both steady and dynamic states [11], [12].

Moreover, BLDC motor control is required to achieve and sustain smooth torque response and speed with minimum ripple content, ensuring excellent performance in speed and position control drives for EVs. Due to uncertain parameter variations and load disturbances from the motor, torque ripple effects are seen in BLDC motors, preventing smooth motor rotation with a gradual increase and decrease in output torque.

Torque ripple is caused by various factors, including interactions between magnetomotive forces (MMF) and air gap flux harmonics, as well as speed fluctuations, which degrade performance and may trigger resonant frequencies in the mechanical parts of the drive system, resulting in acoustic noise. Torque ripple effects are particularly undesirable in some motion-control EV motor drive applications, and generally, the average value of the torque ripple produced by a motor depends on the motor's construction, design, and control parameters [13].

Regarding motor control methods, different types of control strategies, such as scalar and vector-based controls, are initiated to mitigate torque ripples for BLDC motors in EVs. Most commonly, the regulation of torque ripple by advanced vector controls in closed-loop operation is compared to the scalar method because it offers high speed and a more dynamic response against the overall constraints of the motor. It also improves motor output response over a wide speed range while maintaining high torque at zero speed, which is the most essential feature for BLDC motor drives in EVs.

In this context, a conceptual review of various vector control strategies leads to the conclusion that BLDC motor torque ripple mitigation is necessary to enhance driving performance and meet specific power requirements for EVs. The literature review includes various research studies conducted to date and suggests ambiguities that future engineers should investigate to further improve the performance and significance of BLDC motors in EVs.

In a discussion focused on BLDC motor hardware, the emphasis is primarily on different classifications, operating performance characteristics, advantages, and disadvantages of various electric motors used in EVs [14], [15], [16]. The development of different converter topologies to minimize current and voltage ripples due to switching power loss issues is also discussed [17]. Various BLDC motor control strategy discussions explore different control schemes in terms of sensors or sensorless controllers to improve motor performance and address different power optimization issues in real time [18], [19]. Furthermore, the optimal control strategy to regulate torque ripples in various control methods [20], [21], [22], [23], [24], [25], [26], [27], [28], [29], [30] and the investigation of various commutation techniques and PWM schemes to control stator current in BLDC motors have been discussed [31], [32], as mentioned in Fig 1. According to the review, some control strategies have been developed to improve BLDC motor performance to meet vehicle performance requirements, such as driving range and energy optimization in real-time operating conditions.

II. MOTIVATION AND OBJECTIVE OF PRESENT WORK

Torque control of BLDC motors has always been an important area for research in the field of electric vehicles, and its control strategies, as well as ripple reduction, have consistently been crucial for the development of high-performance vehicles in the future. The extensive literature review on various control strategies is more concerned with describing the unique control modules and their development than taking a critical approach to torque control strategies for BLDC motors in the development of EVs. There is a need for future research and development of efficient control operations, and improving the control strategies for torque control in BLDC motors is associated with electric vehicle performance. This

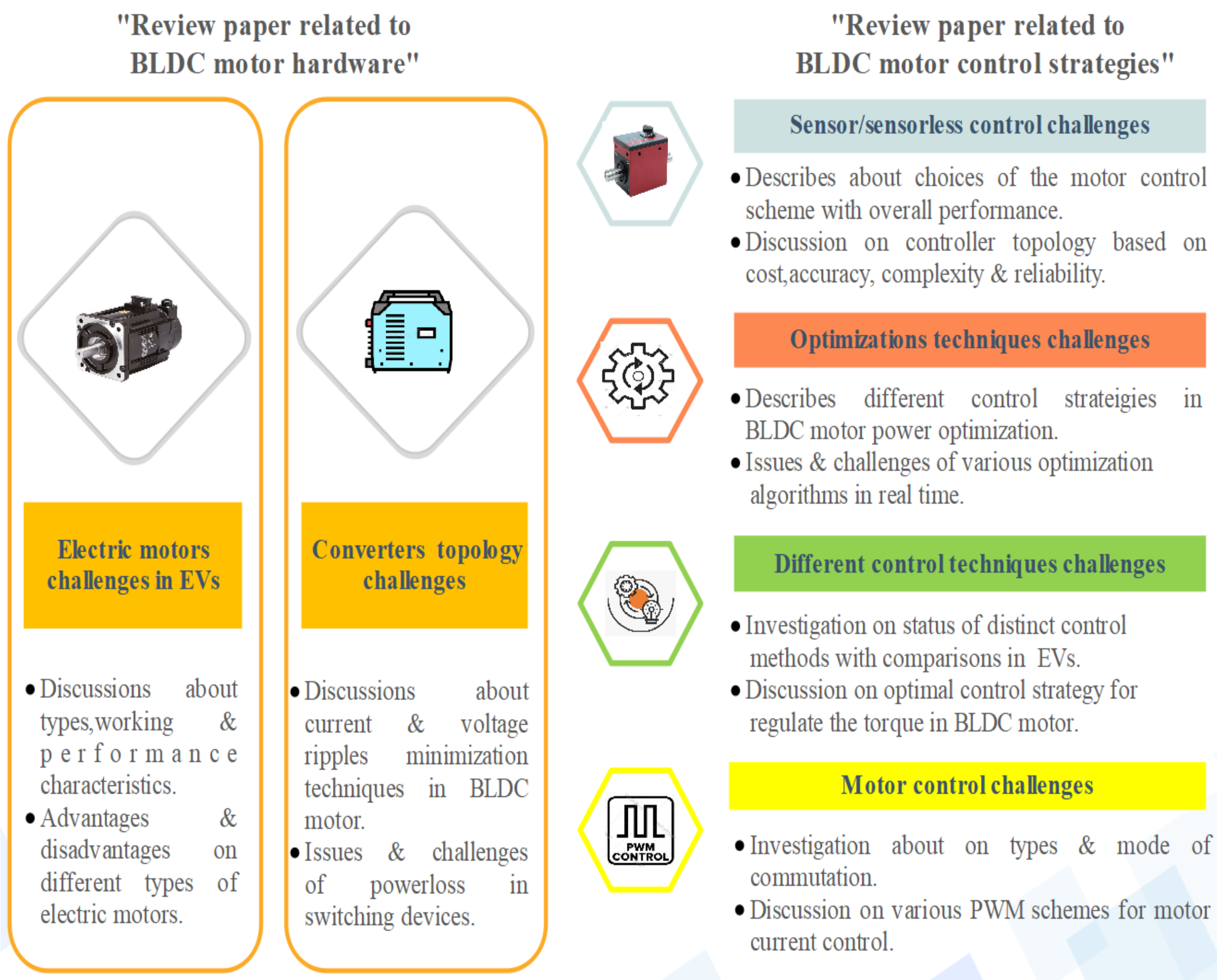

FIGURE 1. Status of existing review work on various control strategies of BLDC motor in electric vehicles.

still prompts extensive work on torque ripple mitigation in BLDC motors to clarify the various goals associated with distinct control strategies and future guidelines for the research. Even though numerous studies on torque ripple mitigation control strategies are available, an evaluation article on the in-depth structure of BLDC motors with advanced control techniques in EVs has not been published, and certain objectives for this work were developed in response to this research gap. Moreover, such a category of studies will pave the way for improving the overall performance of BLDC motors in EVs in the future. Within this context, the objective of the present work focuses on the critical review of advanced and essential control strategies for reducing torque ripples in BLDC motors in a holistic manner. The novelty of this review stems from the collection and integration of studies that examined architectural systems, thereby increasing methodological and technical approaches to motor torque control in EVs. Eventually, the various literature gaps are presented in Fig. 2. The outcome of the stated objective will serve as an essential guide for future studies and provide a wide range of BLDC motor control strategies for EVs in real-time evaluation. Moreover, this review paper provides insight and a critical interpretative view to the readers about BLDC motor torque control performance in EVs. This review paper will not impose any new results; instead, it will formulate the various research activities on torque ripple regulation for BLDC motors in EVs, additionally discussing the future prospects of advanced control strategies for torque ripple regulation in the future to meet the demands of real-time vehicle performance. Finally, the method used in this investigation supports an overview of the possible directions for future research in this field. To attain these outcomes, Fig. 3 gives brief information about the structure and flow of the present study.

III. STRUCTURAL ARCHITECTURE ARRANGEMENT OF BLDC MOTOR IN ELECTRIC VEHICLES

The BLDC motor's structural configuration includes a hall sensor, motor controller unit, power inverter, or motor driver as shown in Fig 4. BLDC motors are similar to DC motors

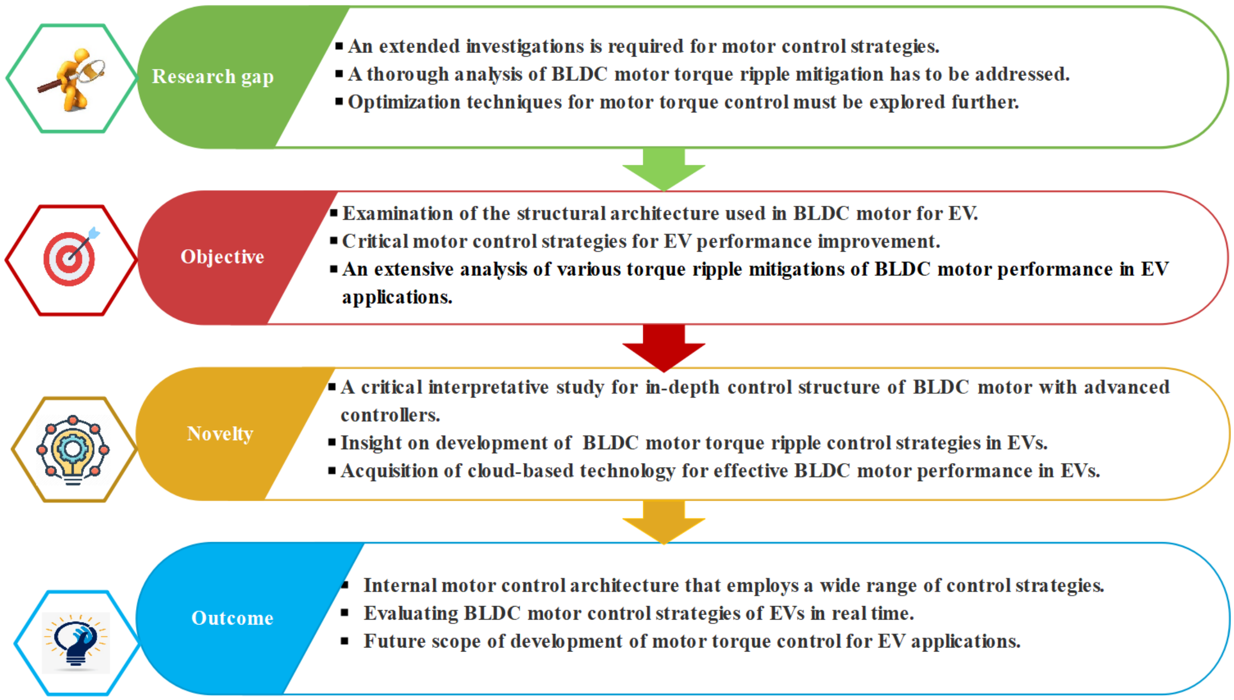

FIGURE 2. A schematic illustration of research gap and original contribution of the work.

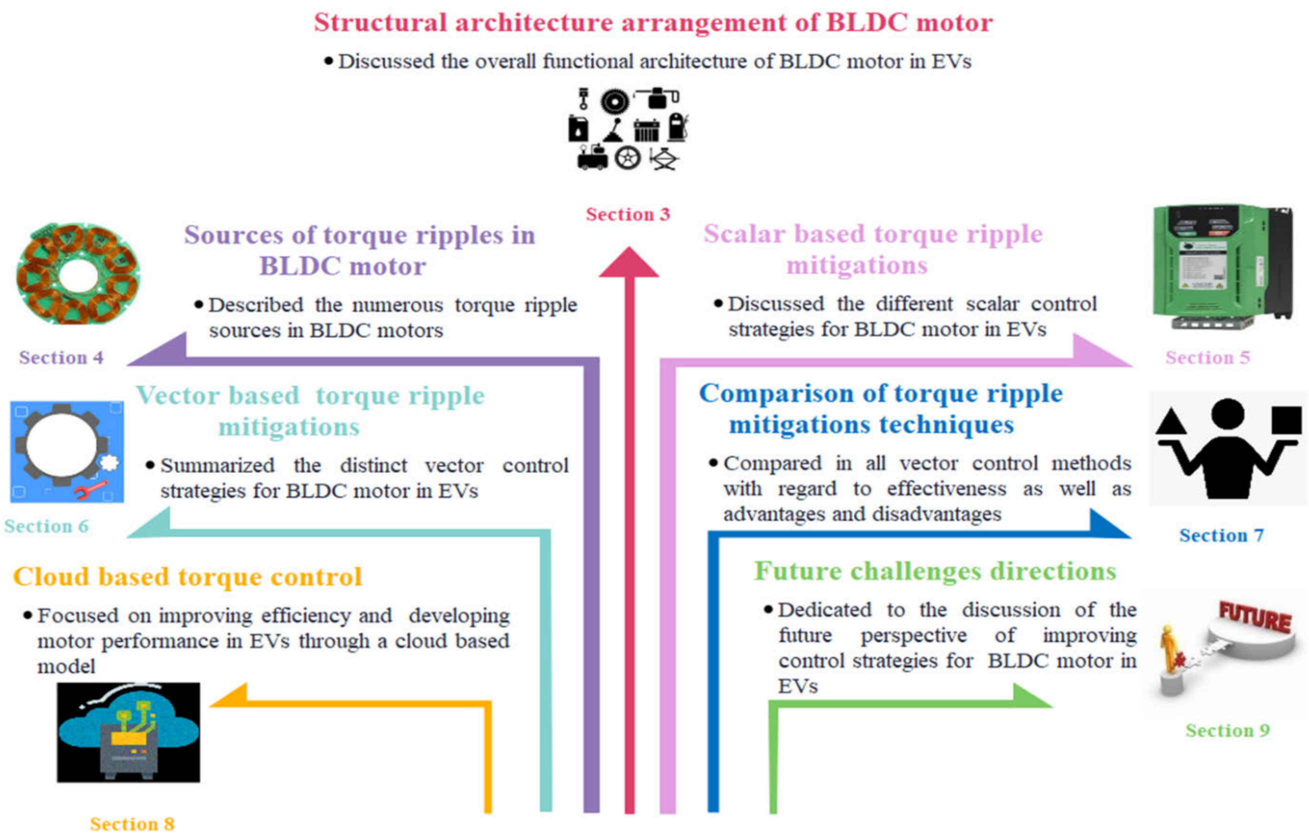

FIGURE 3. Structural overview of a current review article along with section constituents.

with permanent magnets and are referred to as brushless because they lack a commutator and brush arrangement, therefore these motors are sometimes referred to as 'electronically commutated motors'. In addition, it eliminates problems associated with the brush and commutator arrangement, such as sparking and commutator brush wear, making

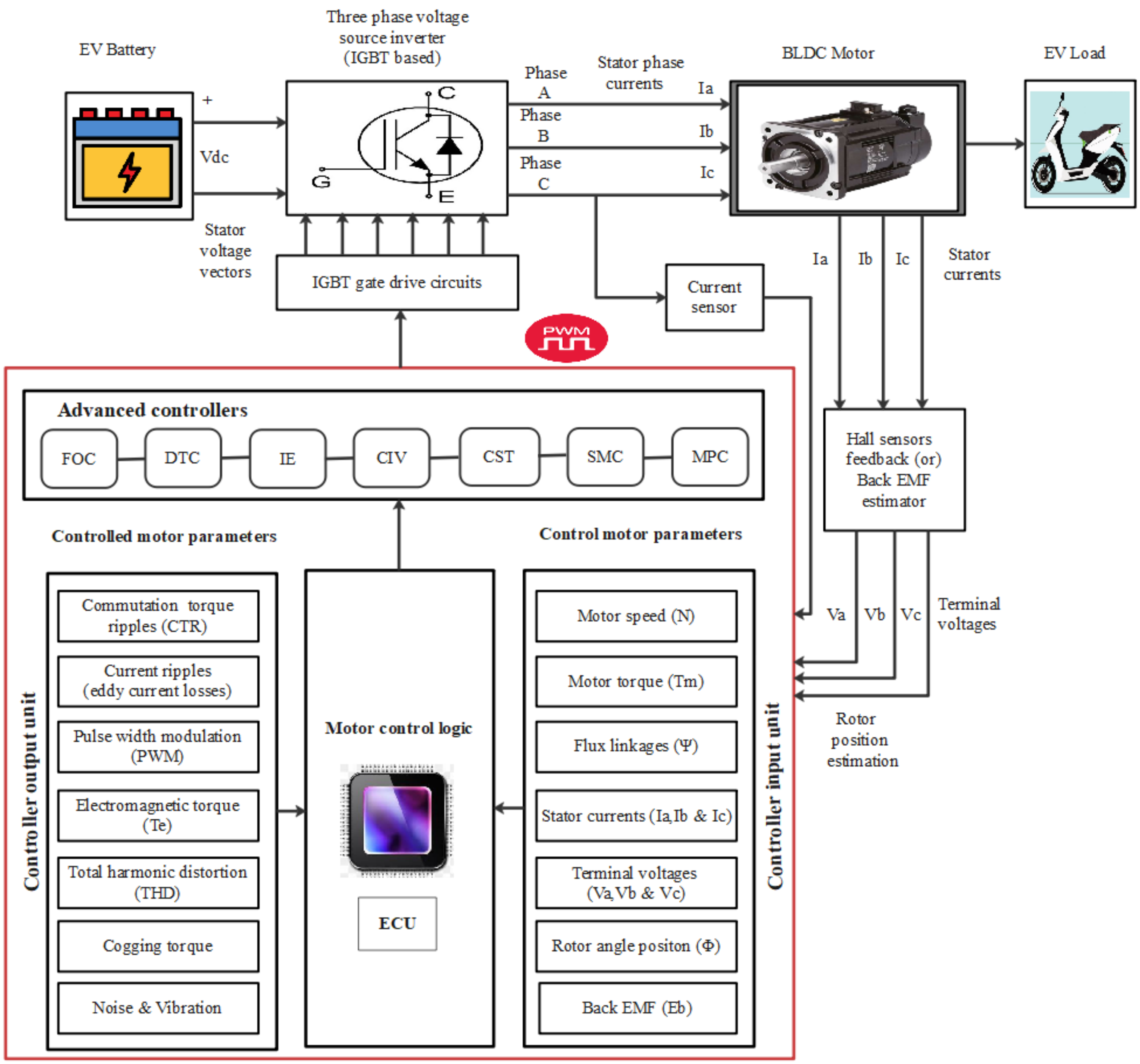

FIGURE 4. Internal structural architecture arrangement of BLDC motor in electric vehicles.

a BLDC more rugged than a DC motor. Moreover, a BLDC motor, unlike a conventional DC motor, has an ''inside-out'' construction in which the field poles rotate while the armature remains stationary. The stator is made of silicon steel stampings with a specific number of poles and windings connected to a DC supply through a power inverter circuit, and the armature is wound on a slotted laminated iron structure. The two layouts of a motor are ''Out runner'' and ''In runner''. The out runner is designed for high torque requirements, while the runner is designed to produce less torque and is more capable of rotating at very high speeds, in that the permanent magnet rotates around the stator and the rotor is external.

A sensor is required to provide input to the motor control system indicating when the rotor has attained the desired position. Motor control sensors include voltage, current, and Hall signals. If the commutation is performed quicker or slower than the rotor's speed, the magnets maintain interaction with the stator's magnetic field. So, in both types of motor layouts, the rotor position must be sensed for electronic commutation and control of the entire motor operation through the controller also the rotor shaft's position and speed, are measured using a Hall effect sensor [33], [34]. This sensor is a solid-state device that uses the Hall effect principle to determine how stator armature excitation synchronizes with rotor position, speed, and various other aspects such as torque and the voltage required to run a BLDC motor efficiently, additionally providing rotor position information to a motor controller [35], [36].

In addition to current detection, the motor is regulated by a number of control methods or algorithms that are linked to the current sensor's accurate monitoring of the motor's current. This enables precise synchronization and orientation control while measuring power, diagnosing control systems, measuring current supply, and controlling complex loads generated by electric motors. Voltage sensors can also measure voltage in a variety of methods, such as detecting low current levels and high terminal voltages. This allows for the detection of load defects, power failures, the regulation of power demand, temperature, and so on. It's al crucial to regulate the motor's speed and torque to obtain transient output suitable for driving an electric vehicle. Based on the torque requirements from the driver and other vehicle accessories, the control strategy in the motor controller unit (MCU) will calculate the current to be regulated by the power inverter circuit. It controls the source voltage from the battery based on the PWM signal from the MCU in that PWM signals include the command signal for measuring the coil's energization and current according to the required torque [37].

Based on the regulated current input, the three-phase stator windings are energized sequentially, which creates the magnetic stator poles. In contrast, the permanent magnet field in the rotor with North and South poles accommodates the stator poles, which build the motor, which in turn creates the torque in the rotor shaft. The magnitude of the torque produced mainly depends on the number of turns of the stator windings, the amplitude of current, the length of the rotating winding, the MMF, the size of the permanent magnets, also the air gap between stator and rotor windings. A typical BLDC motor's design and operation parameters refer to variations in the torque produced at the rotor shaft that produces torque ripples.

It is mainly due to the rotor magnet's interaction with the stator slots, the relation of magneto motive forces produced by the stator current and air gap flux harmonics, and electromagnetic torque fluctuations [38]. In the electric vehicle perceptive, the torque ripple in BLDC motors will affect the vehicle's performance and further, it will cause large vibrations at specific vehicle speeds during the drive, which will lead to instability of rotational speed. By properly designing the structural uniformity and position of stator poles, the torque ripples are mitigated. Consider the many applications oriented towards BLDC motors for electric vehicles; torque ripple minimization is very important for improving the comfort and overall performance of the vehicle.

IV. SOURCES OF TORQUE RIPPLE AND THEIR INFLUENCE IN BLDC MOTOR FOR ELECTRIC VEHICLE APPLICATIONS

To achieve high performance in speed and position control drives of electric vehicles, smooth torque output is necessary. The most impact on the machines with high specific torque has an inherently large torque ripple. The magnitude of the produced torque ripples is based on three factors, such as the construction of the motor, motor parameters, and motor control strategies, [13], [39] as shown in Fig 5.

A. TORQUE RIPPLE SOURCE BASED ON THE MOTOR CONSTRUCTION

According to the behavior structure, torque ripples are associated with BLDC motors by three factors: cogging torque, reluctance torque, and electromagnetic torque.

1) COGGING TORQUE

The interaction between the permanent magnet rotor slots and the stator pole slots in BLDC motors is a major factor in the generation of cogging torque. The magnetic attraction varies according to the magnetic field's intensity, and this variation leads to the production of unequal torque. Some permanent magnet motor designs exhibit cogging when a motor is operated in an unfavorable manner, particularly at low speeds, which leads to fluctuations in the motor's output torque and causes torque ripples [40], [41], [42]. Additionally, it is influenced by other factors, including the slot opening width, magnet width, skewing, etc., that make the BLDC motor unstable and reduce overall performance. Reduce cogging torques when building a motor, increase the air gap, increase the number of slots per pole, thicken the tooth tips to prevent saturation, reduce the slot opening, skew the magnet poles, provide dummy slots, and lower the magnet flux density while creating a motor [43], [44], [45].

2) RELUCTANCE TORQUE

A reluctance torque is produced simply due to a change in reluctance because of the stator teeth's angular fluctuation in the magnetic circuit's reluctance as viewed by the rotor magnets. The reluctance torque, phase coupling, or the rotor magnets themselves can be a result of ripple torque [46], [47]. The unequal direct and quadrature inductances of the rotor provide the reluctance torque in an internal permanent magnet motor and affect the control accuracy of the drive system. Eccentric permanent magnet teeth and compensatory windings reduce reluctance torque variability.

3) ELECTROMAGNETIC TORQUE

The torque electromagnetic a motor's rotation, which is typically equal to the load torque, is known as the electromagnetic torque. The load torque at no load is equal to the output electromagnetic torque, which is the torque generated by the armature on the air gap. The back-EMF waveform is a crucial factor in determining the quality of the generated torque and its ripple. Significant torque ripple can be caused by the waveform of the back-EMF in conjunction with the waveform of phase currents, and then the choice of control strategy determines the waveform of phase currents [48]. Additionally, it is influenced by electromagnetic torque, which is developed as harmonics depending on the type and structure of the motor. Harmonics are produced by non-idealities in

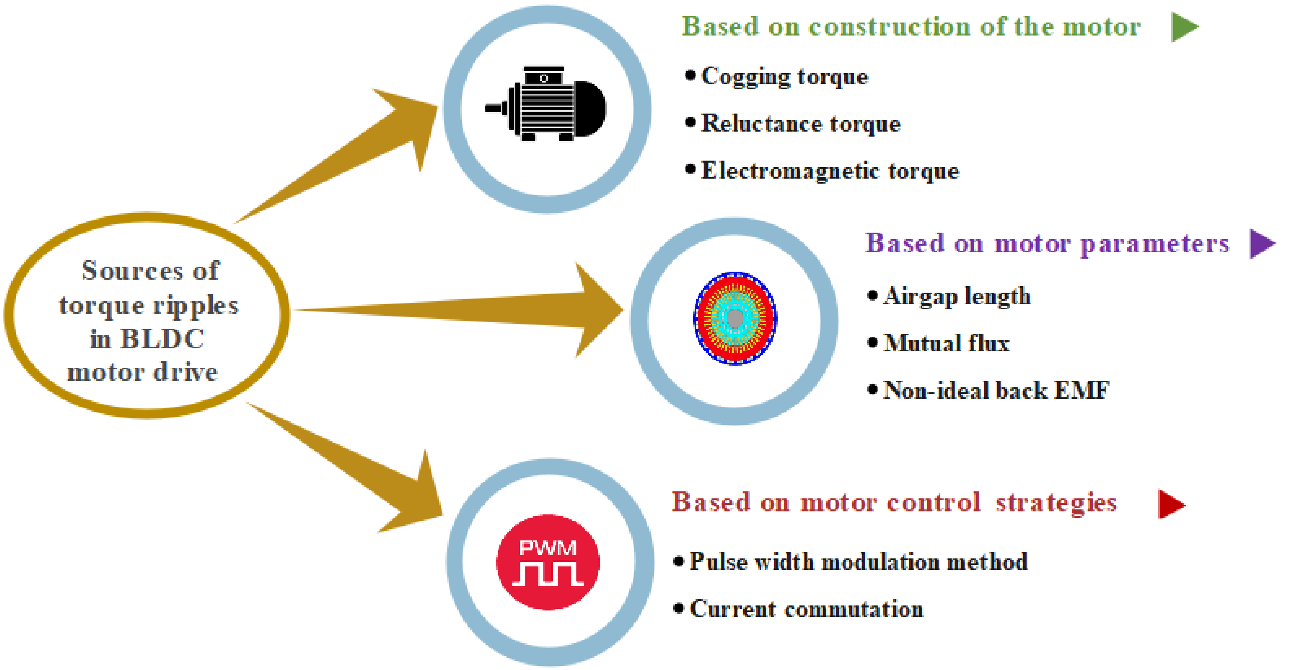

FIGURE 5. Sources of torque ripples of BLDC motor in electric vehicles.

the electromagnetic fields created by the interaction of the rotor and stator. However, the overall electromagnetic torque ripples are significantly lower than in comparable drives with magnetically insulated winding sets, making it advisable to use concentrated windings with non-intersecting winding ends.

B. TORQUE RIPPLE SOURCE BASED ON MOTOR PARAMETERS

According to the designing parameters, the torque ripples are associated with BLDC motors by three factors: airgap length, mutual flux, and non-ideal back-EMF.

1) AIRGAP LENGTH

The process of designing and operating a BLDC motor involves several procedures, including material selection, machine structure selection, and component geometric sizing. One of the essential geometrical characteristics is the airgap length, which is determined by mechanical, thermal, and electromagnetic factors [49], [50]. The overall strength of the magnetic circuit and the motor efficiency are both impacted by the air gap length, which is a crucial design element. The electromagnetic torque is directly influenced by the motor's back-EMF, so airgap length reduction increases airgap flux density, which in turn increases flux linkage and back EMF produced in the stator phases.

2) MUTUAL FLUX

To improve motor performance through the design and control of the stator parameters by reducing the leakage 8 reactance and increasing the magnetic flux linkages. The rotor magnet generates flux, which is connected to the stator [51], [52]. The motor construction behavior mainly depends on various factors like power, speed, and loading conditions.

3) NON-IDEAL BACK-EMF

The majority of high-specific torque machines have a big torque ripple by nature, which is a drawback that restricts their employment in high-bandwidth applications. Current harmonics, which depend on control strategy and inverter dead time and EMF harmonics are the primary electrical factors in BLDC motors that contribute to torque ripple. Electrical machines with non-sinusoidal electromotive forces (EMF) which give rise to current harmonics and the torque ripple typically result from the need to increase specific torque, decrease volume and weight, and create motors with less active materials [53]. Regarding the torque ripples of BLDC motors with non-ideal back-EMF, there are primarily two types of resolvents. In one method, the motor's back-EMF waveform functions can be used to control current, while direct torque control is used in the other. Regarding the direct torque, although a control strategy is used, it is necessary to measure the back-EMF and phase current, so the complexity of the circuit and software is increased.

C. TORQUE RIPPLE SOURCE BASED ON MOTOR CONTROL STRATEGIES

According to various control techniques, the torque ripples are associated with the BLDC motor by two factors pulse width modulation method and current commutation.

1) PULSE WIDTH MODULATION METHOD

Nowadays, designing and controlling rotating systems is more difficult when building an electronics controller that uses the PWM technique to operate a BLDC motor; therefore, while possible, integrate the PWM driver with the motor to avoid unexpected performance issues. In this driver, a linear amplifier is used to change the power delivered to the motor by a linear variation of voltage, which is done by control electronics and causes the motor to move in the desired position. Because the integrated linear amplifier dissipates power that is not delivered to the motor, it is difficult to integrate into the application and must be compensated for with a large heat sink. Conversely, a chopping amplifier power transistor uses turn-on and turn-off logic in terms of altering the duty cycle at a constant frequency to change the stator voltage and currents within the desired target value while also making a device more compact, decreasing heating, and improving battery life. Chopping amplifiers frequently use PWM techniques to determine average current and motor torque by changing the duty cycle ratio while the current is operating to increase and decrease over each cycle to generate heat losses in terms of ripple current and an effect on the root mean square (RMS) current without increasing the torque.

Ripple current still uses energy, which could reduce battery life in portable applications and result in iron losses, generating circulation eddy currents that are proportional to the square of both the motor's current and speed. Due to the squared relationship between iron losses and motor power, large current ripples in terms of torque ripples are created in BLDC motors to reduce their performance characteristics [54], [55], [56]. To prevent current ripples in the BLDC motor, adjust the power supply voltage without consideration of speed or power, while also considering PWM frequency as an option to reduce current rise time and reduce ripples effectively [57], [58], [59].

2) CURRENT COMMUTATION

BLDC motors typically use a 120-degree commutation mechanism with three hall sensors to determine rotor position and require a trapezoidal back-EMF waveform due to direct input current. The current spike phenomenon, on the other hand, reduces efficiency and increases noise and vibration because of current harmonics. Because of this effect, the current changes quickly during commutation in BLDC motors. Nevertheless, inductances are present in the motor's windings, and when current is commutated from one phase to another, a transient process occurs, resulting in electromagnetic torque fluctuations known as commutation torque ripple (CTR) [60], [61], [62]. The CTR effect reduces efficiency due to iron and copper losses, while accurate phase current control weakens during phase current commutation periods. Also, the CTR of BLDC motors is limited by the output voltage of the power inverter, making it difficult to change rapidly the incoming phase and outgoing phase current when operating in their high-speed range. To prevent CTR in the BLDC motor, use current sensors to adjust CTR by measuring the commutation interval and computing a PWM duty ratio based on the measured commutation interval. On the other hand, the charged capacitor is used during the non-commutation time to effectively minimize the CTR and also uses a power inverter that is controlled to make the motor's input voltage equal to four times the back-EMF amplitude [63], [64].

V. SCALAR-BASED TORQUE RIPPLE MITIGATION TECHNIQUES OF BLDC MOTOR

BLDC motor drives are used in such a wide range of applications, that the constant torque these devices deliver is important for producing outcomes that are efficient, smooth, and desirable. The efficiency of the motor drive system depends on how effectively the pulsating effects of undesirable harmonic components of torque are mitigated. The undesirable torque pulsations are caused by any source of deviation from ideal circumstances in either the motor or the related power converter in a BLDC motor drive. The variation in torque might be divided into three types: in the first, the interaction of the rotor's magnetic flux and the stator's magnetic reluctance variations causes cogging torque [41], [42]; in the second, the action of the magneto-motive force of the stator current with electromagnetic characteristics created by rotor motion causes mutual torque; [51] and in the third, the identical MMF and the rotor's magnetic reluctance's angle deviation causes reluctance torque [46], [47]. In order to reduce the fluctuations caused by these torque components, requires enhancing the BLDC motor drive construction for comfort and ensuring that their characteristics are at an optimal level. Various construction modifications, such as skewing the stator slots or altering the width of the poles, might reduce torque ripple, although these involve higher manufacturing costs and are undesirable operations.

Another strategy of utilizing control techniques to adjust for variations of excitation current in the stator is to control the motor's output parameters, like rotor flux, torque current, stator magnetic flux linkages, motor torque, rotor back-EMF, commutation angle, and speed. This technique is most adaptable for controlling torque ripples (torque pulsation) because of current ripple and commutation time in BLDC motors, which have a low cost of manufacture and are more efficient compared to the torque ripples mitigated by all other sources. In this paper, we focus on the control-side approach to mitigating the torque ripples in BLDC motors. The torque and speed control methods applied for variable frequency drives are classified into two types: scalar-based and vector-based control.

A. SCALAR-BASED CONTROL

The scalar control techniques are used to control the electrical machines in terms of speed and torque as a function of voltage amplitude and frequency. This method is easy to implement and controls the motor parameters, among them a simple design, lower steady state error rate, and lower cost. In addition, this control method is mostly used in all manufacturing and industrial settings for controlling the speed required with a low initial current. Scalar control involves a steady-state model of the motor because it controls the stator flux by varying the amplitude of the voltage and frequency to obtain the control torque [65], [66]. Scalar control techniques of BLDC motors can be achieved in two categories based on variable supply voltage control and constant voltage/frequency (V/F) control.

1) VARIABLE SUPPLY VOLTAGE CONTROL

This control method is a simple and efficient way to control the speed and torque of a BLDC motor by varying the supply voltage. However, by changing in terms of reducing stator voltage, the developed speed and torque were also reduced. It is undesirable for many applications oriented toward EVs. While vehicles may be moving slowly uphill, the maximum torque is required, but it is unable to be provided by the specific control strategy [67]. For this condition, controlling motor speed is done by varying the frequency of the stator voltage and also by obtaining the maximum torque for all-electric drive applications of BLDC motors.

2) CONSTANT VOLTS/FREQUENCY (V/F) CONTROL

This frequency drive control method is used in BLDC motors for a wide range of speed and torque control with higher run-time efficiency. During this control, the air gap flux will tend to saturate if the supply frequency is reduced while maintaining the rated supply voltage, which causes excessive stator current and stator flux wave distortion in the motor. To keep the airgap flux constant, the stator voltage should be decreased proportionally to the frequency because the stator voltage and its frequency are correlated with the magnitude flux of the stator [68]. Therefore, if the voltage-to-frequency ratio stays constant, the flux stays constant. Additionally, maintaining the V/F constant at the specified levels to achieve variable speed with maximum air-gap magnetic flux keeps the developed torque constant, providing the soft start capability. As a result, the BLDC motor's electromagnetic torque capacity is maximized.

VI. VECTOR-BASED TORQUE RIPPLE MITIGATION TECHNIQUES OF BLDC MOTOR

The vector control technique is the frequency drive control, and it is widely used in high-performance control system applications-oriented with the BLDC Motor drives in order to maximize the torque and speed performance. In this vector control, various constraints present in the scalar control are addressed, like low-speed operation and poor dynamic torque responsiveness, also the phases of stator current magnitude and frequency. In addition to frequently requiring precise parameter knowledge or rotor flux position, vector controls are more expensive and difficult than scalar ones. Even though it's able to obtain excellent performance in controlling the magnitude, frequency, and instantaneous phases of the stator and rotor phase currents and minimize the changes in flux linkages. Vector control has been used to reduce torque ripples in BLDC motors, which mainly includes field-oriented control, direct torque control, intelligent control, controlling input voltage, current shaping techniques, model predictive and sliding mode control, etc.

A. TORQUE RIPPLE MITIGATION BASED ON FIELD-ORIENTED CONTROL

Field-oriented control (FOC) techniques, commonly refer to as vector control, are used to manage BLDC motors with good control capability of the entire torque and speed ranges. It operates the motor very smoothly and efficiently to reduce the torque ripples with greater high load efficiency. FOC is utilized to make the stator magnetic field orthogonal to the rotor magnetic field in order to provide the desired output in a BLDC motor, and vector representation is used to modulate the current flowing through the stator as shown in Fig 6.

It is the best and is often used in speed control techniques to manage the amplitude and angle of the stator phase current and voltages. Initially, express the relationship between the electrical angles (ω_{m}) of the stators and the rotors and the angles (θ_m) of the winding stators that are described by the following equations (1 & 2).

$$\omega_{\mathrm{m}} = \frac{\omega_{s1} + \omega_{s2}}{\mathrm{P}} \tag{1}$$

$$\theta_m = \theta_{s1} + \theta_{s2} \tag{2}$$

The FOC also referred to as decoupling control, is employed to achieve the independent control of torque and flux converting to three-phase stator currents ($\mathrm{I_a}$, $\mathrm{I_b}$, and $\mathrm{I_c}$) from torque-producing components in a stationary reference frame and flux-producing components in a rotating magnetic frame. The three-phase stator currents are measured and determined by Kirchhoff's current relation is expressed in equation (3).

$$\mathrm{I_a} + \mathrm{I_b} + \mathrm{I_c} = 0 \tag{3}$$

This measured motor stator current is mathematically translated into two orthogonal current components (I_α & I_β) with amplitudes that are aligned with the quadrature axis ($\mathrm{I_q}$) and direct axis ($\mathrm{I_d}$) respectively, by using Clark and Park's transformation given by the equation (4 & 5).

$$\mathrm{I}_\alpha = 0.816[\mathrm{I_a} - \sin(30)\,\mathrm{I_c} - \sin(30)\,\mathrm{I_b}] \tag{4}$$

$$\mathrm{I}_\beta = 0.816[\cos(30)\,\mathrm{I_c} - \cos(30)\,\mathrm{I_b}] \tag{5}$$

The stator current controls in the d-axis components regulated the rotor flux magnitude, while the q-axis components handled the output torque. On that axis, the one along the reference vector or rotating magnetic field is called the direct axis ($\mathrm{I_d}$), and the other axis that makes 90 degrees with the direct axis is called the quadrature axis ($\mathrm{I_q}$) [69], [70] are presented in equation (6&7).

$$\mathrm{I_d} = \mathrm{Cos}\ominus\mathrm{I}_\alpha - \mathrm{Sin}\ominus\mathrm{I}_\beta \tag{6}$$

$$\mathrm{I_q} = -\mathrm{Sin}\ominus\mathrm{I}_\alpha + \mathrm{Cos}\ominus\mathrm{I}_\beta \tag{7}$$

In steady-state conditions, both $\mathrm{I_d}$ and $\mathrm{I_q}$ are constants, and their values are compared with the desired reference current

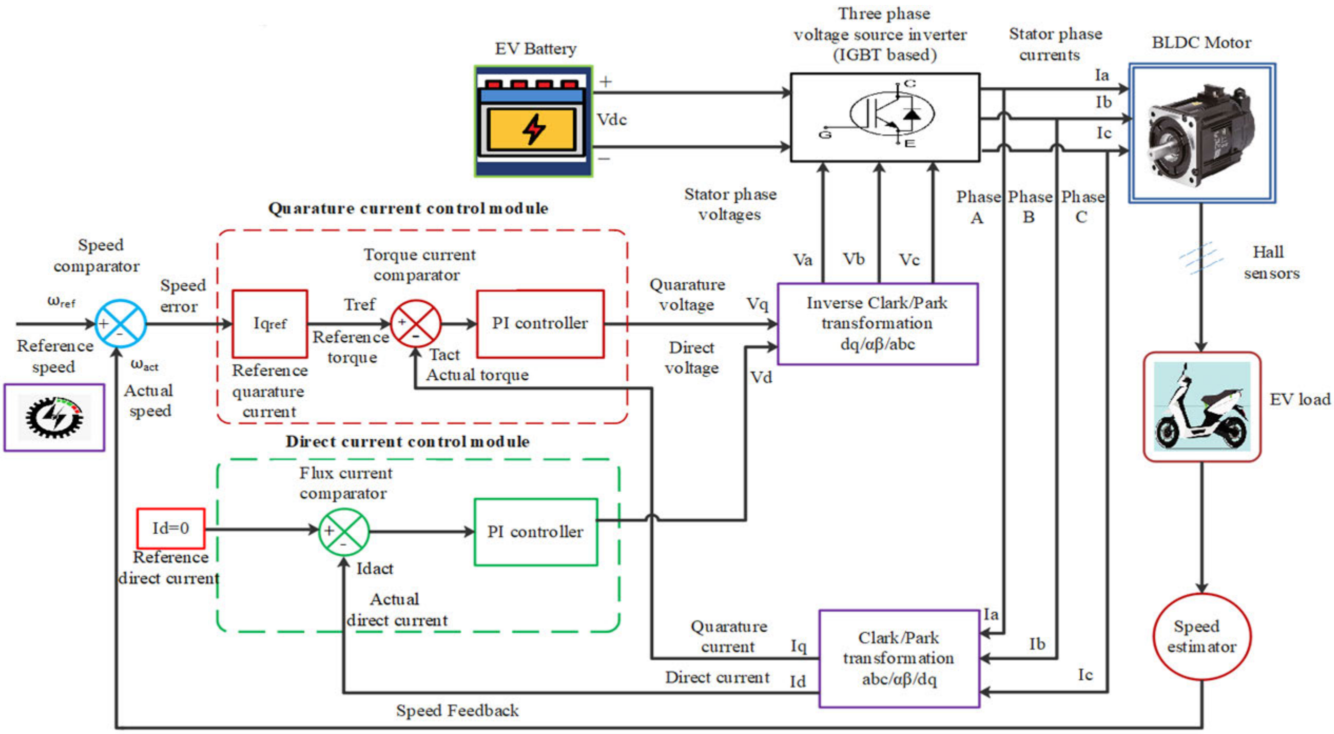

FIGURE 6. Field-oriented control strategies of torque ripple mitigations in BLDC motor for electric vehicles.

values, I_{dref} & and I_{qref} respectively, to control the rotor magnetic flux and torque output of the motor. It is based on the comparison error difference signals that are produced and fed to the two PI controllers. To achieve the maximum torque, when it makes the reference of flux component I_{dref} is zero and reference of torque component I_{qref} generated to maximum [71], [72], [73]. The output values from the PI controllers provide the voltage vectors V_d and V_q, which are represented in a rotating constant reference frame. The measured voltages V_d and V_q were transformed into three-phase stator voltages (V_a, V_b, and V_c) by using the inverse Clark and Park transformation [74], [75] obtained by the following equations (8,9&10).

$$V_a = 0.557 V_d \tag{8}$$

$$V_b = 0.557[V_q \cos(30) - V_d \sin(30)] \tag{9}$$

$$V_c = 0.557[-V_q \cos(30) - V_d \sin(30)] \tag{10}$$

In this manner, new PWM duty cycle values are determined, and the motor is supplied with optimal voltages to create the maximum amount of electromagnetic torque while minimizing reduced torque ripples produced by angular fluctuations between the stator and rotor teeth due to variation in reluctance. Thus, the examination of the electromagnetic torque can be divided into partial sections focused on the specific components in terms of, analyzing the form of the current and the back-EMF component leading to the location and definition of the torque ripple source. The produced torque component described in equation (11),

$$T_e = T_{avg} + T_{ripple} \tag{11}$$

where, T_e is the electromagnetic torque (N-M), T_{avg} is the average or smooth torque (N-M) and T_{ripple} is a sum of the harmonics content in torque.

The total torque ripples are primarily related to estimating the rotor and stator flux linkage in that way, the phase current must be chosen to calculate the motor speed based on the rule that the value of rotor flux of the chosen phase changes with rotor position whereas the other two phases have constant flux value [77]. The amount of torque ripple (equation 12) is calculated as the difference between the resultant electromagnetic torque T_e and the cogging torque reference T_{cogg}.

$$T_{ripple} = T_e - T_{cogg} \tag{12}$$

The BLDC motor was controlled using the FOC-controlled method; the results were effective, and the pursuit of speed was perfect despite some sort of disruption in the transition between portions.

The various FOC controllers have been improved to satisfy the distinct demand for electric vehicles (EVs). In general, the different techniques used in conjunction with FOC controllers to obtain the optimum voltage for motor torque control in EVs are summarized in Table 1.

Most popularly, the strategy of two control loop modules for motor torque control mitigates torque ripples, such as through a speed and current control module. According to

TABLE 1. Performance comparisons of field-oriented control for BLDC motor in electric vehicles.

Control Strategy Adopted	Rotor position estimation	Torque ripple analysis	Complexity	Robustness	Outcomes	Ref.
6wire-3phase inverter topology	Sensor	THD=0.15% I_{rms} =0.594A with 150w	Increased switches & drivers cause heat dissipation in inverter components	Increase voltage swing for greater motor speeds without over-modulation	Reduce third harmonic components to increase motor efficiency	[76]
Novel flux estimation algorithm	Sensorless	Transient time (before 0.085 s) 1.55 Nm rated load torque at 1.5 s	The control drive has a low-speed handling capacity	Actual flux & predicted flux were perfectly matched after 0.085 seconds	Improve starting torque without position sensors by mapping rotor & flux linkage	[77]
FTC-FOC	Voltage & Current	Current transition from DTC to FOC=5s FOC to DTC=5.5s	Insufficient FTC scheme causes voltage sensor fault	Address sensor failures using FTC relevance	Synchronize two controlling systems to improve EV reliability & safety Prevent excessive transients during switching operation	[78]
FOC-SMO	Sensorless	T_s=3.5s for 800rpm T_s=6s for 1600rpm	Tuning gain procedure of the SMO	To reduce chattering, the sign function is replaced by a saturation function	Improve speed tracking accuracy, torque, current ripples, and performance wide speed range	[79]
Dither signal injection	Hall sensors	T_s=2.7s for 500Hz T_s= 2.4s for 10kHz T_s= 1.8s for 20kHz	Gearbox installation causes nonlinearity backlash in BLDC motors	Minimize nonlinearity & prevent uncontrollable oscillation in closed-loop control systems	Adding sinusoidal dither to minimize backlash nonlinearity	[80]
FOC-DTC	Sensorless	T_r= 0.015s for 1000rpm T_s=0.022s for 1000 rpm T_r= 0.012s for 600rpm T_s=0.015s for 600 rpm	Inaccurate data due to erroneous input makes it unreliable	Hybrid ZSI-BLDC motor drive controller resists harmonics	Enhance current shape through THD optimization to reduce CTR	[81]
FOC-CHC	Hall sensors	5% peak ripple lower than conventional FOC	Design complexity for precise harmonic signal control in bandwidth	Accurate of tracks periodic alternating signal & suppresses disturbances	Reduce current harmonics to optimize torque & smoothness	[82]
FOC-AFFC	Sensorless	THD=0.213% at no load THD=1.896% at load	EMF harmonics remain constant at high speeds without controller action	To minimize current harmonics in the presence of significant measurement noise.	Periodic tracking & disturbance to improve system stability	[83]
ACC-FOC	Sensorless	The host vehicle's 35 m/s relative distance equals a safe distance	Adaptability in various driving scenarios	To ensure torque load control stability	Driver must ensure acceleration, velocity, speed, torque response & safe distance	[84]
Novel current control	Encoder & current	Provide less than optimal flux interaction angle at Duty cycle 50%	The current controller design is difficult in low-duty cycles	High-speed, smooth system weight and inertia applications minimize ripples	Reduce switching loss, vibrations, and audible noise to improve controller efficiency	[85]
WLC-FOC	Sensorless	T_s=0.05s for 60km/hr	The minimal description length (MDL) criterion selection wavelet controller	For fine-tuning gain parameters under various operating conditions	Reduce peak overshoot & settling time to achieve smooth torque	[86]
FLC-FOC	Hall sensors	T_s=0.5s,M_p=0% with high speed T_s=0.2s,M_p=0% with low speed	Compute control inputs for general FLC within loop controller sampling time	To regulate torque changes, a quick response with great accuracy	Transmission/drive system with high stability, accuracy & fast response Improve motor torque dynamic &steady state response	[87]
Cogging torque reduction algorithm	Sensor	Cogging torque compensation 5 Hz and 10 Hz BW	Load torque observer involves more mathematical operations	Accurate tracking of harmonic current reference	Compensate cogging torque & reduce torque ripples	[88]
FOC-PWM	Sensorless	T_L increased from 0.8 Nm to 2 Nm at 1sec N increased from 1000 rpm to 1400 rpm at 1.6sec	Delta modulation enables triangular wave oscillation in the hysteresis band	Creating conditions like speed variation, load torque change, and initial rotor angle mismatch.	Obtained high performance, load torque control & speed response	[89]
Lab view FPGA	Hall sensors	T_{ss}=0.04s for 120rpm	Semiconductor design for power converters & digital signal processors	FGPA improves complex conversion and control procedures	Reduce switching harmonics & provide fast processing for complex operations	[90]

TABLE 1. ***(Continued.)*** **Performance comparisons of field-oriented control for BLDC motor in electric vehicles.**

Modified FOC	Sensorless	T_{rip} reduction= 0.3% THD=0.55% I_{rms}= 1.8615A	Real-time implementation requires adding decoupling voltage terms to current controllers	Minimizing harmonic distortion	Currents inject currents to maintain harmonic ratio & reduce torque ripple	[91]
New Zero voltage vector	Sensorless	T_{rip} reduction= 2.62%	Voltage vector, not zero in conducting phase windings analysis is difficult	New ZVVs short circuit conducting phase windings improve performance	Reveals the zero voltage vectors exactly to improve system stability & reliability	[92]
Six-step with FOC	Sensor	T_{rip} reduction= 0.62%	Due to a lack of commutation, fluctuations in torque occur in a rotating d-q coordinate system	Maintaining constant current in q axis amidst back-EMF changes	Examines the quantitative evaluation of torque ripple & motor power losses	[93]
Low-resolution sensors	Sensors	Resolution of 0.935deg	FPGAs require more design effort and resources	Balance economic constraints with computational performance	Optimize FPGA resource utilization to balance economic & computational performance	[94]
Space vector modulation	Encoder	T_{rip} reduction= 6%	Implementation of high voltage approaches is complicated	Improves bus voltage utilization & eliminates overall harmonic distortion	Reduce torque ripples & maximize efficiency in large EV applications	[95]
FOC-ANN	Sensorless	Flux variation (-0.5 to 0.5) wb, Rotor angle = 5.5 deg	Due to non-linear interactions, real-time implementation becomes difficult	Improves mechanical resistance to noise and noise immunity	Fast dynamics & improved parameter adaption ripples to reduce torque ripples	[96]
SVPWM	Sensorless	T_s = (0.06-0.12) s with an amplitude of 7.5V, 1.4 A for low load and 2.5 A for high load	Complex techniques require device design	Total harmonic distortion in the output voltages of VSI	Modulation scheme-based inverter provides low harmonic distortion, good output quality	[97]
Power factor correction	Sensor	Non-regulated mode TL = 10 Nm at speed 3166.5 rpm	The control circuit manages the RMS current with a complex, almost unity power factor	Enhance power consumption quality	Controlling motor speed when load changes improve power usage	[98]
FTC-SV modulation	Sensorless	Torque control mode at Maximum reference DET of 15 Nm	Complex switching sequence selection implementation	Increased phases lead to better physical capability & electric actuation system	Control signals are provided to servo steering, braking & traction systems	[99]
Position sensorless control	Sensorless	Only (4-8 %) error at low speeds	Processor advancements simplify strategy complexity, reducing computational time	Predicting back EMF speed at slower speeds	Evaluation of driving cycle schemes to control rotor position sensor failure	[100]

the speed control module way, the FOC is paired with modified sliding mode control (SMC) to regulate the reference speed accurately when the performance of the controller is weak in the motor because of uncertainty and nonlinearity parameters. Even though motor parameter fluctuations are present, the sliding mode observer (SMO) is used to estimate the continuous rotor position and improve the speed tracking accuracy at all operating conditions [79]. Besides, it limits speed overshoot, minimizes steady-state error, and provides good dynamic responsiveness and quick rising and settling times for the minimum phase system motor drive. Although an adaptive feedforward controller (AFFC) is used in a non-minimum phase system to regulate the motor speed by adding modulation action to the stator at various harmonic frequencies. It periodically tracks disturbances so that the adaption gain can be changed automatically without disturbing system stability to improve the stator voltage waveform along with this motor drive controller [83], regarding this motor driver, employs adaptive cruise control (ACC) to maintain a constant speed, while field-oriented control (FOC) was used to regulate the motor to maintain the desired speed independent of the torque load on the motor. It also generates a negative acceleration to reduce velocity and maintain safe spacing between the vehicles [84]. Correspondingly, the wavelet controller (WC) enhances stability and provides smooth control of the two rear drive wheels in EVs, especially on 12 curved roads [86]. According to the current control module way of thinking, FOC works together with SMC to suppress the torque ripples in the inner loop current control [79]. To improve the performance of this controller from backlash nonlinear action, the high-frequency dither signals are injected in different types of modulation and enhance the motor system performance in EVs [80]. Similarly, it is possible to improve system performance by reducing electromagnetic torque ripples and enhancing current shape through THD by using of fuzzy logic concept [81]. Additionally, the fuzzy logic controller (FLC) ensures four quadrant operations to control the motor torque without any fluctuations during the accelerating, decelerating, and reversing states. It provides a fast response with the transmission in EV systems compared to all other controllers [87]. More distantly, the smoother torque control with less current motor operation is analyzed by space vector pulse width modulation (SVPWM) along with this motor drive controller to mitigate the torque ripples [97]. In FOC, control techniques are used to ensure effective steady-state performance across all load torque and speed ranges. It generates precise torque with a high switching frequency, which may result in higher energy costs. Furthermore, EVs do not always require precise torque output.

B. TORQUE RIPPLE MITIGATION BASED ON DIRECT TORQUE CONTROL

Direct torque control (DTC) techniques are reliable and energy-efficient vector control methods that are appropriately used in electric vehicles because of their ability to control the torque directly with the low sensitivity parameters of BLDC motors. It also delivers precise dynamic torque response and flux control with a compact structure. DTC is utilized to make optimal voltage vectors by selecting appropriate switches from space vector modulation control of a three-phase inverter along the variables related to the developed torque and flux linkage of the motor, as shown in Fig 7. This technique consists of three main stages: the motor model, the hysteresis current controller (HCC), and the optimal switching lookup table. The motor model estimates the developed torque (T_d) and stator flux linkage (Ψ) based on the current in the two stator windings and the battery voltage. The DTC method uses the Clark transformation to convert the motor's three-phase currents parameters (I_a& I_b) to a rotating d-q reference axis frame can be expressed by the following equations (13 & 14),

$$I_\alpha = I_a \tag{13}$$
$$I_\beta = \frac{I_a + 2I_b}{1.732} \tag{14}$$

& two-phase independent vector current components (I_d & I_q) are given by the following equations (15 & 16),

$$I_d = \frac{\Psi_{sd} - \Psi_{rd}}{L_d} \tag{15}$$
$$I_q = \frac{\Psi_{sq} - \Psi_{rq}}{L_q} \tag{16}$$

where, Ψ_{sd} and Ψ_{sq} are the stator flux linkages (d-q axis) (wb), Ψ_{rd} and Ψ_{rq} are the rotor flux linkages (d-q axis) (Wb) and L_d &L_q are inductances of motor (d-q axis) (H).

From this conversion, the estimate of the developed torque (T_d) and stator flux linkage (Ψ) can be expressed by the following equations (17 & 18),

$$T_{d(act)} = \frac{3}{2}\frac{P}{2}(\Psi_{sd}I_q - \Psi_{sq}I_d) \tag{17}$$
$$\Psi_{(act)} = \Psi_{sd} + \Psi_{sq} \tag{18}$$

and these actual (T_d & Ψ) are compared with the current command magnitude with each phase of desire reference developed torque (T_{dref}) and flux linkage (Ψ_{ref}) [101], [102].

The stator currents are regulated by the hysteresis current controller in accordance with the torque and flux deviations, (equations 19 & 20) which are the variations in the stator flux linkages and torque and their estimated values from the motor.

$$dT_d = T_{dact} - T_{dref} \tag{19}$$
$$d\Psi = \Psi_{act} - \Psi_{ref} \tag{20}$$

Depending on the hysteresis current controller output, the optimal stator voltage vector is selected from the switching lookup table [103], [104]. According to the switching state of the table, the voltage source inverter controls the stator flux linkages and torque directly, and the motor is supplied with optimal stator currents. This DTC method is used to reduce the torque ripples created by the insufficient commutation effect of electromagnetic fluctuations caused by a motor, along with maintaining a constant current and varying the frequency from minimum to maximum [105], [106].

In a steady state, we may regulate the hysteresis bandwidth to control torque ripple. Hysteresis controllers can be added to each stage of the current controlled inverter to raise the switching frequency. Due to the fast changes in flux waveforms and their unpredictably huge amplitudes brought on by a number of parameters, such as winding inductance, load torque, etc., the DTC motor drive is unable to manage stator flux connections. Only electromagnetic torque can be controlled.

The different DTC controllers have been enhanced to ensure the safety and stability of EVs while also providing good dynamic characteristics of the traction chain. Most of the various approaches used in conjunction with DTC controllers to obtain the optimal stator phase currents for controlling torque in motor drives are summarized in Table 2. The DTC is generally built around two hysteresis controller modules that control the switching state voltage vector via torque and flux linkage modules that regulate the stator phase currents. Based on the three-level hysteresis torque controller, the inverter's switching frequency can be balanced while keeping the motor's common mode voltage at a minimum [112].

Moreover, it reduces torque ripples during sector-to-sector commutation and achieves maximum efficiency with low frequency, torque ripple-free direct control. Even though a hysteresis controller (HC) combined with PWM improves the lookup table of switching devices, the torque ripple in commutation is overcome [125]. Here, the four-quadrant operation is obtained to validate the feasibility and effectiveness of this controller in avoiding large current and torque ripples. However, to control the torque effectively and directly without flux linkage observation (FLO), using the shape function in terms of the amplitude of the back-EMF and stator current estimation [119], the optimal voltage vector is

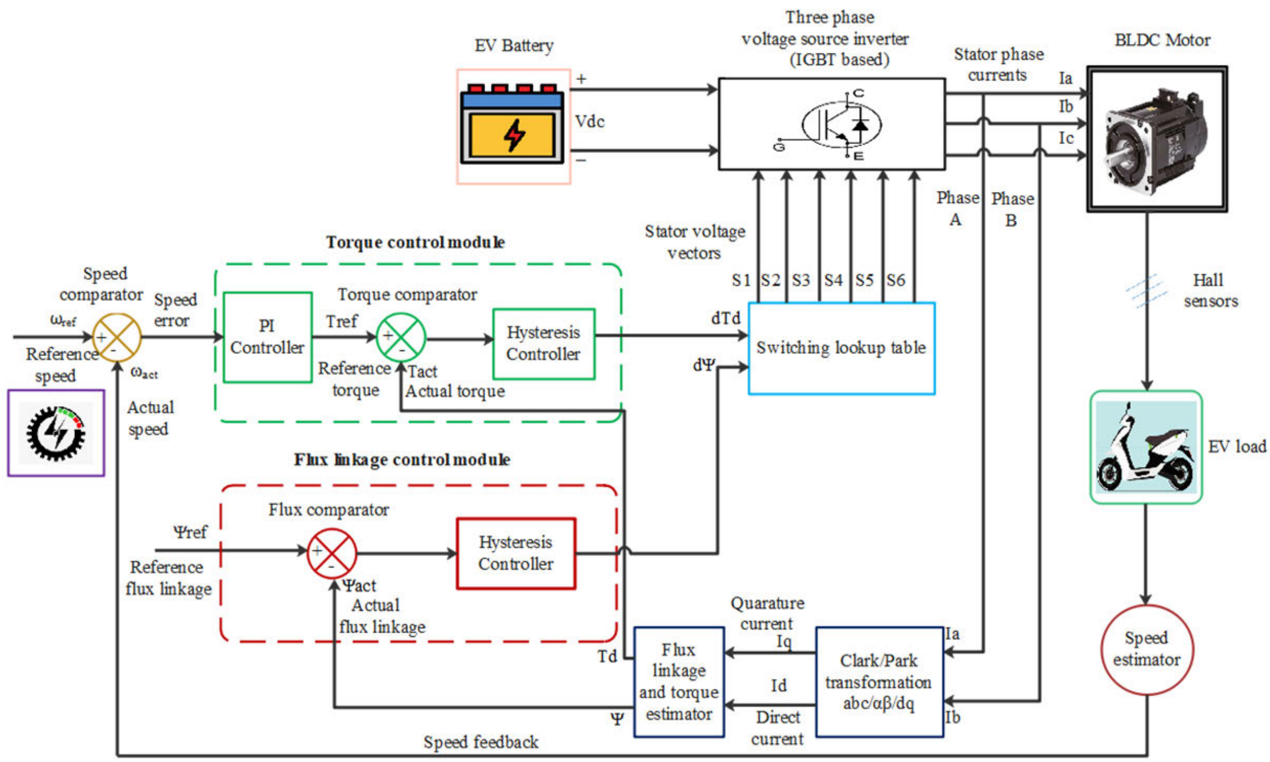

FIGURE 7. Direct torque control strategies of torque ripple mitigations in BLDC motor for electric vehicles.

chosen based on the torque error between the given torque and the actual torque by using of PI controller.

Which are designed to drive light electric vehicles and operate in variable torque and speed conditions with a single reference input. In addition, the FLC-based speed control is proposed instead of PI controllers to reduce starting current, avoid overshoot in torque and speed responses, simplify the design, and minimize complicated mathematical equations. Furthermore, the SVPWM combined DTC is preferred for optimum steady-state performance in terms of torque ripple minimization and speed regulation, apart from the necessity for a switching table and a hysteresis controller [115].

Here, an optimal PI controller has been properly tuned to reduce uncertainties due to load variations. Similarly, DTC used the synthesized current phase compensation (SCPC) technique to effectively minimize torque ripples in BLDC motors. Here, stator current has been synthesized using voltage vector selection and a new switching technique to modify three-phase supply currents. Also, the injection of synthesized currents with angle advancement increases the torque capacity of the motor control [117]. For further improvement of the BLDC motor drive by DTC, the nonlinear model predictive controller (NMPC) scheme is used to control the desired torque and speed of the motor by minimizing energy while limiting the supplied current and maximum speed [127].

Moreover, this NMPC can be enhanced for real-time implementation to achieve torque ripple reduction, controlled degradation, etc. NMPC is a challenging control strategy that has emerged as an attractive solution for electric vehicle applications due to its energy-efficient performance. Regarding, this DTC control scheme can provide faster torque response, and furthermore it is frequently utilized in high-performance motion control of electric drives [110], [127].

C. TORQUE RIPPLE MITIGATION BASED ON INTELLIGENT CONTROL

Intelligent control techniques are one of the most efficient methods to use for most common problems present in BLDC motors for electric drives, like electromagnetic inference, fault tolerance, and torque ripples. Today, several conventional controllers are used in electric vehicle drive applications, like PI and PID controllers, but for more optimal electric vehicles with maximum efficiency, accuracy, and performance, fuzzy-based intelligent control systems are mostly preferred, as shown in Fig 8. The fuzzy control method has more features to mitigate the torque ripples with good steady state and dynamics performance of the electric drive system by integrating a phase current (square wave) within a portion of the steady back EMF magnitude [131], [132], [133]. A mostly fuzzy logic-based control system is used to increase the reliability of the electric vehicle system and improve the time domain specifications of the motor control system, like minimizing the rise time, starting current, settling time, speed fluctuation, and peak overshoot. It is mainly afforded to non-linearity by the small torque ripples in low-speed

TABLE 2. Performance comparisons of direct torque control for BLDC motor in electric vehicles.

Control Strategy Adopted	Rotor position estimation	Torque ripple analysis	Complexity	Flux / Torque control	Drive Robustness	Outcomes	Ref.
Non-sinusoidal back-EMF	Sensorless	I_p=0.25 pu/div T_e=0.2 pu load torque Time base=3.4 ms/div	Unpredictable sharp dips in stator flux linkage, complicating control strategy	Torque	Improve torque response by adjusting voltage vectors & keeping stator flux amplitude constant	Reduce non-ideal trapezoidal back-EMF induced low-frequency oscillations	[107]
DTC-low resolution sensors	low-resolution sensors	Speed curve measured from 360rpm to 140rpm in 0.6s	Inaccuracies in closed-loop control systems	Both	Remove pricey position sensors to improve drive reliability	An efficient way to stop freewheeling current during switching OFF period	[108]
Modified switching algorithm	Hall sensors	T_{ripple} reduction 1.1% for 50rad/s 0.9% for 75rad/s	Balancing switching frequencies for enhanced reliability is a little more complicated	Both	Switching table implementation for control strategy	High steady& transient state capability during speed reversal & load changes	[109]
Finite control-DTC	Sensorless	Torque tracking=5 ms T_s=50μs	Control performance not yet comparable to optimal controllers	Both	Controllers enable efficient drive operation	Maintaining good steady-state performance while retaining rapid dynamic reaction	[110]
Maximum torque/ampere control	Sensorless	T_{ripple} index 4.2% for 1.5Nm 2.8% for 3 Nm 2.6% for 4.5Nm 2.2% for 6 Nm	To track the fast-changing desired currents, a high-speed inner current controller	Torque	Underestimation of iron loss due to robust MTPA realization	Maintain current magnitude to improve dynamic performance & track changing intended current	[111]
Direct torque & indirect flux control	Sensorless	T_s=15μs T_{band}=0.001Nm Flux band= 0.001 Wb	Torque estimation using the Fourier approximation	Both	Close torque tracking, friction compensation & steady-state rotor speed	Simple design & fast torque response for sensorless & field weakening	[112]
Firefly algorithm based PID controller	Hall sensors	T_{ripple} reduction 14.7% for 300rpm 19.8% for 1000rpm	Multiple fireflies attract, causing oscillations & computational time	Torque	Optimum controller parameter modifying	Optimized torque is achieved through optimization techniques	[113]
Adaptive neuro-based fuzzy inference system controller	Sensorless	T_r=0.1s,M_p=0% for rated speed	Reduce the complexity of arithmetic formulas	Torque	In the optimum tuning scenario, eliminate overshoot in speed response & torque	Reducing math complexity & simplifying design to reduce overshoots	[114]
SVPWM-DTC	Hall effect sensors	T_r= 0.0200s T_s= 0.4063s T_p= 0.0283% M_p= 1.61% T_{ripple} = 9.7% for 1231rpm	BLDCM drive's sampling frequency limited due to the complex process	Both	Robust problem-solving, finding optimal optimization tasks for unconstrained & constrained tasks	Regulate gain parameters to reduce speed & torque ripple	[115]
FOC-DTC	Sensorless	Mean square error 0.6823 for 1394 rpm	Adaptive bias and gain method for efficient closed-loop electronic speed control	Both	Ensures inductance & resistance parameters are accurate across rotor speeds	High robustness to improve torque level & reduce steady-state error	[116]
DTC-SCPC	Hall sensors	T_s=25μs Traces the current 33% of $N_{nominal}$ & 35% of $T_{nominal}$	Less complexity of computational costs in controller design	Flux	Compensate current commutation error	Motor phase currents are determined to simplify system controller design Calculating conduction & switching periods reduces commutation phase error	[117]
Torque control with un-ideal back-EMF	Hall sensors	T_{ripple} control at T_e=2.54Nm, I_{stator}=10A	Torque control using finite DC bus supply voltage	Torque	Robust pulse action time calculation using back EMF waveforms for switch control	Selecting appropriate current harmonic during commutation might minimize CTR	[118]
DTC without FLO	Sensorless	T_{ripple} reduction Te=0.24Nm at speed ripple 120rps	Difficult to differentiate non-sinusoidal flux linkage components from other noise signals	Torque	Rapidly obtaining shape function (E_b α N_r)	Analysis of voltage vectors to manage torque by calculating stator phase currents & back-EMF	[119]
Three-level hysteresis torque controller	Hall sensors	T_{ripple} reduction T_e=0.5Nm, I_{stator}=10A at sector commutation=2	Multiple transformations are required & complicating torque control	Torque	Fast inverter switching frequency balancing & motor CMV average value reduction	Null voltage vectors are used to reduce CTR during sector commutations	[120]

TABLE 2. ***(Continued.)*** **Performance comparisons of direct torque control for BLDC motor in electric vehicles.**

Position sensorless DTC	Sensorless	Rotor position error is less than 5 degrees	Stator flux magnitude cannot be easily controlled due to sharp dips in vectors	Both	SMO robustly estimates back-EMF accuracy due to parameter uncertainty	Rotor flux vector location is used for choosing a switching pattern to reduce CTR	[121]
DTC-HCC	Sensorless	T_{ripple} calculation Stator current= 0.52% Torque = 0.08%	Advance control approach using BLDC voltage & current regulation	Both	Ensuring torque generation while minimizing power losses	Multi-loop approach to regulate variable signals & reduce torque ripples	[122]
Delay in gate firing Circuits	Hall sensors	T_{ripple}=10 % for 400 rpm,2 ms OFF delay T_{ripple}=20% for 1000 rpm,0.3 ms OFF delay	In practice, constant speed and load torque cannot be guaranteed, making delay impractical	Torque	Commuting currents' slopes balance quickly	OFF delay is used to reduce torque ripple for specific operating speeds	[123]
One-cycle average torque control algorithm	Hall sensor	Speed = 1200 r/min Load torque =1.6 Nm	Complex exponential decomposition enables closed-form solution for current harmonics	Both	Delta modulation technique for tracking motor winding currents	Observers can measure stator flux & torque to reduce torque ripples	[124]
HC&PWM	Position sensors	T_{ripple}=12%	High switching frequency causes undesirable harmonics	Both	Enhancing control accuracy over peak current control	4 quadrant level hysteresis controller improves torque control also PWM controller prevents current & torque ripple	[125]
Modified DTC	Sensorless	T_{rip} reduction Torque band= ±0.02 Flux band= ±0.005	Computational time complexity	Both	High-resilience controller with minimal computational load	Variable torque reduces torque ripples in light EVs	[126]
NMPC	Sensorless	Transient steady state $P_{consumption}$=1741w P_{saving}=13.79%	Computational complexity is less for NMPC	Torque	Fast convergence without oscillations	EV applications benefit from energy-efficient performance also real-time torque & loss reduction, control degradation.	[127]
FLC	Encoder	T_{ripple} reduction T_L= 6Nm ,M_p=0% for rated speed	Reduce the complexity of arithmetic formulas	Torque	Eliminate overshoot in speed & torque responses	It reduces starting current, torque overshoot and also addresses complicated problems	[128]
Modified integrator	Sensorless	Tracks the reference speed of 500 rad/s within 0.0125sec	Choosing the appropriate torque hysteresis band size	Both	Three-phase conduction pulse width modulation enhances torque control reliability is more.	Reduce initial transient in flux linkage during the first switching interval to make torque control robustness	[129]
Current observer	Encoder	Torque is controlled in 0.05s	The current control algorithm reduces the complexity	Torque	Estimated torque accurately tracks output torque	Estimates motor current for given voltage/speed Motor torque can be accurately & reliably controlled	[130]

operation and is designed for stabilization in EV applications [134], [135], [136], [137].

In BLDC Motor the back-EMF mainly depends on rotor position and the BEMF of each phase differs by 120 deg phases from the others, hence the equations (21,22 & 23) are described by,

$$e_a = K_b f_a(\lambda)\omega \tag{21}$$
$$e_b = K_b f_b(\lambda)\omega \tag{22}$$
$$e_c = K_b f_c(\lambda)\omega \tag{23}$$

where, λ is rotor angle (electrical degree), ω is angular speed (rad/sec), K_b is the back EMF constant, and, f_a, f_b & f_c are the trapezoidal signal functions. From the following back EMF equations, the trapezoidal signal functions can be expressed by the following equations (24,25 & 26),

$$f_a(\lambda) = \begin{cases} \frac{\lambda}{60}, & 0 < \lambda \leq 60^\circ \\ 1, & 60^\circ < \lambda \leq 150^\circ \\ 1 - \frac{\lambda - 150}{60}, & 150^\circ < \lambda \leq 210^\circ \\ -1, & 210^\circ < \lambda \leq 330^\circ \\ -1 + \frac{\lambda - 330}{60}, & 330^\circ < \lambda \leq 360^\circ \end{cases} \tag{24}$$

$$f_b(\lambda) = f_a(\lambda + 120^\circ) \tag{25}$$
$$f_c(\lambda) = f_a(\lambda - 120^\circ) \tag{26}$$

where, the commutation angle functions $f_a(\lambda)$, $f_b(\lambda)$, and $f_c(\lambda)$ are exactly the same shape as e_a, e_b, and e_c with a maximum scale of 1. Also, the electromagnetic torque can be obtained by following equation (27),

$$T_{(actual)} = \frac{e_a I_a + e_b I_b + e_c I_c}{\omega} \tag{27}$$

Intelligent control uses a fuzzy logic estimator to control the torque ($T_{prediction}$) (equation 28) in the motor and an artificial

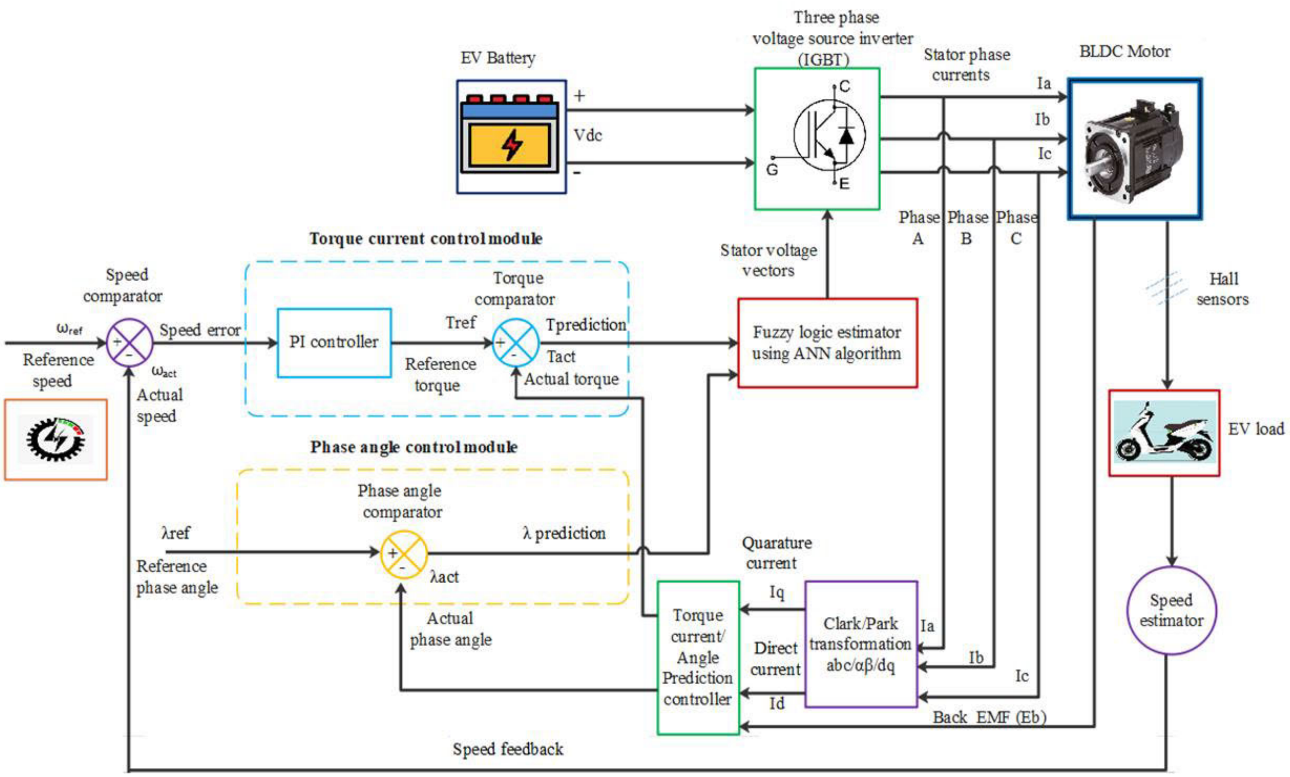

FIGURE 8. Intelligent control strategies of torque ripple mitigations in BLDC motor for electric vehicles.

neural network concept to maintain the commutation angles ($\lambda_{\text{prediction}}$) (equation 29) of the rotor winding. By using this, regulate the commutation angles in the rotor winding to sustain the slew rate of commutated phase currents while keeping non-commutating phase currents constant. Also, it's employed to achieve the new commutation on the analysis of torque control by motor output parameters like rotor phase angle (λ_{actual}) and speed (ω). Here, the actual speed (ω_{act}) of the motor is compared with the reference speed (ω_{ref}) and its difference error signal fed to a conventional PI controller in order to obtain the control torque considered as reference torque (T_{ref}) [138], [139], [140].

$$T_{\text{prediction}} = T_{\text{actual}} - T_{\text{ref}} \tag{28}$$

$$\lambda_{\text{prediction}} = \lambda_{\text{actual}} - \lambda_{\text{ref}} \tag{29}$$

Using a fuzzy logic estimator and ANN algorithms to estimate torque and commutate angles from the intelligent controller to optimum stator voltage vectors, torque, motor output power, and speed are controlled adequately with minimal torque response ripple [17]. Although these techniques are referred to as commutation torque ripple reduction, they merely swap the speed controller with a fuzzy logic one.

Numerous intelligent control methods have been developed to improve the reliability of electric vehicle drives through the design of FLC systems. Fuzzy logic is one of the most advanced control methods for regulating the speed in a wide range of various EV applications. The fuzzy control system is used in accordance with several other techniques to improve the efficiency, performance, and accuracy of the system, resulting in a more optimal electric vehicle, as summarized in Table 3. Fuzzy systems with PI controllers are commonly used for effective speed management to keep the speed constant even when the load fluctuates [141]. Again, it uses a particle swarm optimized (PSO) PI Controller to improve motor speed, reduce error to an absolute minimum, and achieve high performance in both steady state and transient responsiveness [146].

Based on the speed, various braking applications are obtained in electric vehicles to increase driving range. In regenerative braking mode, the fuzzy-PID hybrid controller collaborates to reduce the vehicle's speed, improve system efficiency, and ensure safe charging battery voltage status at desired levels [142]. In electro-mechanical braking mode (EMB), fuzzy logic with SMC is extremely useful in managing the system's non-linearity and uncertain nature. In this case, fuzzy reduces chattering while the SMC achieves the desired drive speed control [143]. Here the state observer is then created to estimate vehicle states like operating speed and directional force while considering both normal and emergency braking conditions. Similarly, handling nonlinearity and unpredictability of motor parameter variations through adaptive PID controller (APIDC) design with fuzzy logic is used to optimize the dynamic performance [148]. Depending on the variations, the membership function is tuned to analyze the steady state, regulation, and motor

TABLE 3. Performance comparisons of intelligent control for BLDC motor in electric vehicles.

Control Strategy Adopted	Torque ripple analysis	Complexity	Robustness	Outcomes	Ref.
Fuzzy-PI controller	T_r=0.007s, T_s=0.007s E_{ss}=5%, M_p=0.9% at T_L=10Nm, 3000rpm	More disruptions problem	Reduced steady-state error & improved steady-state accuracy	Achieved both transient & steady-state performance to maintain speed regulation of motor	[141]
Fuzzy-PID controller	K_P =0.2, K_I = 4, & K_D = 0.04	Challenges in design & implementation	Improve stability & regulation	Efficiently resists the disturbance and continues to track the speed with significant steady-state accuracy	[142]
Fuzzy-SMC	Tracking speed intervals 100r/s at 0.05s,50r/s at 0.1s 0r/s at 0.15s, -50r/s at 0.2s -100r/s at .25s,-150r/s at .3s	Buffeting problem	Speed tracking capability	Improve of speed/torque drive with reduction of chattering effect & adaptive gain adjustment Adaptive drive executing for straight & non-direct loads	[143]
Fuzzy-member ship tuning control	T_L=0.25Nm, E_{ss}=1.2148 T_L=0.5Nm, E_{ss}=1.3248 T_L=0.75Nm, E_{ss}=1.4567 T_L=1Nm, E_{ss}=1.5123% at 3000rpm	Low convergence rate during iterations	Reduced parameter non-linearities & uncertainties when load perturbation	The membership function is set to increase the dynamic performance of the motor based on the fluctuation of motor parameters	[144]
PID supervised online ANFIS	With load condition T_r=0.03s, T_p=0.04s, T_s=0.036s ,T_r=1501.7 rpm M_p=0.1103%, E_{ss}=0.01%	Computational complexity	Accurate speed set tracking	Motor speed regulation efficiency under no load and load conditions Time domain specifications & torque control improved performance	[145]
Fuzzy-PSO algorithm	K_P = 6.5471 & K_I = 3.7717 No. of iteration (PSO)=50	High-dimensional difficulties reduce efficiency	Acquire motor speed control & reduce errors rapidly	Gain tuning of PI controller by PSO algorithm to obtain the speed improvement of EV Motor	[146]
CANFIS	E_{ss}= 0.0015%	No. of membership functions	Improving stability & tracking response	Accomplished positioning & tracking performance without any control delay issues Capable of overcoming issues of non-linearities & uncertainty from motor reference input fluctuations	[147]
Fuzzy adaptive PID controller	T_s=0.041s,T_p=0.041s, N=2997rpm, E_{ss}=3%	Computational complexity	Improving speed regulation	To obtain the motor speed control performance with different load variations & enable good stability and reduced overshoot	[148]
Bat algorithm	$T_{recovery}$=0.2631s, M_p=0%, E_{ss}=0.0641%	convergence rate Reduction	Design controller optimization	Using the BAT algorithm, examine & adjust the tuning of PI parameters to achieve speed control of the motor Capacity to diminish the uncertainty problem arising caused by load variations & set speed variations	[149]
Current control strategy	T_{ripple} reduction T_e=2Nm at 1700rpm	Maximum switching frequency leads to harmonics	Speed tracking error	Employing a fuzzy-based current control strategy to maintain a high stability factor, control torque ripples & regulate motor speed	[150]
Neutrosophic-FLC	K_p=75,K_I=75,K_D=165 T_s=0.005s,E_{ss}=-0.5r/s	Imprecise probability	Reaches the reference speed with less oscillation	It can exert control by compensating for uncertainty and inaccurate data in order to provide a faster settling time and lower steady-state error	[151]
Interval type-2-PID- FLC	$T_{control}$ at above 2000rpm with load deviation at T_e=30Nm	More difficult to understanding	Torque control ability	It addresses motor uncertainty & variations in speed by modifying the PID gain using fuzzy logic It outperforms standard fuzzy logic algorithms for speed control	[152]
Fuzzy-PWM	Total harmonic distortion current (THD_I)=16.15	Implementing fuzzy logic-based control algorithms optimal switching angle offline calculation & storing	Harmonic current removal	Based on a speed & load-dependent fuzzy rule matrix, optimize both the converter switching losses and the machine core and copper losses	[153]
PID parameters tuned by FLC	With load condition Set point 700 T_r=115.79s, T_s=1.99s, M_p=0.21%	Long-term delay is challenging	Leading to enhanced efficiency & torque in EV	Optimize the speed control of motors, resulting in improved performance & responsiveness in real-world driving conditions	[154]

TABLE 3. ***(Continued.)*** **Performance comparisons of intelligent control for BLDC motor in electric vehicles.**

Mamdani's Fuzzy Inference	Accelerating time reduced 3.5% with 0 to 50km/h	Challenges in design & implementation	Formulate rules set	Optimization of the drivetrain control strategy is critical to enhancing the energy economy and performance of EV	[155]
FLC	T_s=0.4s,T_s=1.3s, M_p=0%, Starting torque=0.4Nm	The iterative convergence rate is low	Computation process of PSO	It offers better speed control & torque ripple minimization in a steady state or even at transient conditions, achieving high starting torque with minimum torque ripple	[156]
Variable universe Fuzzy APIDC	Torque control at 1000rpm with optimal values in (λ_1, λ_2)=(0.7912,0.4299), (k_1,k_2)=0.6527,0.2211)	Implementation challenges	Overcomes the shortcomings of long regulation time	Proposes a variable universe fuzzy APDIC system for motor speed regulation that overcomes the issues of significant overshoot & long adjustment time	[157]
PI & Fuzzy - SVPWM	Space vector PWM with T_{ripple}=5 N-m at speed 120rps	DC bus efficiency is Reduced	Oscillations reduction in speed	When paired with PI and fuzzy control, the usage of space vector pulse width modulation (SVPWM) can significantly decrease torque ripples & increase motor performance	[158]
Self-tuned - Fuzzy PID controller	T_r=0.0025s,T_p=0.01s, T_s=0.02s, E_{ss}=0.5328, Speed ripple=0.0003%	An angle control signal is noisy	Fast speed tracking capability	The controller ensures the desired control response at various operating conditions by appropriately switching between PID & STFPID based on speed error	[159]
FLC of high-speed sensorless	T_{ripple} reduction at 15000rpm with sampling time (T_s) 1s after the steady state	Harmonics challenge	Regulate the PWM duty cycle	Based on terminal voltage measurement & is intended to control the speed of a BLDC motor in the presence of various disturbances, such as the loading effect	[160]

output parameters like voltage, current, speed, and torque. Moreover, for better dynamic performance the Fuzzy PID supervisor online uses the adaptive neuro-fuzzy interface system (ANFIS) controller to validate motor effectiveness and performance under all operating conditions with constant loads and different loads with varying set-up speeds [145]. It also analyses the speed response from the time domain specifications, like peak time, rise time and peak overshoot, etc. Regarding, the rotor position, the dynamic behavior of the motor is analyzed through the fuzzy-governed coactive neuro-fuzzy inference system (CANFIS) to obtain a more attractive tracking performance without the chattering effect [147].

It also addresses the issue of nonlinearities and uncertainty caused by changes in the reference input of the BLDC motor. Even though a fuzzy inference system was used to develop a neutrosophic FLC (NFLC) to efficiently implement BLDC motor speed control, it provides better steady-state error and settling time than all other controllers [151]. The FLC system is one that is frequently used to develop the best optimal, effective, and reliable control system for EVs.

D. TORQUE RIPPLE MITIGATION BASED ON CONTROLLING INPUT VOLTAGE

Control input voltage techniques are one of the reliable methods for eliminating torque ripples in BLDC motors when the trapezoidal back-EMF is non-equivalent to the phase current of the stator windings due to the commutation of power inverter switches, as shown in Fig 9. The torque ripples are determined by the back-EMF and current waveform; they're also mainly affected by the current ripple because of the inductances and resistances influenced by the stator windings of the motor.

The current ripple causes PWM- controlled power stages and produces power losses in windings, then eddy current losses in the iron core, because of which the motor gets heated. By this condition reducing the current ripples by controlling the PWM voltage and frequency is obtained from PWM schemes along with power converters.

The PWM scheme comprises two controller stages, the first stage controls the commutation in terms of maintaining the trapezoidal back-EMF (E_b) in phase with the stator phase currents (I_a, I_b, and I_c). This PWM scheme is employed to achieve the new commutation on the basis of reducing current ripples and torque control by motor output parameters like speed (N) and rotor position done by back-EMF (E_b). Here, the actual speed (ω_{act}) of the motor is correlated with the reference speed (ω_{ref}) and its difference error signal in order to obtain the PWM switching stages of the inverter, with this speed control, the BLDC motor's current can also be controlled [171], [172]. The second controller stage uses a power converter (buck converter) to regulate the current amplitude and create the three-phase rectangular current pulse width of 120 degrees with a power inverter. The buck converter is installed between the DC power supply and the inverter's DC-link and depending on the motor speed, the DC-link voltage is modified then it's calculated in equation (30).

$$V_{out} = \frac{D_b}{1 - D_b} V_{in} \tag{30}$$

where, V_{in} is the input source voltage (volts), V_{out} is the output buck converter voltage (volts) and D_b is the duty ratio of the buck converter.

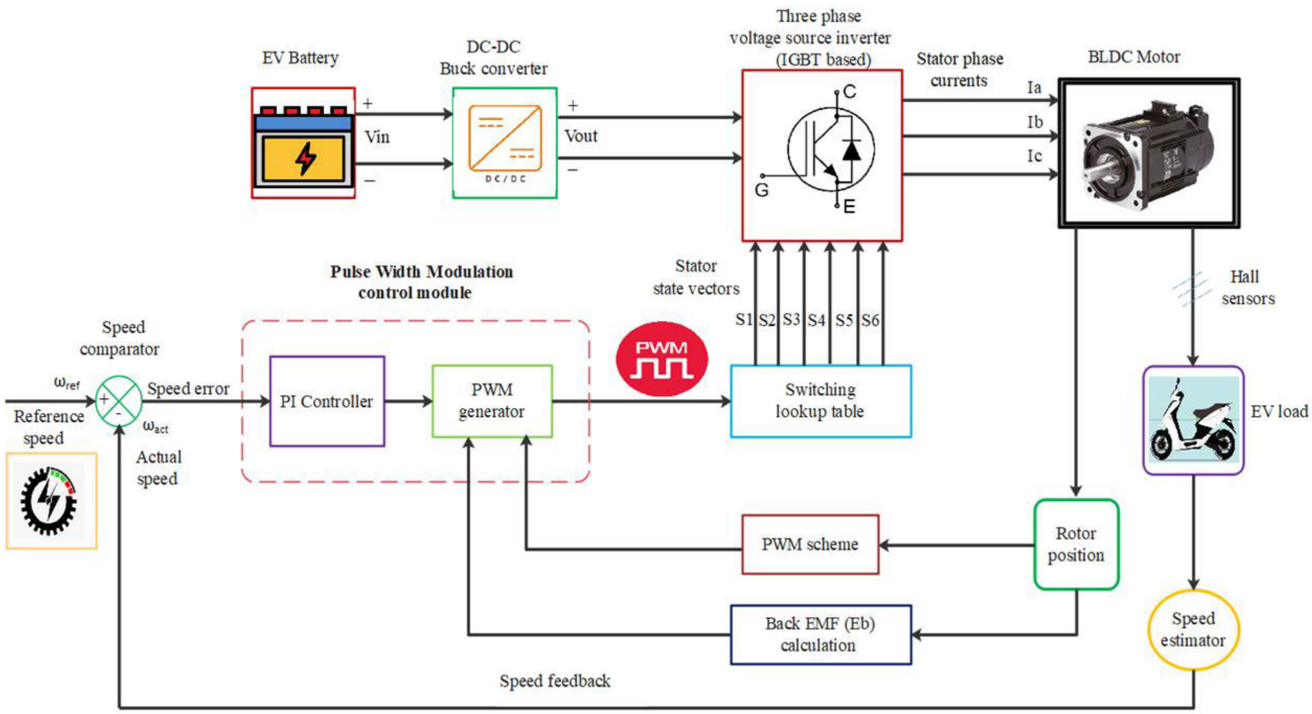

FIGURE 9. Controlling input voltage strategies of torque ripple mitigations in BLDC motor for electric vehicles.

PWM is utilized to control the phase currents of a high-speed BLDC motor and the PWM duty cycle is changed to reduce phase current ripple during commutation. The output of both controllers' stages is combined to produce a new duty cycle and it's compared with high-frequency saw tooth waveform to produce PWM signals in the PWM generator. The commutation current control duty ratios (Dc) are expressed by the equations (31&32).

$$\mathrm{Dc} = 1 \text{ means, } \mathrm{V_m} = \mathrm{V_{in}} \tag{31}$$

$$\mathrm{Dc} = 0 \text{ means, } \mathrm{V_m} = \mathrm{D_b V_{in}} \tag{32}$$

The resulting switching pulses are applied to the inverter's switches in order to energize the winding and control the stator input voltages to suppress the torque ripples and maintain the speed and torque at the specified level [161], [162].

This technique is easy to implement and has a low computational complexity for dynamic performance in EVs. It also reduces torque ripple by varying the input voltage, which also reduces the current ripple. By lowering current spikes in the DC-DC converter output along with the PWM-based technique as well as by using the space vector PWM technique with more vectors, torque ripples in the input voltage technique are now being reduced, as summarized in Table 4.

Here, an electronically switched inverter powered by a DC power supply commutates the currents, and commutations are addressed by rotor position, which can be determined by the position sensor in order to keep the trapezoidal back-EMF in phase with the stator phase currents [166]. Commonly, a DC link voltage controller's (DC-DC converter) PWM duty cycle signal can be changed to vary the motor voltage in order to limit the output signal of the torque controller; in this case, a buck converter is used, which transforms the fixed voltage into a mutable voltage.

To improve the torque controller even further, the DC-DC converter has been modified using PWM techniques to control the duty cycle length of the firing signals, resulting in a controlling speed [172]. Again, here PWM techniques use a cuk converter to increase the three-phase bridge inverter's input voltage and then meet the voltage demand of the commutation period while reducing the torque ripple by maintaining a constant non-commutated current in BLDC motor drives [164]. Moreover, in this PWM scheme, the motor driving system uses a digital controller to control the speed and torque of the motor output along with the duty cycle of the PWM output in low and high states. Because of the reduced torque ripple and improved current waveform, it produces the most average torque with optimal speed response and less overshoot and settling time [171]. In terms of improving the current waveform and achieving a controlled DC voltage from the single-ended primary-inductance converter (SEPIC), it provides effective current ripple suppression during the commutation interval.

E. TORQUE RIPPLE MITIGATION BASED ON CURRENT SHAPING TECHNIQUES

Current shaping techniques are mostly used in BLDC motors for high operating speeds and fast response output with optimal current drive in EVs. This can significantly mitigate the

TABLE 4. Performance comparisons of controlling input voltage for BLDC motor in electric vehicles.

Control Strategy Adopted	Torque ripple analysis	Complexity	Robustness	Outcomes	Ref.
Sensorless drive control	T_{ripple} reduced by controlling the time and degree of compensation	A high requirement of algorithms is needed	Evaluate the commutate compensation	Fast response & no complex calculations Regulating switching time & compensation to reduce torque ripple	[163]
Cuk converter	Motor speed steady at 3000 r/min T_L=(0.11 to 0.23 Nm)	More reactive components are used & High current strains on the switch	Regulating the inverter voltage	PAM technique regulates stator voltage & reduces voltage spikes	[164]
Twelve voltage space vectors with overlap angle control	The optimum overlap angle between (120 deg to150 deg)	Inverter expense and winding losses	Improving DC bus utilization	Increase switching space vector to reduce commutation interval & current	[165]
Single DC current sensor	Commutation compensation delays 50 µs sampling time	Saturation of the controller during commutation times	Compensate unavoidable time delays in systems	The compensation technique reduces CTR by the whole motor speed range with a single sensor Commutation can equalize current slopes during commutation interval	[166]
PR compensator	Stabilization switching frequency =10KHz	Reference signals tuning	Regulating DC link voltage & switching losses in inverter	PR compensator suppresses current ripple to ensure reliability & effectiveness Controlled DC voltage with minimal overshoot & high robustness	[167]
Back-EMF wave shaping	Optimization parameters Coils=156, N=1256rpm, Te=13.68Nm, η=67.72%	A challenge in making winding layers	Make the trapezoidal shape of the back EMF	Modifying winding arrangement can improve motor characteristics	[168]
Reference voltage PWM	20,520 rpm at 5 V 49,200 rpm at 20 V η=80%	Motor controller designing	Reducing inefficient tail current by using PWM	High switching frequency & regulated phase current reduce torque ripple	[169]
Neoteric PWM-ON-PWM buck converter	T_{ripple} reduction T_L= 2Nm ,M_p=0% for 1000 rpm	A significant amount of power is lost due to resistance in the converter	Compensating torque ripples during the conduction period	Combination of buck converter & inverter to compensate for CTR during the commutation period & partially removes torque ripples resulting from current introducing in the turn-off phase	[170]
Digital PWM	$N_{response}$=1ms $T_{settling}$=2ms M_p=10%, N_{ripple}= 5.7%	Speed ripple, throughout the steady state	More average torque can be produced via a better current waveform	Digital controller allows for maximum torque, speed response & less overshoot	[171]
Varying input voltage	Vin = 180 V N= 6660 rpm T_{ripple} reduction=10%	Complex calculations	Rapid response to torque fluctuations	Laplace transforms are used to regulate input voltage to reduce current ripple Maintain a constant current in the freewheel region	[172]

torque ripples when the motor is caused by non-ideal trapezoidal back-EMF due to insufficient commutation, [173], [174] as shown in Fig 10. Because of this effect. phase current distortion and excitation of torque ripples in terms of current harmonics are happening in the motor. During this effect, the stator current is commutated from one phase to another very transiently without a commutation interval period, resulting in the electromagnetic fluctuations produced by the commutation torque ripple in the motor. In BLDC motors, a perfect trapezoidal back-EMF waveform is needed; however, the spiking phenomenon of current and the negative impact of harmonic components produced in the motor causes mechanical vibration, and acoustic noise, and reduce overall life performance and efficiency [175], [176], [177].

This current shaping method is a popular one to obtain an exact commutation point and optimal torque control of a BLDC motor drive for an EV. Also using this method to suppress the torque ripples in the motor in two ways, likewise, using the current sensor and charged capacitor in electric drive. In first known way to determine the exact commutation interval from the terminal voltage of stator phase windings and reduce the commutation ripple by using a current sensor is to flow out-of-phase current information as feedback to motor drive control and improve motor performance. Here the current is controlled by regulating the terminal voltage, which is obtained using current hysteresis control (CHC) [178], [179], [180].

CHC is most widely used to control a current-controlled voltage source inverter and determines the switching states

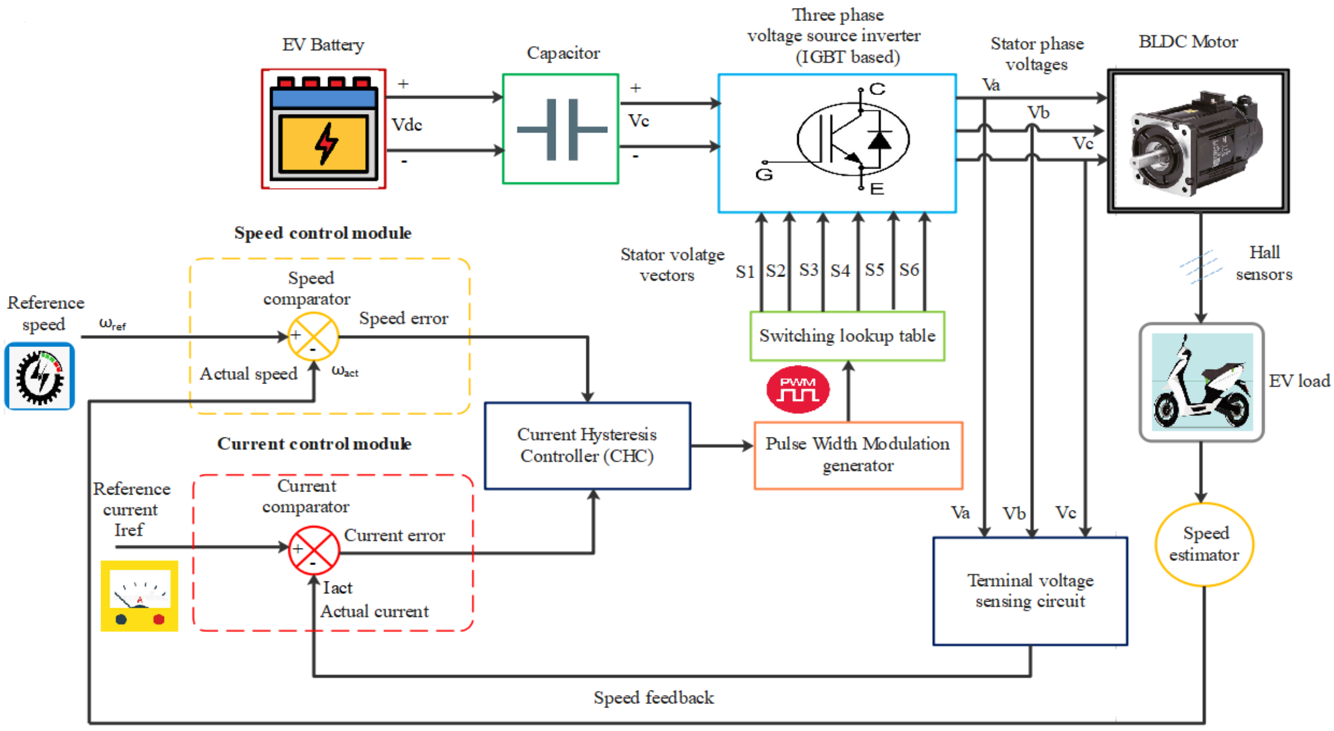

FIGURE 10. **Current shaping techniques strategies of torque ripple mitigations in BLDC motor for electric vehicles.**

given motor output parameters like rotor-sensing current (I_{act}) and speed(ω).

The switching states of the inverter are mostly implemented by modifying the duty cycle of the PWM in order to eliminate phase current ripple during commutation. It is expressed in equation (33),

$$V_{dc} = \frac{D}{1-D} V_{in} \tag{33}$$

where, V_{in} is input source voltage(volts), V_{dc} is output DC link voltage(volts) and D is the duty ratio of the controller.

In a second way, charged capacitors are added to a voltage source that is inverter-controlled to deliver a more steady DC voltage while limiting variations due to the inverter's irregularly high current demands, and is also used to step up the voltage during the commutation period [181], [182]. It's described in equations (34,35 & 36),

$$V_{in} = 4E_b \text{ (In ideal condition)} \tag{34}$$

$$V_{in} > 4E_b \text{ (In low-speed condition)} \tag{35}$$

$$V_{in} < 4E_b \text{ (In high-speed condition)} \tag{36}$$

This technique is one of the predictive current controllers that analyses the various switching logic levels to provide adequate powered low-voltage DC current to various components used in EVs. This technique employs various operations to change the switching vectors to regulate non-commutation phase current and efficiently mitigate CTR in low-and high-speed applications, as summarized in Table 5. To regulate the electromagnetic torque in terms of CTR, the non-commutating current is directly controlled using current hysteresis control (CHC), and its function is obtained by employing various PWM techniques and an adjustable DC-DC converter to maintain a dc-link voltage with constant voltage [190]. In addition, CHC has unconditional stability, is insensitive to system parameters, has a fast response time, is simple to implement, has a low CTR, and responds quickly to transients that occur during insufficient commutation. In terms of commutation control, self-commutation is used to keep the rotor's rotation in sync with the rotary field velocity on the BLDC motor stator, as well as its combination with fuzzy controllers to improve steady performance and more effectively control current strategies to reduce commutation torque control [188]. For more improvement in motor current control, switching vectors are combined with a diode-assisted inverter to suppress CTR and motor speed regulation during both the commutation and normal conduction periods.

This method effectively controls insufficient commutation across the entire speed range by employing unified switching vectors during the commutation period, and it can be developed to prevent increasing the voltage stress in inverter bridge switching devices [183]. Although achieving a smooth CTR with a fast response is relatively difficult, this is typically based on the varied fast switching rate line current during the commutation period. For this reason, it is necessary to maintain constant incoming and outgoing current phase rates throughout the commutation period for the hysteresis-based field programmable gate array (FPGA) controller to function during both the conduction and commutation intervals [184].

TABLE 5. Performance comparisons of current shaping techniques for BLDC motor in electric vehicles.

Control Strategy Adopted	Torque ripple analysis	Complexity	Robustness	Outcomes	Ref.
Diode-assisted buck-boost inverter	200 to 600 r/min for T_L = 3.2 Nm	High inverter DC link voltage is required for design parameters	Suppressing CTR's entire speed range	Reduce switching components to reduce power dissipation & torque ripples	[183]
FPGA-based current control	T_{ripple} reduction=8.6% at T_L =0.25 Nm T_{ripple} reduction=11.5% at T_L =2 Nm	Undesirable harmonics are caused by high switching frequency	Current loop & inherent-peak current limiting capability in CHC	Maintaining slew rate of incoming/outgoing current in conduction/commutation interval FGPA controller improves speed, reliability & power efficiency	[184]
IDO converter	T_{ripple} reduction=4.99% at 100 rpm T_{ripple} reduction=16.2% at 1000 rpm	The system's bulk & complexity are increased by system components	Capable of obtaining the essential voltage during conduction & commutation times	Motor torque can be improved by obtaining optimal voltage quickly	[185]
PWM-ON-PWM	Control pulse on Duty cycle=0.4 at t_{comm}=0.0013s	Power switching losses during commutation	Preventing CTR across the full-speed range	Preserve optimal commutation period to reduce CTR Control system without torque ripple at both low & high speeds	[186]
Braking PWM technique	$T_{braking}$=(−0.2T_N to −T_N) 1.7 ms in 600 r/min & 1.9 ms in 300 r/min	Switching sequence changes during braking	Duty cycle calculation for braking operation	Reduce CTR effectively & maintain braking torque with superior dynamic performance	[187]
Self-commutation technique	T_{ripple} = 0.1520 Nm at T_{ss}=0.8s	Computational complexity	A combination of a logic commutation circuit & PWM	A hybrid combination maintains synchronization between rotor position & field velocity Improves steady state performance to reduce CTR	[188]
Improved PWM-OFF-PWM	Don = 0.77ms& Doff = 0.03ms	A challenge in maintaining turn-off time less than the turn-on time	Reduction of fluctuation from non-commutation current	It improves system stability in terms of controlling non-commutating current in commutation intervals to reduce CTR at low speed	[189]
Multimode CHC	Torque signal control at frequency (0-2500Hz),0.1% linearity deviation	The transition & communication process is complex	Rapid speed tracking	Easy implementation, low CTR & quick response Multimode operation to minimize CTR with proper commutation	[190]
Three-segment modulation	T_L=0.75 Nm at d1=1, d2=0.5, Nc =11	Undesirable for the motor's smooth operation.	Maintaining current slew rates in switching phases	Divide the PWM period into three segments to reduce CTR Commutation speed is controlled to reduce commutation time	[191]
Current controlled SVPWM	T_{ripple} =12% at T_L = (0.88 to 0.78Nm)	Switching configurations	Inverter switching loss reduction	Motor current slew rates can be adjusted to reduce torque & current ripple	[192]
PWM compensation	I_{ripple} reduction=23% at N=500 to1000 (r/min)	A wider commutation region is necessary	Optimizing inverter switching stress & current regulation	Selecting the right PWM duty ratio can reduce switching loss & torque ripple	[193]
Adaptive soft start-up control	Torque error reduced at 10 electrical degrees under 800 rpm	Switching losses	Reduced excess start-up current	Adaptive ramping current profile provides stable start-up in different load situations	[194]
BLDC motor drive with minimized dc-link capacitor	Torque control at 50µs period of time base & 2000 µs period of reable signal	Keeping the capacitor temperature stable	Reduce the fluctuation in phase current	Maintain current & safeguard VSI for current limit strategies Reduces temperature rise in capacitor by reducing voltage ripple	[195]
One-cycle average torque control	T_L= (0 to 1.5 Nm) at 20% rated speed	More harmonics components	Keeping the real input energy consistent during each control cycle	One-cycle control reduces torque ripple in electric machine drive systems	[196]

Here, the FPGA controller generates control pulse signals to regulate the stator current, and in comparison, to other digital implementation methods, it improves speed, reliability, power efficiency, simplicity, and low cost. Similarly, control the stator phase current in the reverse direction during the braking operation; as a result, the CTR can be reduced in the speed range from the rated speed to zero using only common braking PWM strategies, and the braking torque can be maintained with superior dynamic performance [187].

To improve braking even further, the PWM-OFF-PWM method can reduce non-commutation torque ripple caused by non-conductive freewheeling and address the CTR generated by the turn-off time being shorter than the turn-on time. Controlling the PWM duty periods to the non-commutation current in the commutation interval will make the system more stable in terms of reduced CTR at low speeds and prevent an increase in the power dissipation on the switching devices in the inverter [189].

F. TORQUE RIPPLE MITIGATION BASED ON MODEL PREDICTIVE CONTROL TECHNIQUES

The Model predictive control (MPC) is the most popular and has been extensively implemented in BLDC motors due to its simple control architecture and improved output [197]. It is a feedback control technique that employs a system to predict future outputs of a motor drive in an EV in order to manage complex dynamics, handle multiple input and multiple output systems, and deal with constraints in a systematic manner [198]. The MPC approach regulates electromagnetic torque by considering possible future states for all available voltage levels, as shown in Fig 11. It can solve the problems of commutated phase current control by eliminating complicated current controllers, suppressing the commutation torque ripple over the full range speed, and then providing good steady-state performance while maintaining a fast dynamic response [208]. This technique consists of two main loops, called the inner and outer control loops, respectively, the current control loop, performed as the inner loop depending on a hysteresis controller, regulates the BLDC phase currents, while the speed control loop, performed as the outer loop, is designed using MPC to regulate the motor speed in accurately and rapidly [212].

The non-commuting currents obtained from the MPC controller are described as equations (37,38 & 39),

$$I_{dnon-comm}(K+1) = I_d(k) + \frac{dt}{L} * (V_d(k)(R^* I_d(k) + (\omega(k)^* L^* I_q(k))) \quad (37)$$

$$I_{qnon-comm}(K+1) = I_q(k) + \frac{dt}{L} * (V_q(k)(R^* I_q(k) + (\omega(k)^* L^* I_d(k))) \quad (38)$$

$$I_{non-comm}(k+1) = I_{dnon-comm}(k+1) + I_{qnon-comm}(k+1) \quad (39)$$

where, $I_{q(k)}$ & $I_{d(k)}$ are quadrature and direct current in K^{th} time, $V_{q(k)}$ & $V_{d(k)}$ are quadrature and direct voltage in K^{th} time, R, L are resistance (ohm), the inductance of motor (henry), & $\omega(k)$ is the speed in k^{th} time (rad/sec).

To achieve the desired control effect, the current control loop bandwidth must be high while the speed control loop bandwidth must be low. Depending on HCC, the stator phase currents are governed by a defined switching frequency by effectively generating the switching pulse commands to three-phase voltage source inverters based on the rotor position information [159]. Here, PID controllers are used to generate the reference current (I_{qref}) to control the speed and the reference current (I_{dref}) is zero in accordance with the speed error [199]. The MPC uses the cost function (CF) to calculate the future control signals to achieve the optimum reference tracking performance by comparing reference and predicted currents.

The objective function expands as the difference between the reference ($I_{ref(k+1)}$) and predicted non-commutated currents ($I_{non-comm(k+1)}$) develops, therefore it is possible to use the simple sum of errors of the currents in d and q as the target function. However, the sum of squared errors is preferred for extensive tracking.

The cost function is described as equation (40),

$$CF = I_{qref}(k+1) - I_{qnon-comm}(k+1) + I_{dref}(k+1) - I_{dnon-comm}(k+1) \quad (40)$$

where, $I_{qref}(k+1)$& $I_{dref}(k+1)$ are the output of the speed loop (reference quadrature and direct current), $I_{qnon-comm}$ (k+1)& $I_{dnon-comm}$ (k+1) are the output of the current loop predictive value of non-commutated phase current during commutation (non-commutated quadrature & direct current) and k+1 is the $(k+1)^{th}$ sampling time.

It is the best model-based method for predicting the future behavior of a system over a specific time horizon. According to the predefined cost function, the optimal switching state is directly selected and applied during the next sampling period, to maintain a constant non-commutated stator phase current during commutation and efficiently minimize commutation torque ripples [200], [201]. For a BLDC motor, the Model predictive controller provides each of the three-phase primary voltages required to exactly follow the reference path, in order to ensure the future output error is equal to zero by minimizing the cost function value.

This MPC approach is an advance over conventional control methods in that it can effectively mitigate torque ripples and current ripples without affecting the dynamic performance of a BLDC motor to simulate the loading effects on the driver motor of the EV.

This scheme is proposed to provide a popular solution in motor drive and achieve faster dynamic performance with EV controllers. MPC can now be combined with diverse control concepts to create an adaptable controller design that regulates electromagnetic torque at desired voltage levels, as summarized in Table 6. Most commonly, MPC controllers use two control loop modules to mitigate torque ripples in different speed conditions via the current and speed loop modules. As specified by the current module, the model predictive deadbeat current controller (DBCC) employs the motor model to generate reference voltage for state vec-

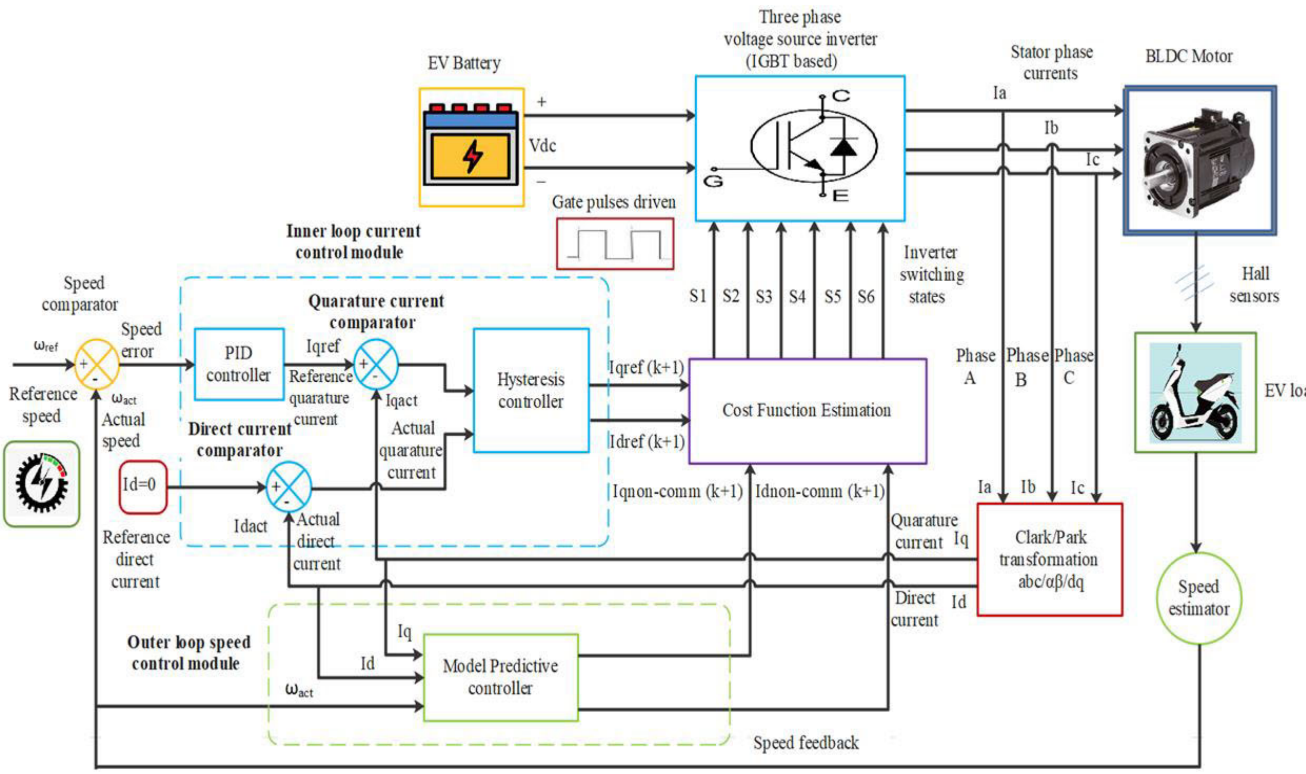

FIGURE 11. **Model predictive control strategies of torque ripple mitigations in BLDC motor for electric vehicles.**

tor PWM during commutation to minimize torque ripples [210], [213]. During the commutation period, the MPC generates the desired current and operates the electric vehicle in constant torque ranges. Besides, it performs admirably in both high and low-speed operations, reducing current and torque ripple while maintaining average torque at its rated value. Similarly, MPC in association with an SMC functions as a current loop to control overcurrent constraints in the motor and enhance its ability to reduce load torque uncertainties [203].

Also, it is used to limit tracking error, peak time, and transient response, and improve stability of motor variables. Additionally, a current control loop has been developed by using of finite control set MPC (FCS-MPC) to handle harmonic current injections, provide the appropriate switching states in terms of the cost function, and obtain the smooth torque [214]. It can reduce machine power dissipation, provide high transient output, and easily incorporate nonlinearities and constraints into controller design. Although this current control scheme does not require any modulators, it significantly reduces implementation complexity, especially in multiphase systems. As specified by the speed module, an NMPC technique has been suggested for the speed control of constrained nonlinear lightweight electric vehicles due to its energy-efficient performance [219]. The proposed NMPC can be further developed for real-time implementation with goals such as torque ripple reduction, loss minimization, controlled degradation, etc. Furthermore, these techniques address the issue of over-excitation in EV applications to reduce the machine's overall energy consumption, thereby increasing the vehicle's driving range. Moreover, an adaptive MPC (AMPC) is used to estimate speed and power demand using a global positioning system (GPS) and to provide control torque to electric vehicles using optimization algorithms [218].

It is much more capable of dealing with constraints by using an open-loop optimization and closed-loop feedback system 28 to continuously evaluate and upgrade the vehicle mass in real time. Even now, MPC uses a deep learning artificial neural network (DLANN) algorithm to control the motor's speed and torque, additionally providing a more robust, simple, and effective operation with less settling time [204]. Again, for future development, the MPC coupled with the PWM method can effectively reduce current and torque ripples at lower or higher speeds without changing the circuit topology [210]. This PWM-MPC control method achieves constant current of the conducted phases during non-commutation and constant non-commutation current during commutation in the full speed range by estimating the PWM duty ratio. In this case, new MPC techniques are used to predict the value of electromagnetic torque and non-commutating current by selecting an appropriate PWM duty ratio that efficiently controls the non-commutating current to reduce CTR. Currently, MPC techniques are used

TABLE 6. Performance comparisons of model predictive control for BLDC motor in electric vehicles.

Control Strategy Adopted	Speed/ Current control	Torque ripple analysis	Complexity	Robustness	Outcomes	Ref.
Model predictive direct power control	Both	Start ramps up to 600 rpm, ramps up to 800 rpm at 0.15 s	Evaluating the duty cycle of a non-zero vector in addition	Ripples in both the torque & the phase current reduced	Duty cycle control algorithm used to reduce errors in complex power T_{ripple} minimization can be improved by reducing computational overhead	[202]
SMC	Both	Control horizon=10 Prediction horizon=20 Weight matrix=1	In low inertial devices, identical time constants prevent dynamic behaviour	Ensuring reliability & feasibility of constraints	The dual loop algorithm reduces uncertainty, tracking error, rise time & stability	[203]
DLANN	Speed	T_L changes Nm at 50 s N_r changes at 25 s	Optimization process & data complexity	Solves non-linearity, parameter variations	It provides a robust, easy implementation & effective operation	[204]
Fault-tolerant MPC	Current	Change in torque=2.3% Change in flux=4% THD=12.10% T_s= 4.6 s for 400r/min	Increased control structure complexity deteriorates the steady-state performance	Maintains load disturbance adaptability	Limit measurement noise & predict stator phase current to compute voltages	[205]
Hybrid intelligent predictive control system	Speed	Offline system training yielded accurate dynamics for adaptive motion control	Challenging high computational burden & complex interpretation	Differentiates fault & normal currents	Imitating electrical failures quickly with no harmonics	[206]
Quadratic programming - MPC	Both	Solve QP in MPC=30ms Average error=3.2684% Overshoot=8 %	Sensor noise may cause poor load motor current	Handles input saturation & solves QP in 30ms	EV test simulator can handle input saturation & regulate motor accurately	[207]
Finite-state MPC	Current	Sample frequency=40 kHz	Commutation without PWM duty ratio computation	Matches rising & falling currents in dynamic processes	Reduces CTR by avoiding complex current controllers	[208]
FCS-predictive direct power control	Current	Sample frequency=10 kHz at 1000 rpm T_0 = 100µs	High BW controllers are necessary to reduce torque ripple frequencies & ensure proper input voltages	Regulates the power exchange between the stator and rotor	Reduce computing cost & complexity to optimize control signal	[209]
PWM	Current	T_{ripple} reduction 11.5% at 500rpm 9.04% at 1500rpm	A complex H/W circuit is necessary to increase the slot rate of the outgoing phase current during commutation	Reduces current fluctuation & torque ripple with duty ratio	Reduce torque ripple effectively without modifying circuit design Prevents current surges during the commutation period	[210]
Direct torque control – multi-phase FCS	Current	DC-link voltage = 24 V Switching frequency=20 kHz Motor speed = 50 rpm	Performance is influenced by parameter uncertainty	Resilience of the inverter to nonlinearity & non-ideal model parameters	VSI can detect open and & short circuit defects as well as tolerate transients	[211]
Four-switch inverter-fed drives	Both	Control horizon=1 Prediction horizon=2 Weight matrix=0.7 T_s= 100µ s (5% of steady state value)	The microcontroller developed to calculate time weight is complex	Obtaining quasi-square current waveforms by selecting voltage vectors from a look-up table	It reduces capital cost & optimizes speed transient response	[212]
DBCC	Current	T_{avg} near the nominal value & the ripple within 25%	Complex analytical problems increase controller complexity	Ensure the current aligns with the reference current	Operate EV in constant torque range to reduce torque & current ripples	[213]
FCS-MPC	Current	T_s = 25 µs $Torque_{ref}$ = 500 r/min at $Torque_{Load}$ = 2 Nm	The fourth leg enhances the control complexity by increasing the number of gating signals	Constraints in controller design & rapid dynamic response with the inclusion of nonlinearities	Power dissipation reduced, dynamic output provided, smooth torque operation	[214]
Takagi–Sugeno fuzzy systems	Speed	SSE=1.0019 MAE=0.0055 MSE=0.05011	Low-gain controller originated for actuator-saturated T-S fuzzy systems	Constructing a stabilizing controller against system parameters	Provides robust outcomes in EV operational conditions with less computational complexity	[215]

TABLE 6. ***(Continued.)*** **Performance comparisons of model predictive control for BLDC motor in electric vehicles.**

Fault-tolerant MPC	Current	Under defective conditions, achieving smooth & sufficient high-torque	Current steady-state error cannot to be zero due to the lack of an integrator	Select appropriate actuation & optimize predefined criterion	Predicting stator current & measuring voltages to reduce current errors	[216]
New MPC	Current	Load Torque Tracking 15N.m at t=0.2s 7.5N.m at t=0.5s	Prediction of non-commutating current	Fast transient is to track load torque	Control non-commutating current with minimal CTR & reference current tracking	[217]
Adaptive MPC	Speed	Control horizon=3 Prediction horizon=10 Weight matrix=10^{-5} T_s= 0.01s	Traction controllers are challenges of numerical stability	Proposes the driver with excellent traction	It can handle constraints & solve numerical stability issues in real time	[218]
Nonlinear MPC	Both	NISE=0.0132 NIAE=0.512 Control input power=214.154	Challenge to solve their convex linear equivalents	Controller against the changes in system parameter constraints	Reduce torque per current pulse without impacting dynamic response	[219]
Inbuilt stator current control	Current	Torque ripple control by reducing high switching harmonics	Challenging to produce quasi-square wave currents	Neglecting the phase over the current	The current controller equalizes all phase currents & prevents over-currents	[220]
Phase modulated MPC	Current	T_{ripple}=22% at 8 KHZ T_{ripple}=29% at 4KHZ T_{ripple}=36% at 2 KHZ	Constant switching frequency	Improving the switching frequency	Reduces surges of stator current & equalizes incoming/outgoing currents	[221]
MPC-four quadrant	Speed	Reduced torque ripple at the time of 0.025s	Difficult to act on input voltage oscillations & mechanical interruptions	Handling unknown dynamics	Four quadrants operated to achieve high speed, long lifespan, low noise & efficiency	[222]
Multi-model-based predictive controller	Speed	T_s = 1 ms	Exhibit transient current peak behaviour	Faster control tune capability	Multimode operation provides better dynamic performance & precise control tunings	[223]

in EVs to enhance fast torque generation, steady-state, and dynamic performance along with vehicle performance. However, in terms of computational burden, EVs are the main issue with MPC, but this burden is alleviated by various advanced techniques such as artificial neural networks (ANN) and machine learning (ML) algorithms, among others.

G. TORQUE RIPPLE MITIGATION BASED ON SLIDING MODE CONTROL TECHNIQUES

The sliding mode controller (SMC) presents a robust control strategy for dealing with nonlinear BLDC motor states and parameter uncertainty, assuring system stability and flexibility. This strong and versatile technology is gaining popularity because to its ability to handle the complex terrain of electric motors in electric vehicles [EV]. The design and development of the SMC for managing the speed dynamics of the BLDC motor is a challenging exploration inside this environment. The SMC approach efficiently reduces commutation torque ripple (CTR) over the whole speed range and achieves good performance in both dynamic and steady-state modes by effectively switching the power inverter's three conduction states during commutation [224], [225], [226], as shown in Fig 12.

The procedure begins with two critical steps, each of which is part of the complicated control system: as a design of sliding surface and as a selection of control law. The first step design a sliding surface to make sure the system meets the necessary design constraints. An essential part of the control strategy, the sliding surface controls how the system's states evolve while it is in operation. During the procedure, the Hall effect estimator serves two primary operations. It estimates the rotor's position and serves as a communication switch with the inverter. It also assesses the BLDCM's actual speed by determining the difference between the desired and measured speeds. Here speed error(e) is introduced in equation (41),

$$e = \omega_{ref} - \omega_{act} \tag{41}$$

where, N_{ref} and N_{act} are the respective reference torque and the actual torque is developed by motor and e is the torque error. Establishing a straight-line switching surface in terms of speed error(e), its derivative is given as equation (42),

$$\sigma = e + C\frac{de}{dt} \tag{42}$$

where, $C > 0$ is a strictly positive real constant $\frac{de}{dt}$ is the speed error at K^{th} sampling interval.

The second step is to choose a suitable control law (U) that ensures the system's state is drawn to the sliding surface. The control input (U) is defined by the equation (43) below as,

$$U = -K\,\text{sign}(s) \tag{43}$$

TABLE 7. Performance comparisons of sliding mode control for BLDC motor in electric vehicles.

Control Strategy Adopted	Torque ripple analysis	Complexity	Robustness	Outcomes	Ref.
SMC-Fuzzy	T_r=4ms, M_p=0%, T_s=4ms, Speed variation in sudden load=0%	Buffeting issue	Proper tuning controller gain to reduce the max overshoot & settling time	Improved the motor's performance while loaded, reducing speed fluctuation when the reference speed or load changed suddenly It addresses the critical issue of speed control in BLDC motors, which have a large speed range	[229]
Adaptive SMC	Parameter optimize values α= 78.31, β=54.67, γ=72.95, δ=58.29 T_s=0.291s,	Low convergence accuracy & lagging search speed algorithm	Robust ability to withstand a variation in the parameters & load	Two cascaded SMCs are used to control the drive's inner loop current & outer loop speed while taking the exponential reaching law into account Based on the tuning of sliding mode surface parameters, which improves the dynamic control of the motor	[230]
Adaptive Fuzzy SMC	T_r=0.0058s, M_p=0%	Control gain never lessens	Tolerance to parameter uncertainty along with external disturbances	For effective speed regulation of BLDC motor in the absence & presence of external load Improve the BLDC motor's performance in terms of settling time, steady-state error, rising time, disturbance & noise rejection	[231]
SMC-FOC	N_{ref}=170, Tripple=0.316% N_{ref}=110, Tripple=0.340% N_{ref}=280, Tripple=0.462%	The current dynamic response is slow	Speed tracking response	Eliminates the overshoot present in traditional FOC and reduces torque ripples by 5.84% compared to FOC, making it competitive in EV applications	[232]
SMC-Hysteresis	T_r=11.23ms, M_p=0.51%, T_s=14.38ms, T=0.31Nm, $I_{transient}$= 1.5A, $I_{steady\ state}$= 1A	High switching frequency, resulting in undesirable harmonics	Ability to track the reference signal with a reasonable response time even when motor parameters were changed	This solution is able to mitigate modeling errors and external disturbances, making it suitable for applications with variations in environmental conditions	[233]
Integral time-SMC	THD_i=0.271A, $T_{ripple\ factor}$=0.10% T_r=1.2s, T_f=1.3s	Multidimensional derivatives	Absorption against variations in R_s and L_s	Ability to inject arbitrary reference current to the motor windings without the need to transfer motor currents to the rotational reference frame	[234]
RBFNN-SMC	at 2000 rpm & t=0-4s T_r=0.156s, T_s=0.234s, M_p=1.07%	Require sufficient radial basis function input space coverage	Enhances the system's ability to recover quickly	It showed better transient specification to improve the recovery time when an external load was added to the system.	[235]
SMC-SMO	at speed 3000 r/min T_{ripple}= 0.003%	Chattering effect	A sequential approach to problem-solving	SMO is used to estimate the rotor speed & position using the terminal voltages & currents of the BLDC motor SMC eliminates the derivative of the sliding variable for speed control, simplifying the control scheme while preserving its benefits	[236]
SMC-MPC	$N_{Steady\ state}$= 200rad/s, T_{load}= 6-10Nm at t=0.2s	Low inertial devices restrict dynamic behaviour	MTPA (Maximum torque per ampere) control to improve the system	Uses a current predictive model of BLDCM in discrete steps & a cost function considering torque current tracking and MTPA operation to select the optimal voltage vector for motor control	[237]

where, U is control input, k is the constant parameter, s is the switching function, sign(s) is sign function of switching

The above equation describes the differences from the desirable condition. If the sliding surface is reached and maintained, then $\sigma = 0$. The speed error-switching surface is a straight line in the phase plane. The simplest control input to achieve $\sigma = 0$ using equivalent control are described in equations (44 & 45),

$$U = -1 \text{ for } \sigma > 0 \tag{44}$$

$$U = +1 \text{ for } \sigma < 0 \tag{45}$$

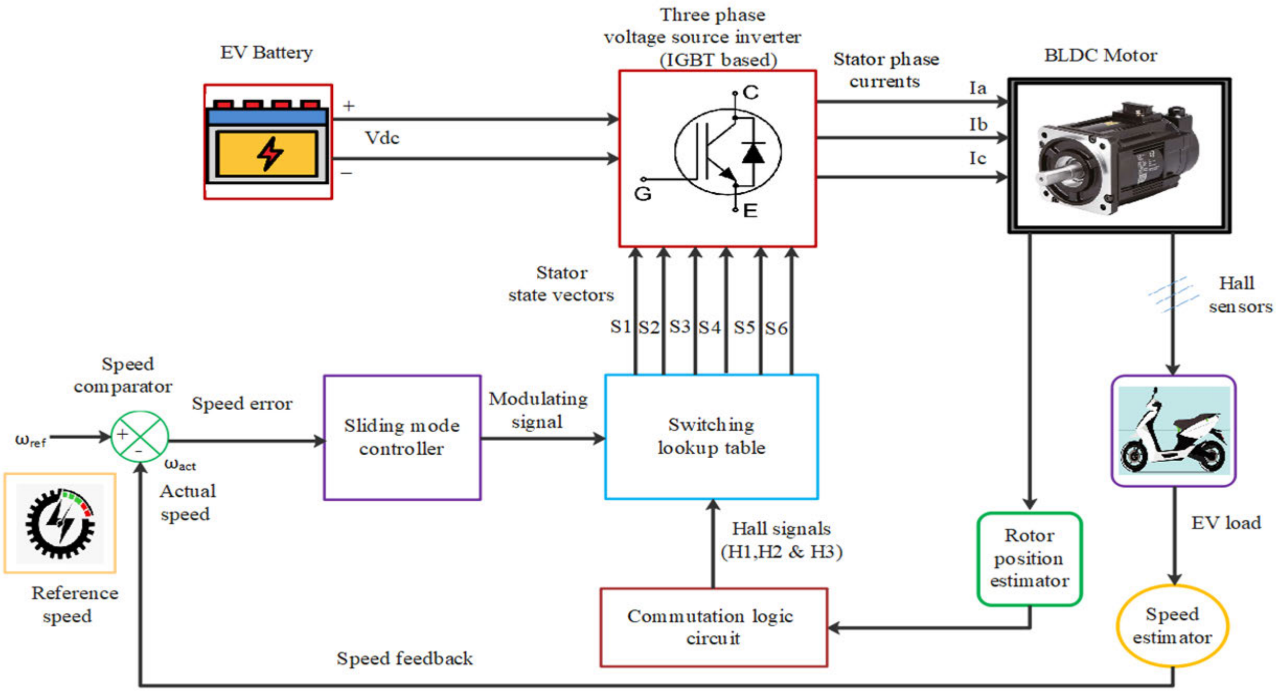

FIGURE 12. Sliding mode control strategies of torque ripple mitigations in BLDC motor for electric vehicles.

According to the error in the current and the error in the rotor speed, the sliding surface (σ) can be changed to a straight line in the phase plane. Here, the real speed is compared to the reference speed by the SMC controller and is capable of maintaining stable operation while precisely tracking desired set points. In this context, SMC maintains constant electromagnetic torque, effectively eliminating commutation torque ripples that are mainly based on stator switching vectors of the three-phase inverter by commutation logic circuit [227], [228].

This algorithm is implemented to drive the BLDC motor with efficient torque control, which is growing popularity in EVs, and it efficiently handles torque ripples, enabling smooth cornering and increased vehicle performance, also the vehicle tracks the input speed and provides the control system's reliability. SMC is currently compatible with a variety of control principles to produce a flexible controller design that manages speed and electromagnetic torque at predetermined voltage levels, as summarized in Table 6. The SMC controller is most typically used alongside the intelligence of a fuzzy inference system to address the critical issue of speed control in BLDC motors, which have a wide range of speed capabilities [229]. Fuzzy SMC (FSMC) eliminates peak overshoot, reduces rise time, and reduces settling time compared to the conventional controller. The use of cascaded sliding mode controllers for inner loop current control and outer loop speed control can improve the performance of the BLDC motor drive system [230].

This can result in more precise control of the motor's speed and current, which is beneficial in applications where accurate control is required in EVs. Furthermore, adaptive fuzzy SMC techniques increase the speed regulation of BLDCM in the absence and presence of external load, improving system parameters such as settling time, steady-state error, rising time, and disturbance and noise rejection [231]. Similar to this, SMC operates senselessly and employs a higher-order sliding mode observer (HOSMO), mostly for speed and position estimates. It is suitable for electric vehicle (EV) applications because it produces consistent results with low estimation error, improved speed tracking efficiency, and minimal torque ripples [232], [236].

In addition, the Hysteresis controller and SMC work together to improve motor current control, it can track the reference signal with a reasonable response time even when the motor's parameters are changed, and SMC does not need any additional sensors for current measurement [233]. To further protect the BLDC motor from torque ripples, an integral time SMC is used, allowing the system states to achieve the equilibrium point in finite time and eliminating chattering with its higher dynamic response and robustness operation [234]. Similarly, using an SMO with RBFNN (Radial Basis Function Neural Network) increases the motor control system's transient specification, making it more responsive to changes in load conditions and improving the overall reliability of the control system [235].

VII. COMPARISONS OF VARIOUS TORQUE RIPPLE CONTROL MITIGATION STRATEGIES IN BLDC MOTOR

The basic control characteristics of all controllers are examined and contrasted to define the nature of the control strategies, and also investigate their impact on drive performance (in steady state & and transient state) with implementation complexity, as shown in Fig 13 (a).

Also, discussed are the advantages and disadvantages of various control strategies for mitigation of torque ripples in BLDC motors, as shown in Fig 13 (b). Advanced control methods are investigated to overcome the complexity of the coordinate transformation, which requires knowledge of the rotor orientation and thus the machine parameters. FOC is not robust against parameter variations, such as stator and rotor resistance being more influenced by temperature, which causes estimation errors and has a negative impact on control accuracy. To avoid coordinate transformation and create a control strategy that is independent of the machine parameters, DTC has been developed. In contrast to FOC, flux, and torque can be directly controlled by adjusting the inverter switching states. DTC is further improved by combining the PWM technology concept used in FOC with DTC to reduce torque ripples without the need for coordinate transformation [238], [239]. DTC is a good alternative to FOC because it has better dynamic performance and a simpler control strategy without knowing the rotor orientation. In most applications, FOC and DTC methods are adequate. However, with the advancement of digital signal processing (DSP) and FPGAs, more research into nonlinear controls has been conducted [240]. Moreover, to provide an accurate evaluation of the performance of the two control schemes, the average switching frequency must be approximately the same. In terms of steady-state performance based on current ripples, the amplitude of the torque ripple in DTC is slightly higher than that of FOC, because of the same average switching and good high-order harmonic suppression effect; as a result, FOC continues to hold the leading position in the field of EVs [241].

According to rotor speed-based transient state performance, DTC has a better torque response in terms of settling time and overshoot, whereas FOC has a longer settling time. Likely, intelligent controllers are thought to provide good control performance for further improvement of time domain specifications to obtain an optimal, effective, and reliable BLDC motor control system. Which has numerous advantages, including reduced overshoot, reduced speed errors, and increased control precision. In this case, if an FLC is used to regulate speed and deliver high performance, then torque ripple could be reduced by increasing the membership functions used in torque and flux fuzzification. The fuzzy-based PID controller provides better and more stable performance than the conventional FOC, along with PI control, reduced speed fluctuation, torque stability, and good control performance. For more enhanced control performance, employ DC-DC choppers to regulate PWM schemes and describe a technique for reducing torque ripple by controlling the input voltage to minimize current ripple and maintain a constant current in the freewheel region [242]. Here digital controllers are used to control the duty cycles of PWM to effectively regulate the speed and torque of the motor driving system during the commutation region, and then reduce the amplitude of the commutating current. Similarly, in order to maintain a constant current in the commutation region, the various PWM switching stages are enhanced by current shaping techniques to provide less commutation torque ripples with minimal switching losses. This technique is more robust and effective than conventional FOC using PWM technology at reducing current ripple and changing the switching logic, while over current, increased speed, or overloading occurs in BLDC motor drive systems [193]. Also, the SMC achieves good speed regulation in order to achieve appropriate time domain specifications and avoid chattering caused by high-frequency switching. Moreover, to improve motor performance in electric vehicles, the concept of MPC techniques is included to easily select switching vectors using a cost function with system constraints. MPC, such as DTC, has fast dynamics and good torque response despite operating with variable switching frequency [242].

The MPC approach outperforms others due to its low torque ripple, low torque and speed pulsations, low power reactive and active ripples, and high-quality waveforms of the stator 34 currents drawn by the motor with low THD [243]. Even though MPC techniques have a higher computation burden than FOC and DTC controllers, this burden might be eliminated with further development of artificial intelligence (AI) like deep learning techniques and machine learning algorithms to improve the performance of vehicles.

The artificial intelligence (AI) technique is being developed to overcome this major issue in BLDC motors in EVs by following variations in speed references and stabilizing output speed during load variations. In this case, the AI approach collaborated with FOC to optimize the speed regulation of an electric current space vector-controlled BLDC motor and improve the drive system's stability, accuracy, and rapid reaction, as well as increase motor torque dynamic and steady-state responsiveness. Using DTC when combined with Artificial Neural Networks (ANN) helps to reduce torque ripples in BLDC motors, resulting in smoother motor operation. In addition, it has a faster time reaction than conventional controllers, which improves the overall performance of the motor system. Fuzzy-based ANN controller for achieving desired steady-state performance and improving dynamic performance of BLDC motor operating parameters.

In this regard, the SMC controller paired with the AI method provides highly effective rejection of disturbances such as load torque and feedback noise, steady state, and transient performance making it suitable for applications requiring high precision position control to obtain efficient torque ripple rejection. Present-day MPC still uses a deep learning artificial neural network (DLANN) algorithm to regulate the motor's speed and torque, producing a more reliable, straightforward, and efficient operation with a shorter settling time.

VIII. CLOUD-BASED TORQUE CONTROL OF BLDC MOTOR IN EV APPLICATIONS

Now a days the improvement of the vehicle's driving range and optimization of its energy usage are key features of EV development. These requirements are dependent on torque

FIGURE 13. (a). Inferences and applications on various control strategies in BLDC motor for electric vehicles. (b). Advantages and disadvantages of various control strategies in BLDC motor for electric vehicles.

control and are met by developing and improving motor performance. Smooth torque output is required for electric vehicles to operate with great performance in their speed and position control drives. The torque ripple affects the motor with high specific torque the most and can lead to noise, vibrations, and problems with motor drives in addition to poor speed-torque characteristics. Recently the development of cloud-based motor torque control has been an advanced research area, integrating them into EVs for improving efficiency as well as providing new ideas for developing motor performance as shown in Fig 14. Cloud-based technology has made significant advances in EVs, bringing feasibility and problem-solving systems to all electrical sectors.

Cloud-based condition monitoring (CM) systems have mostly been used for detecting and diagnosing unexpected motor behavior caused by torque ripples. With the development of cloud-based CM systems, they may now share motor data with experts over the cloud, allowing for better defect detection, faster response times, and reduced machine downtime. Also, gives a direct connection to the cloud, where data from CM systems and devices can be transmitted. The cloud provides more processing capacity and extensive analysis choices due to the coupling of this data with other machine control data. In this context, real-time motor performance monitoring is accomplished by electric motor CM systems using a range of sensors and data analysis techniques. This enables systems to discover potential problems of torque and current ripples before they become serious and take corrective action immediately. Furthermore, these technologies can be utilized to predict the futur motor parameter variations, problems and arrange preventative maintenance appropriately. Here, sensors collect data to monitor critical motor operating parameters such as vibrations, noise, current ripples, and torque on real-time. Besides, cloud-connected computing devices gather and analyses a lot of information to improve motor control parameters performance as part of the Internet of Things (IoT).

It permits the real-time transmission of data to the cloud, where it can be analyzed and processed using artificial intelligence (AI) based learning techniques. This enables the detection of defects and the identification of their potential occurrence, allowing for timely maintenance activities to eliminate the need for extensive checking. Based on the transmission of information in real-time between the cloud and vehicles, is a critical aspect in calculating and satisfying the driving motor torque ripples minimization solution.

IX. FUTURE CHALLENGES AND OPPORTUNITIES

In this paper, a sustainable review of the long-established used control strategies of torque ripple mitigations in BLDC motors for EVs is presented. EVs have enormous potential and interesting opportunities in the future. The most significant barriers to attaining excellent torque control BLDC motor to EV driving performance are overcome with a high level of safety and trust. Under all conditions, EVs must operate consistently and without errors or malfunctions 36 in order to get acceptance and widespread deployment. Furthermore, the prior challenges of torque, current ripples, total harmonic distortion, achieving desired steady-state performance and so on must be overcome to ensure the technology's smooth development. Based on the review conducted and presented in this study, a few salient points are emphasized as well as suggested below on the further research on this topic as shown in Fig 15.

1. Developing and improving high computing techniques with advanced controller design strategies is the capability to manage and engage the performance together with safety in EVs in real-time. It might be influenced by developed vehicle models under all distinct operating circumstances and to deploy vehicles in emergence for specific missions' impact on reliability, comfort, efficiency, and stability. The emergence and execution of an EV controller utilizing optimization techniques, such as artificial intelligence (AI) machine learning programs, to continue and learn complex functions in order to achieve optimal performance.

2. To integrate the two control strategies into a single unit in order to demonstrate the BLDC motor's superior performance, particularly at steady state, by adopting these techniques to obtain better dynamic performance like mitigating torque ripple, maintaining the lowest possible THD in the stator current, improve the power density, uncertainties of load torque and over current constraints of the motor.

3. The development of autonomous driving in EVs accomplished the optimal overall power management result over the duration of a driving cycle and it quickly achieves starting, stopping, and steering control, which is then attained by specific electric motor systems. It employs an embedded-based communication system linked with high-resolution sensors to operate vehicles safely and collect accurate road along with operation data without a driver being present.

4. A potential future change in the direction of the wireless motor (WM) control drive entails improving the flexibility and performance of the EVs system, with the electric motor being directly fed by the wireless power transfer (WPT) system. Also, with the rapidly increasing demand for WPT in various motors, use a broad range of potential applications prospects which include eliminating power components in the system, power conversion inverters, as well as reducing the size and weight of motor drives.

5. Additional advances in cloud-based technology for motor torque control drives could increase the dependability and intelligence of EVs and solve many problems with energy management control system fault diagnostics. It analyses the torque distribution and energy consumption relationship via online cloud mode to adjust the vehicle torque based on current speed and road condition. Furthermore, its integration with electric motor drive systems via IoT and AI satisfies the driving motor power requirement to provide intellectual, robust, secure, and reliable vehicle systems.

6. Multilevel topology converters are becoming increasingly important in modern power electronics applications

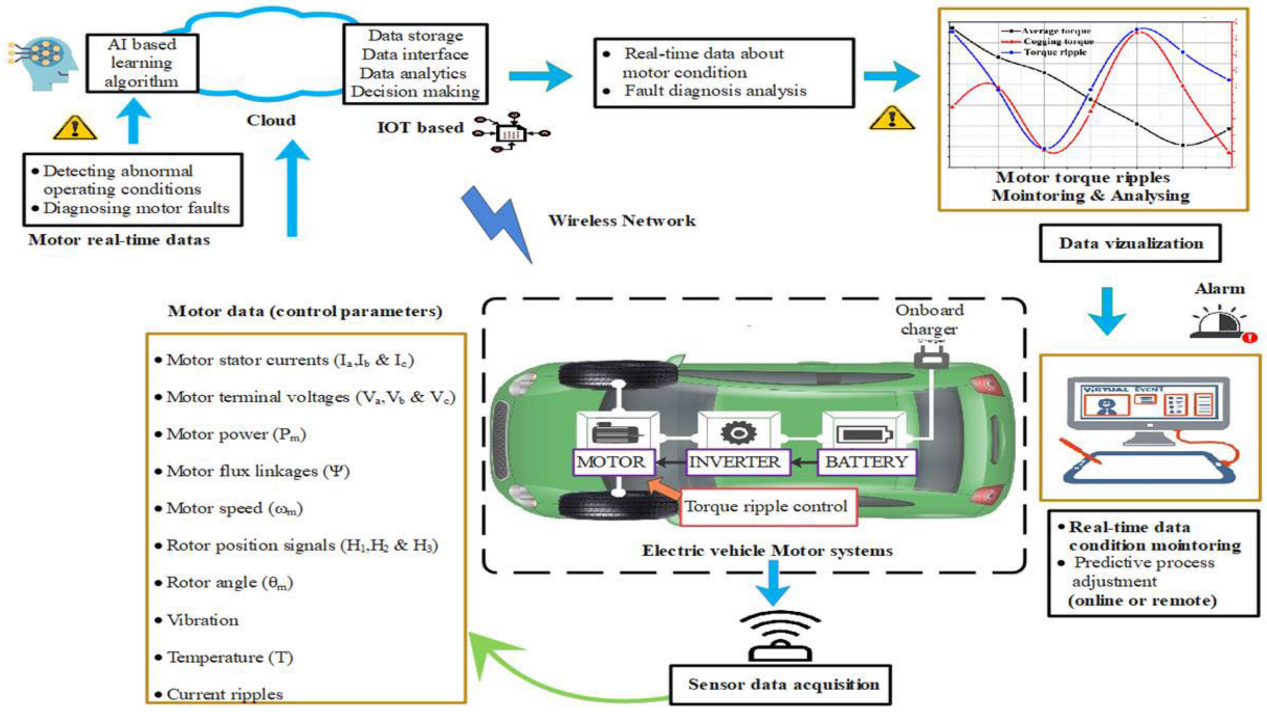

FIGURE 14. Cloud-based control strategies of torque ripple mitigations in BLDC motor for electric vehicles.

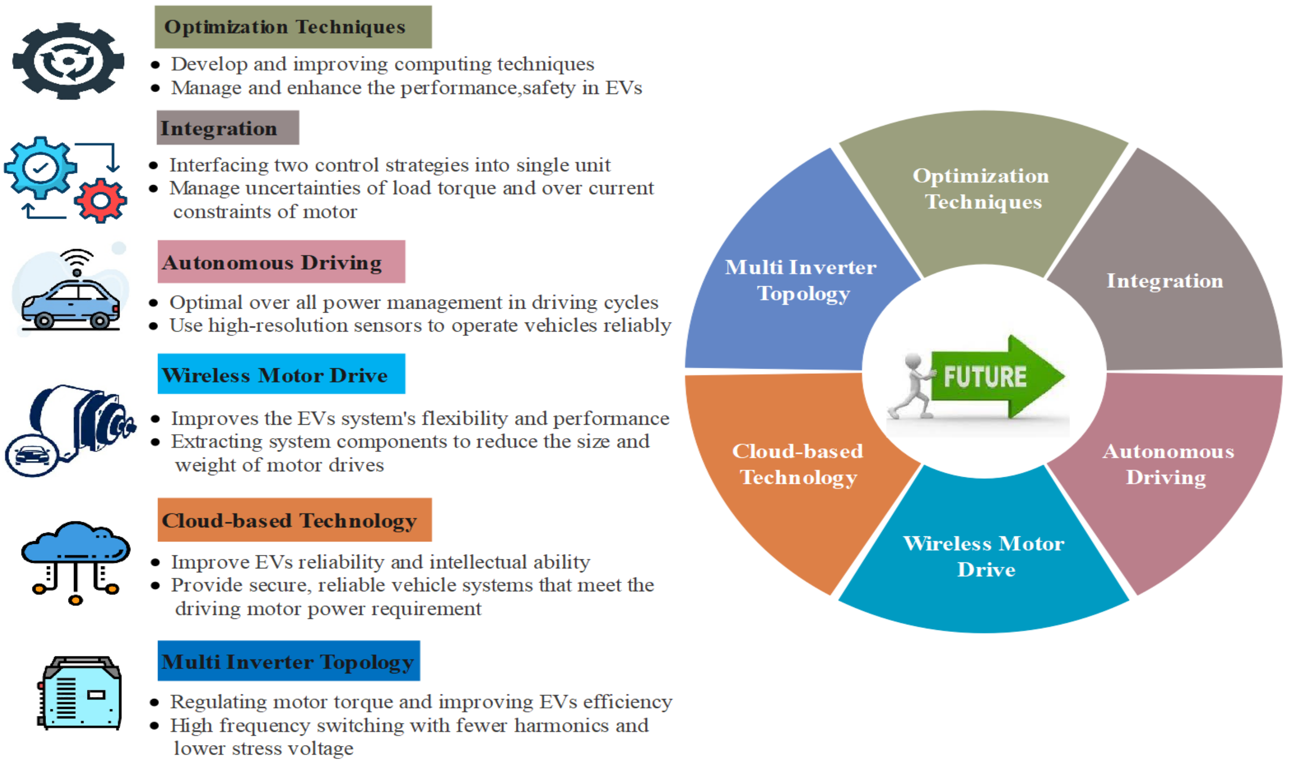

FIGURE 15. Future challenges for the advancement of control strategies in BLDC motor for electric vehicles.

for controlling motor torque and making EVs more efficient by utilizing AC-DC, DC-DC, and DC-AC converters. The output of the converter is simple and smoothly functioning as the number of levels increases (such as flying capacitor, diode clamped, and H-bridge) with less harmonic and reduced stress voltage in addition to the use of high switching frequency to minimize the excitation torque ripple with high-speed operation.

X. CONCLUSION

This work presents a comprehensive review of various control strategies associated with mitigating the torque ripples of BLDC motors in EVs that have been meticulously examined in terms of their function and control procedures. The studies reviewed in this paper focus on BLDC motors, which have become increasingly popular for use in EV applications due to their compactness, accuracy, and cost-effectiveness. Along with a fundamental understanding of torque ripple mitigation for the development of effective control techniques with a high degree of dynamic performance and superior efficiency. This performance is mainly based on the architecture of the control system for BLDC motors in vehicles, which includes controlled and uncontrolled variables such as speed, torque, stator phase currents, terminal voltages, back-EMF, hall sensors, etc. Although machines with a high specific torque inherently have large torque ripples, the significance of torque ripples produced is determined by three factors: motor construction, motor parameters, and motor control strategies. Moreover, an in-depth examination is conducted on regulating the torque ripples, where various control strategies (field-oriented control, direct torque control, intelligent control, controlling input voltage, current shaping techniques, model predictive control, and sliding mode control) are addressed, and their essential features are comprehended.

A similar field-oriented control method is used to manage BLDC motors with good control capability throughout the entire torque and speed ranges and satisfy the distinct demand for EVs. It makes the stator magnetic field orthogonal to the rotor magnetic field to provide the desired output very smoothly and efficiently, reducing torque ripples with greater high load efficiency. Then, the direct torque control method has the capacity to directly control the torque with low sensitivity to BLDC motor parameters, providing reliable and energy-efficient vector control and improving the stability and safety of EVs. Further, intelligent control techniques are an effective way to address some of the most prevalent issues that arise with BLDC motors for EVs, including electromagnetic interference, fault tolerance, and torque ripples, in order to enhance the reliability of EV drives by developing FLC systems.

Consequently, another reliable method of controlling input voltage is to reduce torque ripples and ensure proper commutation of power inverter switches when trapezoidal back-EMF is equivalent to the phase current of the stator windings, providing low computational complexity for dynamic performance in EVs. Like current shaping techniques, optimal current drive in EVs provides high operating speed together with a fast response output while significantly reducing torque ripples caused by non-ideal trapezoidal back-EMF due to insufficient commutation in the motor. Additionally, sliding mode control obtains speed regulation to increase EV motor drive performance. Moreover, model predictive control uses a system to forecast future motor drive outputs in EVs as a feedback control technique to handle complex dynamics and multiple input and output systems, also providing a popular solution in motor drive and achieving faster dynamic performance with EV controllers. Even though recent advancements in research have focused on cloud-based motor torque control, which can be integrated into EVs to increase efficiency and offer fresh perspectives on how to improve motor performance compared to all vector controllers. It can also more precisely predict information about the vehicle's current driving conditions for improved power distribution between the motor and battery system. These control approaches are used to improve motor system performance and guarantee smooth torque operation in order to maintain energy efficiency in EVs. Furthermore, the real-time evaluation processes of control strategies of BLDC motors, as well as crucial characteristics of energy management for the optimum functioning of EVs, have been analyzed.

REFERENCES

[1] J. A. Sanguesa, V. Torres-Sanz, P. Garrido, F. J. Martinez, and J. M. Marquez-Barja, "A review on electric vehicles: Technologies and challenges," *Smart Cities*, vol. 4, no. 1, pp. 372–404, Mar. 2021, doi: 10.3390/smartcities4010022.

[2] S. J. Rind, Y. Ren, Y. Hu, J. Wang, and L. Jiang, "Configurations and control of traction motors for electric vehicles: A review," *Chin. J. Electr. Eng.*, vol. 3, no. 3, pp. 1–17, Dec. 2017, doi: 10.23919/CJEE.2017.8250419.

[3] X. Sun, Z. Li, X. Wang, and C. Li, "Technology development of electric vehicles: A review," *Energies*, vol. 13, no. 1, p. 90, Dec. 2019, doi: 10.3390/en13010090.

[4] X. Men, Y. Guo, G. Wu, S. Chen, and C. Shi, "Implementation of an improved motor control for electric vehicles," *Energies*, vol. 15, no. 13, p. 4833, Jul. 2022, doi: 10.3390/en15134833.

[5] M. Yildirim, M. Polat, and H. Kürüm, "A survey on comparison of electric motor types and drives used for electric vehicles," in *Proc. 16th Int. Power Electron. Motion Control Conf. Exposit.*, Antalya, Turkey, Sep. 2014, pp. 218–223, doi: 10.1109/EPEPEMC.2014.6980715.

[6] N. Hashemnia and B. Asaei, "Comparative study of using different electric motors in the electric vehicles," in *Proc. 18th Int. Conf. Elect. Mach.*, Vilamoura, Portugal, 2008, pp. 1–5, doi: 10.1109/ICELMACH.2008.4800157.

[7] P. Saiteja and B. Ashok, "Critical review on structural architecture, energy control strategies and development process towards optimal energy management in hybrid vehicles," *Renew. Sustain. Energy Rev.*, vol. 157, Jul. 2022, Art. no. 112038, doi: 10.1016/j.rser.2021.112038.

[8] J. X. Shen and K. J. Tseng, "Analyses and compensation of rotor position detection error in sensorless PM brushless DC motor drives," *IEEE Trans. Energy Convers.*, vol. 18, no. 1, pp. 87–93, Mar. 2003, doi: 10.1109/TEC.2002.808339.

[9] J.-W. Park, S.-H. Hwang, and J.-M. Kim, "Sensorless control of brushless DC motors with torque constant estimation for home appliances," *IEEE Trans. Ind. Appl.*, vol. 48, no. 2, pp. 677–684, Mar. 2012, doi: 10.1109/TIA.2011.2181774.

[10] A. Attar, J. Bouchnaif, and K. Grari, "Control of brushless DC motors using sensorless back-EMF integration method," *Mater. Today, Proc.*, vol. 45, pp. 7438–7443, 2021, doi: 10.1016/j.matpr.2021.01.861.

[11] T. Shi, Y. Guo, P. Song, and C. Xia, "A new approach of minimizing commutation torque ripple for brushless DC motor based on DC–DC converter," *IEEE Trans. Ind. Electron.*, vol. 57, no. 10, pp. 3483–3490, Oct. 2010, doi: 10.1109/TIE.2009.2038335.

[12] Y. R. Hais, M. Rameli, and R. Effendie, "Design of torque control strategy for hybrid electric vehicle (HEV) with maximum work of self commutation brushless DC motor using fuzzy-PI," *IPTEK J. Proc. Ser.*, vol. 4, no. 1, p. 39, Jan. 2018, doi: 10.12962/j23546026.y2018i1.3504.

[13] M. Sumega, Š. Zoššák, P. Varecha, and P. Rafajdus, "Sources of torque ripple and their influence in BLDC motor drives," *Transp. Res. Proc.*, vol. 40, pp. 519–526, 2019, doi: 10.1016/j.trpro.2019.07.075.

[14] S. Sakunthala, R. Kiranmayi, and P. N. Mandadi, "A study on industrial motor drives: Comparison and applications of PMSM and BLDC motor drives," in *Proc. Int. Conf. Energy, Commun., Data Anal. Soft Comput. (ICECDS)*, Chennai, India, 2017, pp. 537–540, doi: 10.1109/ICECDS.2017.8390224.

[15] S. A. Niapour, G. H. Garjan, M. Shafiei, M. R. Feyzi, S. Danyali, and M. B. Kouhshahi, "Review of permanent-magnet brushless DC motor basic drives based on analysis and simulation study," *Int. Rev. Elect. Eng.*, vol. 9, no. 5, pp. 57–930, 2014, doi: 10.13140/RG.2.1.2949.4883.

[16] A. E. Aliasand and F. T. Josh, "Selection of motor foran electric vehicle: A review," *Mater. Today, Proc.*, vol. 24, pp. 1804–1815, 2020, doi: 10.1016/j.matpr.2020.03.605.

[17] S. Arunkumar and S. Thangavel, "A review paper on torque ripple reduction in brushless DC motor drives with different multilevel inverter topology," *TELKOMNIKA Indonesian J. Elect. Eng.*, vol. 13, no. 1, pp. 65–75, 2015, doi: 10.11591/telkomnika.v13i1.6904.

[18] A. Dimri, R. D. Kulkarni, S. R. Gurumurthy, and J. Nataraj, "Design and simulation of sensorless control algorithms of brushless DC Motor: A review," in *Proc. 2nd IEEE Int. Conf. Power Electron., Intell. Control Energy Syst. (ICPEICES)*, Delhi, India, 2018, pp. 948–952, doi: 10.1109/ICPEICES.2018.8897324.

[19] J. C. Gamazo-Real, E. Vázquez-Sánchez, and J. Gómez-Gil, "Position and speed control of brushless DC motors using sensorless techniques and application trends," *Sensors*, vol. 10, no. 7, pp. 6901–6947, 2010, doi: 10.3390/s100706901.

[20] M. M. Raj and S. K. Moganti, "A Comprehensive study on techniques to reduce torque ripple and cogging torque in surface mount BLDC motors," *Int. Res. J. Modernization Eng. Technol. Sci.*, 2021.

[21] A. Usman, B. M. Joshi, and B. S. Rajpurohit, "A review of modeling, analysis and control methods of brushless DC motors," in *Proc. Int. Conf. Comput. Power, Energy Inf. Commuincation (ICCPEIC)*, Melmaruvathur, India, Apr. 2016, pp. 337–343, doi: 10.1109/ICCPEIC.2016.7557254.

[22] P. Saiteja, B. Ashok, B. Mason, and S. Krishna, "Development of efficient energy management strategy to mitigate speed and torque ripples in SR motor through adaptive supervisory self-learning technique for electric vehicles," *IEEE Access*, vol. 11, pp. 96460–96484, 2023, doi: 10.1109/ACCESS.2023.3311851.

[23] A. B. Jadhav and M. S. Patil, "A review on torque and current ripple minimization techniques in a BLDC motor drive for EV applications," in *Proc. IEEE 4th Int. Conf. Cybern., Cognition Mach. Learn. Appl. (ICCCMLA)*, Goa, India, Jul. 2022, pp. 7–12, doi: 10.1109/ICCCMLA56841.2022.9989245.

[24] R. Goswami and D. Joshi, "Performance review of fuzzy logic based controllers employed in brushless DC motor," *Proc. Comput. Sci.*, vol. 132, pp. 623–631, Dec. 2018, doi: 10.1016/j.procs.2018.05.061.

[25] A. Swaminathan, K. Malavika, N. Narayanan and M. Jayakumar, "Review on different topologies of power electronic converters and control strategies for motors in electric vehicles," in *Proc. Innov. Power Adv. Comput. Technol. (i-PACT)*, Kuala Lumpur, Malaysia, 2021, pp. 1–7, doi: 10.1109/i-PACT52855.2021.9696849.

[26] M. Karthika and K. C. R. Nisha, "Review on torque ripple reduction techniques of BLDC motor," in *Proc. Int. Conf. Inventive Comput. Technol. (ICICT)*, Coimbatore, India, 2020, pp. 1092–1096, doi: 10.1109/ICICT48043.2020.9112523.

[27] H. S. Chuang, Y.-L. Ke, and Y. C. Chuang, "Analysis of commutation torque ripple using different PWM modes in BLDC motors," in *Proc. Conf. Record IEEE Ind. Commercial Power Syst. Tech. Conf.*, Calgary, AB, Canada, 2009, pp. 1–6, doi: 10.1109/ICPS.2009.5463966.

[28] D. Mohanraj, R. Aruldavid, R. Verma, K. Sathiyasekar, A. B. Barnawi, B. Chokkalingam, and L. Mihet-Popa, "A review of BLDC motor: State of art, advanced control techniques, and applications," *IEEE Access*, vol. 10, pp. 54833–54869, 2022, doi: 10.1109/ACCESS.2022.3175011.

[29] D. Mohanraj, J. Gopalakrishnan, B. Chokkalingam, and L. Mihet-Popa, "Critical aspects of electric motor drive controllers and mitigation of torque ripple—Review," *IEEE Access*, vol. 10, pp. 73635–73674, 2022, doi: 10.1109/ACCESS.2022.3187515.

[30] C. H. Apribowo and H. Maghfiroh, "Fuzzy logic controller and its application in brushless DC motor (BLDC) in electric vehicle—A review," *J. Elect. Electron., Inf., Commun. Technol.*, vol. 3, no. 1, pp. 35–43, 2021, doi: 10.20961/jeeict.3.1.50651.

[31] S. R. Misal and N. R. Bhasme, "A review of multi-switch BLDC motor drive," in *Proc. Innov. Power Adv. Comput. Technol. (i-PACT)*, Vellore, India, 2017, pp. 1–7, doi: 10.1109/IPACT.2017.8245188.

[32] W. A. Salah, D. Ishak, and K. J. Hammadi, "Minimization of torque ripples in BLDC motors due to phase commutation—A review," *Przeglad Elektrotechniczny*, vol. 87, pp. 183–188, Jan. 2011.

[33] P. B. Bobba and K. R. Rajagopal, "Compact regenerative braking scheme for a PM BLDC motor driven electric two-wheeler," in *Proc. Joint Int. Conf. Power Electron., Drives Energy Syst. Power*, New Delhi, India, 2010, pp. 1–5, doi: 10.1109/PEDES.2010.5712566.

[34] Y. Bektaş and N. F. Serteller, "Brushless direct current (BLDC) motor driving experimental set," *Energy Educ. Sci. Technol. A, Energy Sci. Res.*, vol. 27, no. 2, pp. 455–466, 2011.

[35] T. Nama, A. K. Gogoi, and P. Tripathy, "Application of a smart Hall effect sensor system for 3-phase BLDC drives," in *Proc. IEEE Int. Symp. Robot. Intell. Sensors (IRIS)*, Ottawa, ON, Canada, Jul. 2017, pp. 208–212, doi: 10.1109/IRIS.2017.8250123.

[36] X. Gao, *BLDC Motor Control With Hall Sensors Based on FRDM-KE02Z*, document AN4776, Sep. 2021. [Online]. Available: https://www.nxp.com/docs/en/application-note/AN4776.pdf

[37] J. W. K. Jayasundara and D. A. I. Munindradasa, "Novel sinusoidal PWM controller stratagy for axial flux permanent magnet motors," in *Proc. 1st Int. Conf. Ind. Inf. Syst.*, Tirtayasa, Indonesia, 2006, pp. 507–509, doi: 10.1109/ICIIS.2006.365780.

[38] K. I. Laskaris and A. G. Kladas, "Internal permanent magnet motor design for electric vehicle drive," *IEEE Trans. Ind. Electron.*, vol. 57, no. 1, pp. 138–145, Jan. 2010, doi: 10.1109/TIE.2009.2033086.

[39] Y. Sangsefidi, S. Ziaeinejad, and A. Shoulaie, "Torque ripple reduction of BLDC motors by modifying the non-commutating phase voltage," in *Proc. Int. Conf. Elect., Control Comput. Eng. (InECCE)*, Kuantan, Malaysia, 2011, pp. 308–312, doi: 10.1109/INECCE.2011.5953897.

[40] T. Srisiriwanna and M. Konghirun, "A study of cogging torque reduction methods in brushless DC motor," in *Proc. 9th Int. Conf. Elect. Eng./Electron., Comput., Telecommun. Inf. Technol.*, Phetchaburi, Thailand, 2012, pp. 1–4, doi: 10.1109/ECTICon.2012.6254191.

[41] M.-H. Hwang, H.-S. Lee, and H.-R. Cha, "Analysis of torque ripple and cogging torque reduction in electric vehicle traction platform applying rotor notched design," *Energies*, vol. 11, no. 11, p. 3053, Nov. 2018, doi: 10.3390/en11113053.

[42] S. Leitner, H. Gruebler, and A. Muetze, "Cogging torque minimization and performance of the sub-fractional HP BLDC claw-pole motor," *IEEE Trans. Ind. Appl.*, vol. 55, no. 5, pp. 4653–4664, Sep. 2019, doi: 10.1109/TIA.2019.2923569.

[43] P. Dini and S. Saponara, "Cogging torque reduction in brushless motors by a nonlinear control technique," *Energies*, vol. 12, no. 11, p. 2224, Jun. 2019, doi: 10.3390/en12112224.

[44] S. Madhavaraj and B. Venkatalakshmi, "Reduction of cogging torque, harmonics in PM BLDC motor," in *Proc. Int. erence on Innov. Eng. Technol. (ICIET)*, vol. 3, 2014, pp. 1–6.

[45] C. Studer, A. Keyhani, T. Sebastian, and S. K. Murthy, "Study of cogging torque in permanent magnet machines," in *Proc. Conf. Rec. IEEE Ind. Appl. Conf. 32nd IAS Annu. Meeting*, New Orleans, LA, USA, Jul. 1997, pp. 42–49, doi: 10.1109/IAS.1997.643006.

[46] X. Liu, M. Sun, and X. Wang, "Research on reducing reluctance torque of permanent magnet toroidal motor," *AIP Adv.*, vol. 11, no. 2, p. 025302, 2021, doi: 10.1063/5.0031248.

[47] Y. Sozer and D. A. Torrey, "Adaptive torque ripple control of permanent magnet brushless DC motors," in *Proc. APEC 13th Annu. Appl. Power Electron. Conf. Exposit.*, Anaheim, CA, USA, 1998, pp. 86–92, doi: 10.1109/APEC.1998.647674.

[48] I. Shchur and D. Jancarczyk, "Electromagnetic torque ripple in multiple three-phase brushless DC motors for electric vehicles," *Electronics*, vol. 10, no. 24, p. 3097, Dec. 2021, doi: 10.3390/electronics10243097.

[49] M. Fazil and K. R. Rajagopal, "A novel air-gap profile of single-phase permanent-magnet brushless DC motor for starting torque improvement and cogging torque reduction," *IEEE Trans. Magn.*, vol. 46, no. 11, pp. 3928–3932, Nov. 2010, doi: 10.1109/TMAG.2010.2057514.

[50] S. Bentouati, Z. Q. Zhu, and D. Howe, "Influence of design parameters on the starting torque of a single-phase PM brushless DC motor," *IEEE Trans. Magn.*, vol. 36, no. 5, pp. 3533–3536, Sep. 2000, doi: 10.1109/20.908890.

[51] K Krykowski, Z. Gałuszkiewicz, P. Gałuszkiewicz, J. Hetmáczyk, and D. Całus, "High-speed permanent magnet brushless DC motors, properties and prospective applications," *Przegląd Elektrotechniczny*, vol. 95, no. 8, pp. 45–139, 2019, doi: 10.15199/48.2019.08.30.

[52] W. Purwanto, H. Maksum, T. Sugiarto, M. Nasir, M. Martias, and F. Rizal, "The effect of stator winding parameter design to the magnetic flux characteristics in highspeed motor applications," *J. Theor. Appl. Inf. Technol.*, vol. 97, no. 12, pp. 80–3270, 2019.

[53] J. Fang, H. Li, and B. Han, "Torque ripple reduction in BLDC torque motor with nonideal back EMF," *IEEE Trans. Power Electron.*, vol. 27, no. 11, pp. 4630–4637, Nov. 2012, doi: 10.1109/TPEL.2011.2176143.

[54] D. R. B. Divakar, G. Divya, G. S. Yugandhar, and D. Sindhusha, "A review on brushless DC motor control techniques," *J. Pharmaceutical Negative Results*, vol. 13, pp. 6821–6828, 2023.

[55] W. Salah, D. Ishak, and K. Hammadi, "PWM switching strategy for torque ripple minimization in BLDC motor," *J. Elect. Eng.*, vol. 62, no. 3, pp. 141–146, 2011, doi: 10.2478/v10187-011-0023-1.

[56] V. K. Patel and A. K. Pandey, "Modeling and performance analysis of PID controlled BLDC motor and different schemes of PWM controlled BLDC motor," *Int. J. Sci. Res. Publications*, vol. 3, no. 4, pp. 1–4, 2013.

[57] Y.-S. Lai and Y.-K. Lin, "Assessment of pulse-width modulation techniques for brushless DC motor drives," in *Proc. Conf. Rec. IEEE Ind. Appl. Conf. 41st IAS Annu. Meeting*, Tampa, FL, USA, Oct. 2006, pp. 1629–1636, doi: 10.1109/IAS.2006.256754.

[58] H. Patel and H. Chandwani, "Simulation and experimental verification of modified sinusoidal pulse width modulation technique for torque ripple attenuation in Brushless DC motor drive," *Eng. Sci. Technol., Int. J.*, vol. 24, no. 3, pp. 671–681, 2021, doi: 10.1016/j.jestch.2020.11.003.

[59] R. L. Valle, P. M. De Almeida, A. A. Ferreira, and P. G. Barbosa, "Unipolar PWM predictive current-mode control of a variable-speed low inductance BLDC motor drive," *IET Electr. Power Appl.*, vol. 11, no. 5, pp. 696–688, 2017, doi: 10.1049/iet-epa.2016.0421.

[60] Y. Ji, B. Li, and J. Sun, "Harmonic analysis on torque ripple of brushless DC motor based on advanced commutation control," *J. Control Sci. Eng.*, vol. 2018, pp. 1–9, Jul. 2018, doi: 10.1155/2018/3530127.

[61] X. Li, G. Jiang, W. Chen, T. Shi, G. Zhang, and Q. Geng, "Commutation torque ripple suppression strategy of brushless DC motor considering back electromotive force variation," *Energies*, vol. 12, no. 10, p. 1932, May 2019, doi: 10.3390/en12101932.

[62] M. K. Pandey, D. A. Tripathi, and D. B. Dwivedi, "Current harmonics reduction technique in a BLDC motor drive application," *Int. J. Eng. Technol.*, vol. 9, no. 3S, pp. 442–447, Jul. 2017.

[63] S.-Y. Jung, Y.-J. Kim, J. Jae, and J. Kim, "Commutation control for the low-commutation torque ripple in the position sensorless drive of the low-voltage brushless DC motor," *IEEE Trans. Power Electron.*, vol. 29, no. 11, pp. 5983–5994, Nov. 2014, doi: 10.1109/TPEL.2014.2298113.

[64] X. Yao, J. Zhao, J. Wang, S. Huang, and Y. Jiang, "Commutation torque ripple reduction for brushless DC motor based on an auxiliary step-up circuit," *IEEE Access*, vol. 7, pp. 138721–138731, 2019, doi: 10.1109/ACCESS.2019.2943411.

[65] M. A. Aazmi, M. I. Fahmi, M. Z. Aihsan, H. F. Liew, and M. Saifizi, "A review on VFD control and energy management system of induction motor for electric vehicle," in *Proc. IEEE 19th student Conf. Res. Develop. (SCOReD)*, Kota Kinabalu, Malaysia, Nov. 2021, pp. 36–41, doi: 10.1109/SCOReD53546.2021.9652673.

[66] S. Mencou, M. B. Yakhlef, and E. B. Tazi, "Advanced torque and speed control techniques for induction motor drives: A review," in *Proc. 2nd Int. Conf. Innov. Res. Appl. Sci., Eng. Technol. (IRASET)*, Meknes, Morocco, Mar. 2022, pp. 1–9, doi: 10.1109/IRASET52964.2022.9738368.

[67] P. T. Krein, F. Disilvestro, I. Kanellakopoulos, and J. Locker, "Comparative analysis of scalar and vector control methods for induction motors," in *Proc. IEEE Power Electron. Spec. Conf. PESC*, Seattle, WA, USA, Jul. 1993, pp. 1139–1145, doi: 10.1109/PESC.1993.472061.

[68] C. Bejenar, N. D. Irimia, M. Luchian, and F. I. Lazar, "Dynamic behavior analysis of a three-phase BLDC motor under scalar control strategy for automotive actuation systems," in *Proc. Int. Conf. Develop. Appl. Syst. (DAS)*, Suceava, Romania, May 2020, pp. 7–15, doi: 10.1109/DAS49615.2020.9108937.

[69] N. S. Farhan, A. T. Humod, and F. Hasan, "Field oriented control of AFPMSM for electrical vehicle using adaptive neuro-fuzzy inference system (ANFIS)," *Eng. Technol. J.*, vol. 39, no. 10, pp. 82–1571, 2021, doi: 10.30684/etj.v39i10.1969.

[70] A. Flah, I. A. Khan, A. Agarwal, L. Sbita, and M. G. Simoes, "Field-oriented control strategy for double-stator single-rotor and double-rotor single-stator permanent magnet machine: Design and operation," *Comput. Elect. Eng.*, vol. 90, p. 106953, 2021, doi: 10.1016/j.compeleceng.2020.106953.

[71] Y. Lu, Z. Jiang, C. Chen, and Y. Zhuang, "Energy efficiency optimization of field-oriented control for PMSM in all electric system," *Sustain. Energy Technol. Assessments*, vol. 48, Dec. 2021, Art. no. 101575, doi: 10.1016/j.seta.2021.101575.

[72] Y. Wu, Z. Deng, X. Wang, X. Ling, and X. Cao, "Position sensorless control based on coordinate transformation for brushless DC motor drives," *IEEE Trans. Power Electron.*, vol. 25, no. 9, pp. 2365–2371, Sep. 2010, doi: 10.1109/TPEL.2010.2048126.

[73] R. Jauhar, N. Ismail, and N. Sartika, "Design of torque controller based on field oriented control (FOC) method on BLDC motor," in *Proc. 16th Int. Conf. Telecommun. Syst., Services, Appl. (TSSA)*, Lombok, Indonesia, Oct. 2022, pp. 1–5, doi: 10.1109/TSSA56819.2022.10063889.

[74] M. R. Fadli, M. M. Musyasy, J. Furqani, and A. Purwadi, "Modelling of field orientation control (FOC) method in 120 kW brushless DC motor (BLDC)," in *Proc. 6th Int. Conf. Electr. Veh. Technol. (ICEVT)*, Bali, Indonesia, 2019, pp. 383–389, doi: 10.1109/ICEVT48285.2019.8993973.

[75] P. K. Sharma and A. S. Sindekar, "Performance analysis and comparison of BLDC motor drive using PI and FOC," in *Proc. Int. Conf. Global Trends Signal Process., Inf. Comput. Commun. (ICGTSPICC)*, Jalgaon, India, Dec. 2016, pp. 485–492, doi: 10.1109/ICGTSPICC.2016.7955350.

[76] N. A. Macahig, "A 6-wire 3-phase inverter topology for improved BLDC performance and harmonics," in *Proc. IEEE Appl. Power Electron. Conf. Exposit. (APEC)*, New Orleans, LA, USA, Mar. 2020, pp. 741–744, doi: 10.1109/APEC39645.2020.9124358.

[77] P. C. Biswas and B. C. Ghosh, "A novel flux estimation algorithm based position sensorless field oriented vector controlled permanent magnet brushless DC motor drive," in *Proc. 3rd Int. Conf. Electr. Inf. Commun. Technol. (EICT)*, Khulna, Bangladesh, Dec. 2017, pp. 1–6, doi: 10.1109/EICT.2017.8275231.

[78] G. Sajitha, N. Mayadevi, V. P. Mini, and R. Harikumar, "Fault-tolerant control of BLDC motor drive for electric vehicle applications," in *Proc. Int. Conf. Power Electron. Appl. Technol. Present Energy Scenario (PETPES)*, Mangalore, India, Aug. 2019, pp. 1–6, doi: 10.1109/PETPES47060.2019.9003925.

[79] O. Sandre-Hernandez, P. Ordaz-Oliver, and C. Cuvas-Castillo, "Sensorless field oriented control of BLDC motor based on sliding mode observer," in *Proc. Int. Conf. Mechatronics, Electron. Automot. Eng. (ICMEAE)*, Cuernavaca, Mexico, Nov. 2019, pp. 119–124, doi: 10.1109/ICMEAE.2019.00029.

[80] S.-C. Chen and E. T. Mbitu, "Permanent magnet brushless motor field oriented control with dither signal injection," in *Proc. IEEE Int. Conf. Appl. Syst. Invention (ICASI)*, Chiba, Japan, Apr. 2018, pp. 1141–1144, doi: 10.1109/ICASI.2018.8394485.

[81] T. Muthamizhan, P. Saravanan, and R. Maharana, "Sensorless control of z source inverter fed BLDC motor drive by FOC–DTC hybrid control strategy using fuzzy logic controller," in *Proc. 7th Int. Conf. Electr. Energy Syst. (ICEES)*, Chennai, India, Feb. 2021, pp. 358–363, doi: 10.1109/ICEES51510.2021.9383752.

[82] M. Sumega, P. Rafajdus, S. Kocan, and M. Stulrajter, "Torque ripple reduction in PM motors using current harmonics controller," in *Proc. ELEKTRO*, Taormina, Italy, 2020, pp. 1–6, doi: 10.1109/ELEKTRO49696.2020.9130188.

[83] N. A. Qamar and C. J. Hatziadoniu, "Cancellation of selected stator harmonics in BLDC by using an adaptive feedforward controller," *Electric Power Syst. Res.*, vol. 154, pp. 88–94, Jan. 2018, doi: 10.1016/j.epsr.2017.07.032.

[84] A.-M. Petri and D. M. Petreuş, "Adaptive cruise control in electric vehicles with field-oriented control," *Appl. Sci.*, vol. 12, no. 14, p. 7094, Jul. 2022, doi: 10.3390/app12147094.

[85] M. T. Ratcliffe and K. A. Gamage, "BLDC motor power control techniques appraisal: Novel current control technique," in *Proc. 4th Int. Conf. Power Eng., Energy Electr. Drives*, Istanbul, Turkey, May 2013, pp. 1700–1705, doi: 10.1109/PowerEng.2013.6635873.

[86] J. L. F. Daya, P. Sanjeevikumar, F. Blaabjerg, P. W. Wheeler, and J. O. Ojo, "Implementation of wavelet-based robust differential control for electric vehicle application," *IEEE Trans. Power Electron.*, vol. 30, no. 12, pp. 6510–6513, Dec. 2015, doi: 10.1109/TPEL.2015.2440297.

[87] C.-P. Do and D.-K. Le, "Improved of dynamic torque by field oriented control based fuzzy logic for BLDC motor," in *Proc. 7th Nat. Scientific Conf. Applying New Technol. Green Buildings (ATiGB)*, Da Nang, Vietnam, Nov. 2022, pp. 92–97, doi: 10.1109/ATiGB56486.2022.9984089.

[88] M. Sumega, P. Rafajdus, G. Scelba, and M. Stulrajter, "Control strategies for the identification and reduction of cogging torque in PM motors," in *Proc. Int. Conf. Electr. Drives Power Electron. (EDPE)*, The High Tatras, Slovakia, Sep. 2019, pp. 74–80, doi: 10.1109/EDPE.2019.8883892.

[89] Md. A. Islam, Md. B. Hossen, Md. S. Hasan, and B. C. Ghosh, "Field oriented rectangular current regulated PWM control of permanent magnet brushless DC motor," in *Proc. 4th Int. Conf. Adv. Electr. Eng. (ICAEE)*, Dhaka, Bangladesh, Sep. 2017, pp. 346–351, doi: 10.1109/ICAEE.2017.8255379.

[90] G. Tatar, H. Korkmaz, N. F. O. Serteller, and K. Toker, "LabVIEW FPGA based BLDC motor control by using field oriented control algorithm," in *Proc. Int. Conf. Smart Energy Syst. Technol. (SEST)*, Istanbul, Turkey, Sep. 2020, pp. 1–6, doi: 10.1109/SEST48500.2020.9203104.

[91] M. Lazor and M. Štulrajter, "Modified field-oriented control for smooth torque operation of a BLDC motor," in *Proc. ELEKTRO*, Rajecke Teplice, Slovakia, 2014, pp. 180–185, doi: 10.1109/ELEKTRO.2014.6847897.

[92] Y. Guo, J. Yang, Y. Dou, X. Qiu, J. Liu, Y. Zhang, and M. Wang, "New zero voltage vectors in direct torque control of brushless DC motor," in *Proc. 19th Int. Conf. Electr. Mach. Syst. (ICEMS)*, Chiba, Japan, Nov. 2016, pp. 1–4.

[93] F. Li, W. Yao, and K. Lee, "Quantitative characteristic comparison between sensorless six step and field oriented control methods for permanent magnet brushless DC motors," in *Proc. IEEE Energy Convers. Congr. Expo. (ECCE)*, Baltimore, MD, USA, Jul. 2019, pp. 1881–1885, doi: 10.1109/ECCE.2019.8912478.

[94] B. P. Reddy and A. Murali, "SoC FPGA-based field oriented control of BLDC motor using low resolution Hall sensor," in *Proc. 42nd Annu. Conf. IEEE Ind. Electron. Soc.*, Florence, Italy, Oct. 2016, pp. 2941–2945, doi: 10.1109/IECON.2016.7793092.

[95] J. P. John, S. S. Kumar, and B. Jaya, "Space vector modulation based field oriented control scheme for brushless DC motors," in *Proc. Int. Conf. Emerg. Trends Elect. Comput. Technol.*, Nagercoil, India, 2011, pp. 346–351, doi: 10.1109/ICETECT.2011.5760141.

[96] A. M. Saleque, S. M. Ferdous, M. S. Al Hossain, M. Masoom, and T. S. Chowdhury, "An artificial neural network based flux estimator for sensorless field oriented control of interior permanent magnet synchronous motor," in *Proc. Int. Conf. Elect. Mach., Drives Power Syst. (ELMA)*, Oct. 2011, pp. 97–108.

[97] M. N. Gujjar and P. Kumar, "Comparative analysis of field oriented control of BLDC motor using SPWM and SVPWM techniques," in *Proc. 2nd IEEE Int. Conf. Recent Trends Electron., Inf. Commun. Technol. (RTEICT)*, Bangalore, India, May 2017, pp. 924–929, doi: 10.1109/RTEICT.2017.8256733.

[98] A. V. Schagin and D. T. Nguyen, "Development of speed control system for BLDC motor with power factor correction," in *Proc. IEEE Conf. Russian Young Researchers Electr. Electron. Eng. (EIConRus)*, St. Petersburg and Moscow, Russia, Jan. 2020, pp. 2411–2414, doi: 10.1109/EIConRus49466.2020.9038981.

[99] N. D. Irimia, M. Luchian, F. I. Lazar, and A. Ipatiov, "Performant fault tolerant control by using space vector modulation (SVM) technique of a five phases BLDC motor for autonomous driving applications," in *Proc. 10th Int. Conf. Syst. Control (ICSC)*, Marseille, France, Nov. 2022, pp. 317–322, doi: 10.1109/ICSC57768.2022.9993892.

[100] M. A. J. Sadhique, S. Ashok, J. Sandeen, and S. Deepthi, "Position sensorless control for BLDC motor for powertrain applications," in *Proc. 2nd Int. Conf. Intell. Comput., Instrum. Control Technol. (ICICICT)*, Kannur, India, 2019, pp. 322–327, doi: 10.1109/ICICICT46008.2019.8993184.

[101] Z. Li, L. Wang, S. Zhang, C. Zhang, and J. -W. Ahn, "Torque ripple reduction in direct torque controlled Brushless DC motor," in *Proc. Int. Conf. Elect. Mach. Syst.*, Beijing, China, 2011, pp. 1–4, doi: 10.1109/ICEMS.2011.6073659.

[102] M. S. Patil, R. Medhane, and S. S. Dhamal, "Comparative analysis of various DTC control techniques on BLDC motor for electric vehicle," in *Proc. 7th Int. Conf. Smart Struct. Syst. (ICSSS)*, Chennai, India, Jul. 2020, pp. 1–6, doi: 10.1109/ICSSS49621.2020.9201982.

[103] B. Singh, P. Jain, A. P. Mittal, and J. R. P. Gupta, "Direct torque control: A practical approach to electric vehicle," in *Proc. IEEE Power India Conf.*, New Delhi, India, Jul. 2006, p. 4, doi: 10.1109/POWERI.2006.1632617.

[104] F. Korkmaz, I. Topaloglu, and H. Mamur, "DTC control of BLAC and BLDC motors for pure electric vehicles," *Int. J. Instrum. Control Syst.*, vol. 6, nos. 2–3, pp. 9–17, Jul. 2016, doi: 10.5121/ijics.2016.6302.

[105] Y. Ahmad Tarmizi, A. Jidin, K. Abdul Karim, and T. Sutikno, "A simple constant switching frequency of direct torque control of brushless DC motor," *Int. J. Power Electron. Drive Syst.*, vol. 10, no. 1, p. 10, Mar. 2019, doi: 10.11591/ijpeds.v10.i1.pp10-18.

[106] Y. Liu, Z. Q. Zhu, and D. Howe, "Direct torque control of brushless DC drives with reduced torque ripple," *IEEE Trans. Ind. Appl.*, vol. 41, no. 2, pp. 599–608, Mar. 2005, doi: 10.1109/TIA.2005.844853.

[107] S. B. Ozturk and H. A. Toliyat, "Direct torque control of brushless DC motor with non-sinusoidal back-EMF," in *Proc. IEEE Int. Electric Mach. Drives Conf.*, Antalya, Turkey, May 2007, pp. 165–171, doi: 10.1109/IEMDC.2007.383571.

[108] H. Ma, J. F. Yang, Y. P. Dou, X. Qiu, S. L. Dong, and S. X. Li, "A simple control method for direct torque control of BLDCM with low resolution Hall sensors," in *Proc. 21st Int. Conf. Elect. Mach. Syst. (ICEMS)*, Jeju, South Korea, 2018, pp. 493–496, doi: 10.23919/ICEMS.2018.8549281.

[109] K. V. P. Kumar and T. V. Kumar, "Direct torque control of brush less DC motor drive with modified switching algorithm," in *Proc. IEEE Int. Conf. Power Electron., Drives Energy Syst. (PEDES)*, Trivandrum, India, Dec. 2016, pp. 1–5, doi: 10.1109/PEDES.2016.7914500.

[110] M. Schenke, B. Haucke-Korber, and O. Wallscheid, "Finite-set direct torque control via edge-computing-assisted safe reinforcement learning for a permanent-magnet synchronous motor," *IEEE Trans. Power Electron.*, vol. 38, no. 11, pp. 13741–13756, Nov. 2023, doi: 10.1109/TPEL.2023.3303651.

[111] A. Khazaee, H. A. Zarchi, G. A. Markadeh, and H. M. Hesar, "MTPA strategy for direct torque control of brushless DC motor drive," *IEEE Trans. Ind. Electron.*, vol. 68, no. 8, pp. 6692–6700, Aug. 2021, doi: 10.1109/TIE.2020.3009576.

[112] R. Heidari, G. A. Markadeh, and S. Abazari, "Direct torque and indirect flux control of brushless DC motor with non-sinusoidal back-EMF without position sensor," in *Proc. 19th Iranian Conf. Electr. Eng.*, Tehran, Iran, May 2011, pp. 1–5.

[113] B. N. Kommula and V. R. Kota, "Direct instantaneous torque control of Brushless DC motor using firefly Algorithm based fractional order PID controller," *J. King Saud Univ.-Eng. Sci.*, vol. 32, no. 2, pp. 133–140, 2020, doi: 10.1016/j.jksues.2018.04.007.

[114] M. B. B. Sharifian, M. Shafiei, M. S. Sadeghi, and F. Golestaneh, "Direct torque control of brushless DC motor drives based on ANFIS controller with fuzzy supervisory learning," in *Proc. Int. Conf. Electr. Mach. Syst.*, Beijing, Aug. 2011, pp. 1–6, doi: 10.1109/ICEMS.2011.6073444.

[115] M. S. Kumar, G. Satheesh, and S. Peddakotla, "Design of optimal PI controller for torque ripple minimization of SVPWM-DTC of BLDC motor," *Int. J. Power Electron. Drive Syst.*, vol. 14, no. 1, p. 283, Mar. 2023, doi: 10.11591/ijpeds.v14.i1.pp283-293.

[116] K. D. Carey, N. Zimmerman, and C. Ababei, "Hybrid field oriented and direct torque control for sensorless BLDC motors used in aerial drones," *IET Power Electron.*, vol. 12, no. 3, pp. 49–438, 2019, doi: 10.1049/iet-pel.2018.5231.

[117] P. Kumar, D. V. Bhaskar, R. K. Behera, and U. R. Muduli, "A modified torque ripple minimization technique for BLDC motor drive using synthesized current phase compensation," in *Proc. IEEE Int. Conf. Ind. Technol. (ICIT)*, Buenos Aires, Argentina, Feb. 2020, pp. 127–132, doi: 10.1109/ICIT45562.2020.9067134.

[118] H. Lu, L. Zhang, and W. Qu, "A new torque control method for torque ripple minimization of BLDC motors with un-ideal back EMF," *IEEE Trans. Power Electron.*, vol. 23, no. 2, pp. 950–958, Mar. 2008, doi: 10.1109/TPEL.2007.915667.

[119] J. Yang, Y. Hu, W. Huang, J. Chu, and J. Gao, "Direct torque control of brushless DC motor without flux linkage observation," in *Proc. IEEE 6th Int. Power Electron. Motion Control Conf.*, Wuhan, China, May 2009, pp. 1934–1937, doi: 10.1109/IPEMC.2009.5157713.

[120] M. Masmoudi, B. El Badsi, and A. Masmoudi, "Direct torque control of brushless DC motor drives with improved reliability," in *Proc. 8th Int. Conf. Exhib. Ecological Vehicles Renew. Energies (EVER)*, Monte Carlo, Monaco, Mar. 2013, pp. 1–8, doi: 10.1109/EVER.2013.6521562.

[121] G. R. A. Markadeh, S. I. Mousavi, and E. Daryabeigi, "Position sensorless direct torque control of BLDC motor by using modifier," in *Proc. 11th Int. Conf. Optim. Electr. Electron. Equip.*, Brasov, Romania, May 2008, pp. 93–99, doi: 10.1109/OPTIM.2008.4602393.

[122] J. E. Muralidhar and P. V. Aranasi, "Torque ripple minimization & closed loop speed control of BLDC motor with hysteresis current controller," in *Proc. 2nd Int. Conf. Devices, Circuits Syst. (ICDCS)*, Coimbatore, India, 2014, pp. 1–7, doi: 10.1109/ICDCSyst.2014.6926122.

[123] S. Ray and R. Chakraborty, "Torque ripple reduction of BLDC motor introducing delay in the gate firing circuits," in *Proc. Int. Conf. Emerg. Frontiers Electr. Electron. Technol. (ICEFEET)*, Patna, India, Jul. 2020, pp. 1–5, doi: 10.1109/ICEFEET49149.2020.9186980.

[124] S. Jun Park, H. Woong Park, M. Hyung Lee, and F. Harashima, "A new approach for minimum-torque-ripple maximum-efficiency control of BLDC motor," *IEEE Trans. Ind. Electron.*, vol. 47, no. 1, pp. 109–114, Feb. 2000, doi: 10.1109/41.824132.

[125] Z. Li, S. Zhang, S. Zhou, and J. W. Ahn, "Torque ripple minimization in direct torque control of brushless DC motor," *J. Elect. Eng. Technol.*, vol. 9, no. 5, pp. 76–1569, 2014, doi: 10.5370/JEET.2014.9.5.1569.

[126] F. Korkmaz, İ Topaloğlu, and H. Mamur, "Modified direct torque control for BLDC motor drives," *Int. J. Control Theory Comput. Model.*, vol. 6, pp. 1–9, Jan. 2016, doi: 10.5121/ijctcm.2016.6301.

[127] P. Ubare, D. Ingole, and D. Sonawane, "Energy-efficient nonlinear model predictive control of BLDC motor in electric vehicles," in *Proc. 6th Indian Control Conf. (ICC)*, Hyderabad, India, Dec. 2019, pp. 194–199, doi: 10.1109/ICC47138.2019.9123204.

[128] N. Parhizkar, M. Shafiei, and M. B. Kouhshahi, "Direct torque control of brushless DC motor drives with reduced starting current using fuzzy logic controller," in *Proc. Int. Conf. Uncertainty Reasoning Knowl. Eng.*, Bali, Indonesia, vol. 1, Aug. 2011, pp. 129–132, doi: 10.1109/URKE.2011.6007863.

[129] T. E. Joseph and M. V. Sreethumol, "Speed control of BLDC motor drive under direct torque control scheme with modified integrator," in *Proc. IEEE Int. Conf. Electr., Comput. Commun. Technol. (ICECCT)*, Coimbatore, India, Mar. 2015, pp. 1–5, doi: 10.1109/ICECCT.2015.7225931.

[130] L. Zhao, X. Zhang, and J. Ji, "A torque control strategy of brushless direct current motor with current observer," in *Proc. IEEE Int. Conf. Mechatronics Autom. (ICMA)*, Aug. 2015, pp. 303–307.

[131] M. A. Khan, M. N. Uddin, and M. A. Rahman, "A new loss minimization control of interior permanent magnet motor drives operating with a wavelet-based speed controller," in *Proc. IEEE Ind. Appl. Soc. Annu. Meeting*, Orlando, FL, USA, Jul. 2011, pp. 1–8, doi: 10.1109/IAS.2011.6074337.

[132] R. Arulmozhiyal and R. Kandiban, "Design of fuzzy PID controller for brushless DC motor," in *Proc. Int. Conf. Comput. Commun. Informat.*, Coimbatore, India, Jan. 2012, pp. 1–7, doi: 10.1109/ICCCI.2012.6158919.

[133] B. N. Kommula and V. R. Kota, "Mathematical modeling and fuzzy logic control of a brushless DC motor employed in automobile and industrial applications," in *Proc. IEEE 1st Int. Conf. Control, Meas. Instrum. (CMI)*, Kolkata, India, Jan. 2016, pp. 1–5, doi: 10.1109/CMI.2016.7413763.

[134] M. A. Shamseldin and A. A. EL-Samahy, "Speed control of BLDC motor by using PID control and self-tuning fuzzy PID controller," in *Proc. 15th Int. Workshop Res. Educ. Mechtron. (REM)*, El Gouna, Egypt, 2014, pp. 1–9, doi: 10.1109/REM.2014.6920443.

[135] Y. I. Mohammed Al Mashhadany, A. K. Abbas, and S. S. Algburi, "Modeling and analysis of brushless DC motor system based on intelligent controllers," *Bull. Electr. Eng. Informat.*, vol. 11, no. 6, pp. 2995–3003, Dec. 2022, doi: 10.11591/eei.v11i6.4365.

[136] P. Suganthi, S. Nagapavithra, and S. Umamaheswari, "Modeling and simulation of closed loop speed control for BLDC motor," in *Proc. Conf. Emerg. Devices Smart Syst. (ICEDSS)*, Mallasamudram, India, Mar. 2017, pp. 229–233, doi: 10.1109/ICEDSS.2017.8073686.

[137] M. Rif'an and H. Firmansyah, "Intelligent control system for high efficiency electric vehicles," *IOP Conf. Ser., Mater. Sci. Eng.*, vol. 1098, no. 4, 2021, Art. no. 042072, doi: 10.1088/1757-899X/1098/4/042072.

[138] E. Çelik and N. Oztürk, "A new fuzzy logic estimator for reduction of commutation current pulsation in brushless DC motor drives with three-phase excitation," *Neural Comput. Appl.*, vol. 31, pp. 34–1125, Jul. 2019, doi: 10.1007/s00521-017-3083-8.

[139] M. P. Maharajan and S. A. E. Xavier, "Design of speed control and reduction of torque ripple factor in BLdc motor using spider based controller," *IEEE Trans. Power Electron.*, vol. 34, no. 8, pp. 7826–7837, Aug. 2019, doi: 10.1109/TPEL.2018.2880916.

[140] M. K. Umam, R. N. Hasanah, and T. Nurwati, "PID-based fuzzy logic theory implementation on BLDC motor speed control," in *Proc. Int. Seminar Intell. Technol. Appl. (ISITIA)*, Surabaya, Indonesia, 2022, pp. 407–412, doi: 10.1109/ISITIA56226.2022.9855291.

[141] B. N. Kommula and V. R. Kota, "Performance evaluation of hybrid fuzzy PI speed controller for brushless DC motor for electric vehicle application," in *Proc. Conf. Power, Control, Commun. Comput. Technol. Sustain. Growth (PCCCTSG)*, Kurnool, India, Dec. 2015, pp. 266–270, doi: 10.1109/PCCCTSG.2015.7503912.

[142] A. Rubaai, M. J. Castro-Sitiriche, and A. R. Ofoli, "Design and implementation of parallel fuzzy PID controller for high-performance brushless motor drives: An integrated environment for rapid control prototyping," *IEEE Trans. Ind. Appl.*, vol. 44, no. 4, pp. 1090–1098, 2008, doi: 10.1109/TIA.2008.926059.

[143] V. Nigam, S. Hussain, and S. N. Agarwal, "A hybrid fuzzy sliding mode controller for a BLDC motor drive," in *Proc. IEEE 1st Int. Conf. Power Electron., Intell. Control Energy Syst. (ICPEICES)*, Delhi, India, Jul. 2016, pp. 1–4, doi: 10.1109/ICPEICES.2016.7853249.

[144] A. Ramya, M. Balaji, and V. Kamaraj, "Adaptive MF tuned fuzzy logic speed controller for BLDC motor drive using ANN and PSO technique," *J. Eng.*, vol. 2019, no. 17, pp. 50–3947, 2019, doi: 10.1049/joe.2018.8179.

[145] K. Premkumar and B. V. Manikandan, "Fuzzy PID supervised online ANFIS based speed controller for brushless DC motor," *Neurocomputing*, vol. 157, pp. 76–90, Jun. 2015, doi: 10.1016/j.neucom.2015.01.032.

[146] S. Agrawal and V. Shrivastava, "Particle swarm optimization of BLDC motor with fuzzy logic controller for speed improvement," in *Proc. 8th Int. Conf. Comput., Commun. Netw. Technol. (ICCCNT)*, Delhi, India, Jul. 2017, pp. 1–5, doi: 10.1109/ICCCNT.2017.8204006.

[147] M. J. Prabu, P. Poongodi, and K. P. kumar, "Fuzzy supervised online coactive neuro-fuzzy inference system-based rotor position control of brushless DC motor," *IET Power Electron.*, vol. 9, no. 11, pp. 39–2229, 2016, doi: 10.1049/iet-pel.2015.0919.

[148] T. Wang, H. Wang, H. Hu, X. Lu, and S. Zhao, "An adaptive fuzzy PID controller for speed control of brushless direct current motor," *Social Netw. Appl. Sci.*, vol. 4, no. 3, p. 71, Mar. 2022, doi: 10.1007/s42452-022-04957-6.

[149] K. P. kumar and B. V. Manikandan, "Bat algorithm optimized fuzzy PD based speed controller for brushless direct current motor," *Eng. Sci. Technol., Int. J.*, vol. 19, no. 2, pp. 818–840, 2016, doi: 10.1016/j.jestch.2015.11.004.

[150] V. V. Vadla, C. H. Suresh, and R. A. Naragani, "Simulation of fuzzy based current control strategy for BLDC motor drive," *IJSETR*, vol. 4, pp. 32–4626, 2015.

[151] G. Haçat, Y. Çetinceviz, and E. Sehirli, "Speed control of BLDC by using neutrosophic fuzzy logic controller," in *Proc. Innov. Intell. Syst. Appl. Conf. (ASYU)*, Elazig, Turkey, Oct. 2021, pp. 1–5, doi: 10.1109/ASYU52992.2021.9599021.

[152] I. F. Davoudkhani and M. Akbari, "Adaptive speed control of brushless DC (BLDC) motor based on interval type-2 fuzzy logic," in *Proc. 24th Iranian Conf. Electr. Eng. (ICEE)*, Shiraz, Iran, May 2016, pp. 1119–1124, doi: 10.1109/IranianCEE.2016.7585689.

[153] T. Nag, S. B. Santra, A. Chatterjee, D. Chatterjee, and A. K. Ganguli, "Fuzzy logic-based loss minimisation scheme for brushless DC motor drive system," *IET Power Electron.*, vol. 9, no. 8, pp. 1581–1589, 2016, doi: 10.1049/iet-pel.2015.0714.

[154] A. Jaya, E. Purwanto, M. B. Fauziah, F. D. Murdianto, G. Prabowo, and M. R. Rusli, "Design of PID-fuzzy for speed control of brushless DC motor in dynamic electric vehicle to improve steady-state performance," in *Proc. Int. Electron. Symp. Eng. Technol. Appl. (IES-ETA)*, Surabaya, Indonesia, Sep. 2017, pp. 179–184, doi: 10.1109/ELECSYM.2017.8240399.

[155] H. Jianyao, W. Juan, P. Hemeng, P. Qi, and H. Qingli, "Application of fuzzy logic algorithm for optimization of control strategy in electric vehicles," in *Proc. IEEE 2nd Adv. Inf. Technol., Electron. Autom. Control Conf. (IAEAC)*, Chongqing, China, Mar. 2017, pp. 2042–2045, doi: 10.1109/IAEAC.2017.8054375.

[156] J. Joy and S. Ushakumari, "Performance comparison of a sensorless PMBLDC motor drive system with conventional and fuzzy logic controllers," *Proc. Technol.*, vol. 25, pp. 643–651, Jan. 2016, doi: 10.1016/j.protcy.2016.08.156.

[157] Z.-S. Wang, C.-Y. Liu, X.-L. Song, Z.-Y. Song, and Z.-K. Yang, "Improved variable universe fuzzy PID application in brushless DC motor speed regulation system," in *Proc. Int. Conf. Mach. Learn. Cybern. (ICMLC)*, Jeju, South Korea, vol. 1, Jul. 2016, pp. 459–463, doi: 10.1109/ICMLC.2016.7860944.

[158] C. N. Narasimha Rao and G. DurgaSukumar, "Analysis of torque ripple in vector control of BLDC motor using SVPWM technique," in *Proc. 4th Int. Conf. Electron., Commun. Aerosp. Technol. (ICECA)*, Coimbatore, India, Nov. 2020, pp. 519–523, doi: 10.1109/ICECA49313.2020.9297558.

[159] A. Ramya, I. Ahamed, and M. Balaji, "Hybrid self tuned fuzzy PID controller for speed control of brushless DC motor," *Automatika*, vol. 57, no. 3, pp. 672–679, 2016, doi: 10.7305/automatika.2017.02.1769.

[160] J.-S. Wen, C.-H. Wang, Y.-D. Chang, and C.-C. Teng, "Intelligent control of high-speed sensorless brushless DC motor for intelligent automobiles," in *Proc. IEEE Int. Conf. Syst., Man Cybern.*, Singapore, Oct. 2008, pp. 3394–3398, doi: 10.1109/ICSMC.2008.4811822.

[161] M. Dasari, A. S. Reddy, and M. V. Kumar, "A comparative analysis of converters performance using various control techniques to minimize the torque ripple in BLDC drive system," *Sustain. Comput., Informat. Syst.*, vol. 33, Jan. 2022, Art. no. 100648, doi: 10.1016/j.suscom.2021.100648.

[162] R. Çelikel and O. Aydoğmuş, "A torque ripple minimization method for brushless DC motor in high-speed applications," *J. Eng. Res.*, vol. 7, no. 3, pp. 200–214, 2019.

[163] X. Zhang, B. Chen, P. Zhu, and H. Lei, "A new method to minimize the commutation torque ripple in trapezoidal BLDC motor with sensorless drive," in *Proc. 3rd Int. Power Electron. Motion Control Conf.*, Beijing, China, vol. 2, 2000, pp. 607–611, doi: 10.1109/IPEMC.2000.884561.

[164] W. Chen, Y. Liu, X. Li, T. Shi, and C. Xia, "A novel method of reducing commutation torque ripple for brushless DC motor based on cuk converter," *IEEE Trans. Power Electron.*, vol. 32, no. 7, pp. 5497–5508, Jul. 2017, doi: 10.1109/TPEL.2016.2613126.

[165] C. K. Lad and R. Chudamani, "A simple overlap angle control strategy for reducing commutation torque ripple in a brushless DC motor drive," *Eng. Sci. Technol., Int. J.*, vol. 20, no. 4, pp. 1406–1419, 2017, doi: 10.1016/j.jestch.2017.09.005.

[166] C.-H. Won, J.-H. Song, and I. Choy, "Commutation torque ripple reduction in brushless DC motor drives using a single DC current sensor," in *Proc. IEEE 33rd Annu. IEEE Power Electron. Spec. Conf.*, Cairns, QLD, Australia 2002, pp. 985–990, doi: 10.1109/PSEC.2002.1022583.

[167] D. Kumar, H. Tiwari, R. A. Gupta, and R. Sumit, "Elimination of commutation current ripple in the BLDC motor based on DC–DC converter using PR-compensator," in *Proc. IEEE Int. Conf. Power Electron., Smart Grid Renew. Energy (PESGRE)*, 2020, Jan. 2020, pp. 1–6, doi: 10.1109/PESGRE45664.2020.9070364.

[168] K. Pankaj and K. Ragavan, "Analysis of back-EMF wave shaping on performance of PM brushless motor," in *Proc. IEEE Power Energy Conf. at Illinois (PECI)*, Urbana, IL, USA, Feb. 2013, pp. 125–129, doi: 10.1109/PECI.2013.6506046.

[169] W. Lee, D. Han, and B. Sarlioglu, "Comparative performance analysis of reference voltage-controlled pulse width modulation for high-speed single-phase brushless DC motor drive," *IEEE Trans. Power Electron.*, vol. 33, no. 5, pp. 4560–4568, May 2018, doi: 10.1109/TPEL.2017.2731962.

[170] G. Krishnan and K. T. Ajmal, "A neoteric method based on PWM ON PWM scheme with buck converter for torque ripple minimization in BLDC drive," in *Proc. Annu. Int. Conf. Emerg. Res. Areas, Magn., Mach. Drives (AICERA/iCMMD)*, Kottayam, India, Jul. 2014, pp. 1–6, doi: 10.1109/AICERA.2014.6908186.

[171] A. Azarudeen and D. Mary, "Performance analysis of conventional and digital PWM control scheme for speed control of BLDC motor drives," in *Proc. Int. Conf. Adv. Electr. Technol. Green Energy (ICAETGT)*, Coimbatore, India, Sep. 2017, pp. 69–75, doi: 10.1109/ICAETGT.2017.8341460.

[172] K.-Y. Nam, W.-T. Lee, C.-M. Lee, and J.-P. Hong, "Reducing torque ripple of brushless DC motor by varying input voltage," *IEEE Trans. Magn.*, vol. 42, no. 4, pp. 1307–1310, Apr. 2006, doi: 10.1109/TMAG.2006.871937.

[173] S. Murthy, B. Derouane, B. Liu, and T. Sebastian, "Minimization of torque pulsations in a trapezoidal back-EMF permanent magnet brushless DC motor," in *Proc. Conf. Rec. IEEE Ind. Appl. Conf. 34th IAS Annu. Meeting*, Phoenix, AZ, USA, vol. 2, Jul. 1999, pp. 1237–1242, doi: 10.1109/IAS.1999.801661.

[174] D.-K. Kim, K.-W. Lee, and B.-I. Kwon, "Commutation torque ripple reduction in a position sensorless brushless DC motor drive," *IEEE Trans. Power Electron.*, vol. 21, no. 6, pp. 1762–1768, Nov. 2006, doi: 10.1109/TPEL.2006.882918.

[175] A. A. Obed and A. K. Kadhim, "Speed and current limiting control strategies for BLDC motor drive system: A comparative study," *Int. J. Adv. Eng. Res. Sci.*, vol. 5, no. 2, pp. 119–130, 2018, doi: 10.22161/ijaers.5.2.16.

[176] W. Lee, J. H. Kim, W. Choi, and B. Sarlioglu, "Torque ripple minimization control technique of high-speed single-phase brushless DC motor for electric turbocharger," *IEEE Trans. Veh. Technol.*, vol. 67, no. 11, pp. 10357–10365, Nov. 2018, doi: 10.1109/TVT.2018.2866779.

[177] M. S. Boroujeni, G. A. Markadeh, and J. Soltani, "Torque ripple reduction of brushless DC motor based on adaptive input-output feedback linearization," *ISA Trans.*, vol. 70, pp. 502–511, 2017, doi: 10.1016/j.isatra.2017.05.006.

[178] G. Jiang, C. Xia, W. Chen, T. Shi, X. Li, and Y. Cao, "Commutation torque ripple suppression strategy for brushless DC motors with a novel noninductive boost front end," *IEEE Trans. Power Electron.*, vol. 33, no. 5, pp. 4274–4284, May 2018, doi: 10.1109/TPEL.2017.2721439.

[179] F. Salha, F. Colas, and X. Guillaud, "Virtual resistance principle for the overcurrent protection of PWM voltage source inverter," in *Proc. IEEE PES Innov. Smart Grid Technol. Conf. Eur. (ISGT Europe)*, Gothenburg, Sweden, Oct. 2010, pp. 1–6, doi: 10.1109/ISGTEUROPE.2010.5638965.

[180] H. Wang, X. Yue, X. Pei, and Y. Kang, "Improved software current-limiting protection strategy for starting the high-power motor," in *Proc. Int. Conf. Electr. Mach. Syst.*, Tokyo, Japan, Nov. 2009, pp. 1–4, doi: 10.1109/ICEMS.2009.5382846.

[181] Z. S. Ho, C. M. Uang, and P. C. Wang, "Extracting DC bus current information for optimal phase correction and current ripple in sensorless brushless DC motor drive," *J. Zhejiang Univ. Sci. C*, vol. 15, pp. 312–320, Apr. 2014, doi: 10.1631/jzus.C1300247.

[182] H. K. Samitha Ransara and U. K. Madawala, "A torque ripple compensation technique for a low-cost brushless DC motor drive," *IEEE Trans. Ind. Electron.*, vol. 62, no. 10, pp. 6171–6182, Oct. 2015, doi: 10.1109/TIE.2015.2423664.

[183] Y. Cao, T. Shi, X. Li, W. Chen, and C. Xia, "A commutation torque ripple suppression strategy for brushless DC motor based on diode-assisted buck–boost inverter," *IEEE Trans. Power Electron.*, vol. 34, no. 6, pp. 5594–5605, Jun. 2019, doi: 10.1109/TPEL.2018.2866001.

[184] A. Senthilnathan and P. Palanivel, "A new approach for commutation torque ripple reduction of FPGA based brushless DC motor with outgoing phase current control," *Microprocessors Microsystems*, vol. 75, Jun. 2020, Art. no. 103043, doi: 10.1016/j.micpro.2020.103043.

[185] R. Amirthalingam and B. Mahadevan, "A new approach for minimizing torque ripple in a BLDC motor drive with a front-end IDO dc-dc converter," *Turkish J. Elect. Eng. Comput. Sci.*, vol. 25, no. 4, pp. 2910–2929, 2017, doi: 10.3906/elk-1605-40.

[186] G. Meng, H. Xiong, and H. Li, "Commutation torque ripple reduction in BLDC motor using PWM_ON_PWM mode," in *Proc. Int. Conf. Electr. Mach. Syst.*, Tokyo, Japan, Nov. 2009, pp. 1–6, doi: 10.1109/ICEMS.2009.5382974.

[187] T. Shi, X. Niu, W. Chen, and C. Xia, "Commutation torque ripple reduction of brushless DC motor in braking operation," *IEEE Trans. Power Electron.*, vol. 33, no. 2, pp. 1463–1475, Feb. 2018, doi: 10.1109/TPEL.2017.2675444.

[188] M. Rameli, Y. R. Hais, and R. E. A. Kadir, "Design of self-commutation BLDC motor with torque control strategy using fuzzy logic in hybrid electric vehicle (HEV)," in *Proc. Int. Seminar Intell. Technol. Appl. (ISITIA)*, Surabaya, Indonesia, 2017, pp. 211–216, doi: 10.1109/ISITIA.2017.8124082.

[189] Q. Zhou, J. Shu, Z. Cai, Q. Liu, and G. Du, "Improved PWM-off-PWM to reduce commutation torque ripple of brushless DC motor under braking conditions," *IEEE Access*, vol. 8, pp. 204020–204030, 2020, doi: 10.1109/ACCESS.2020.3036724.

[190] W. Jiang, P. Wang, Y. Ni, J. Wang, L. Wang, and Y. Liao, "Multimode current hysteresis control for brushless DC motor in motor and generator state with commutation torque ripple reduction," *IEEE Trans. Ind. Electron.*, vol. 65, no. 4, pp. 2975–2985, Apr. 2018, doi: 10.1109/TIE.2017.2752126.

[191] J. Shi and T.-C. Li, "New method to eliminate commutation torque ripple of brushless DC motor with minimum commutation time," *IEEE Trans. Ind. Electron.*, vol. 60, no. 6, pp. 2139–2146, Jun. 2013, doi: 10.1109/TIE.2012.2191756.

[192] V. Viswanathan and S. Jeevananthan, "Novel space-vector current-control method for torque ripple reduction of brushless DC motor based on three-level neutral-point-clamped inverter," in *Proc. Int. Conf. Green Comput. Commun. Electr. Eng. (ICGCCEE)*, Coimbatore, India, Mar. 2014, pp. 1–5, doi: 10.1109/ICGCCEE.2014.6922420.

[193] S. Kim, J. Park, and D. -H. Lee, "A simple commutation torque ripple reduction method of BLDC motors using a hybrid PWM compensation," in *Proc. 21st Int. Conf. Electrical Mach. Syst. (ICEMS)*, Jeju, South Korea, 2018, pp. 1193–1197, doi: 10.23919/ICEMS.2018.8549453.

[194] K.-S. Kan and Y.-Y. Tzou, "Adaptive soft starting method with current limit strategy for sensorless BLDC motors," in *Proc. IEEE Int. Symp. Ind. Electron.*, Hangzhou, China, May 2012, pp. 605–610, doi: 10.1109/ISIE.2012.6237155.

[195] Y. Wei, Y. Xu, J. Zou, and Y. Li, "Current limit strategy for BLDC motor drive with minimized DC-link capacitor," *IEEE Trans. Ind. Appl.*, vol. 51, no. 5, pp. 3907–3913, Sep. 2015, doi: 10.1109/TIA.2015.2427285.

[196] T. Sheng, X. Wang, J. Zhang, and Z. Deng, "Torque-ripple mitigation for brushless DC machine drive system using one-cycle average torque control," *IEEE Trans. Ind. Electron.*, vol. 62, no. 4, pp. 2114–2122, Apr. 2015, doi: 10.1109/TIE.2014.2351377.

[197] L. Xu, G. Chen, G. Li, and Q. Li, "Model predictive control based on parametric disturbance compensation," *Math. Problems Eng.*, vol. 2020, pp. 1–13, Oct. 2020, doi: 10.1155/2020/9543928.

[198] A. Khanna and T. Gaur, "Model predictive control of DC motor model in MATLAB," *Int. J. Sci. Eng. Res.*, vol. 8, no. 4, pp. 5–82, 2017.

[199] S. N. Vishwanath and K. D. Kusumika, "Effective torque ripple reduction of permanent magnet brushless DC motor," *Int. J. Electron. Signals and Syst.*, vol. 4, no. 1, pp. 1–7, 2022, doi: 10.47893/IJESS.2022.1214.

[200] Y. Wei, Y. Wei, Y. Gao, H. Qi, X. Guo, M. Li, and D. Zhang, "A variable prediction horizon self-tuning method for nonlinear model predictive speed control on PMSM rotor position system," *IEEE Access*, vol. 9, pp. 78812–78822, 2021, doi: 10.1109/ACCESS.2021.3084321.

[201] B. Ma and W. Song, "Model predictive control for torque ripple minimization of brushless DC motor in full speed range," in *Proc. IEEE 2nd China Int. Youth Conf. Electr. Eng. (CIYCEE)*, Chengdu, China, Dec. 2021, pp. 1–6, doi: 10.1109/CIYCEE53554.2021.9676802.

[202] H. Wen and J. Yin, "A duty cycle based finite-set model predictive direct power control for BLDC motor drives," in *Proc. IECON 46th Annu. Conf. IEEE Ind. Electron. Soc.*, Singapore, Jul. 2020, pp. 821–825, doi: 10.1109/IECON43393.2020.9254958.

[203] M. Aghaee and A. A. Jalali, "BLDC motor speed control based on MPC sliding mode multi-loop control strategy–implementation on MATLAB and Arduino software," in *Proc. Electr. Eng. (ICEE), Iranian Conf.*, Mashhad, Iran, May 2018, pp. 795–800, doi: 10.1109/ICEE.2018.8472464.

[204] T. Porselvi, S. Y. A. Barathwaj, S. V. T. Sangeetha, and J. S. Priya, "Deep learning based predictive analysis of BLDC motor control," in *Proc. IEEE 3rd Global Conf. Advancement Technol. (GCAT)*, Bangalore, India, Jul. 2022, pp. 1–6, doi: 10.1109/GCAT55367.2022.9972193.

[205] H. Wang, W. Zhao, H. Tang, T. Tao, and S. Saeed, "Improved fault-tolerant model predictive torque control of five-phase PMSM by using deadbeat solution," *IEEE Trans. Energy Convers.*, vol. 37, no. 1, pp. 210–219, Mar. 2022, doi: 10.1109/TEC.2021.3099813.

[206] T. P. Banerjee, J. Roychoudhury, S. Das, and A. Abraham, "Hybrid intelligent predictive control system for high-speed BLDC motor in aerospace application," in *Proc. 3rd Int. Conf. Emerg. Trends Eng. Technol.*, Goa, India, 2010, pp. 258–262, doi: 10.1109/ICETET.2010.48.

[207] H. F. Prasetyo, A. S. Rohman, H. Hindersah, and M. R. A. R. Santabudi, "Implementation of model predictive control (MPC) in electric vehicle testing simulator," in *Proc. 4th Int. Conf. Electric Veh. Technol. (ICEVT)*, Bali, Indonesia, Oct. 2017, pp. 48–54, doi: 10.1109/ICEVT.2017.8323532.

[208] C. Xia, Y. Wang, and T. Shi, "Implementation of finite-state model predictive control for commutation torque ripple minimization of permanent-magnet brushless DC motor," *IEEE Trans. Ind. Electron.*, vol. 60, no. 3, pp. 896–905, Mar. 2013, doi: 10.1109/TIE.2012.2189536.

[209] A. G. de Castro, W. C. A. Pereira, T. E. P. de Almeida, C. M. R. de Oliveira, J. R. B. de Almeida Monteiro, and A. A. de Oliveira, "Improved finite control-set model-based direct power control of BLDC motor with reduced torque ripple," *IEEE Trans. Ind. Appl.*, vol. 54, no. 5, pp. 4476–4484, Sep. 2018, doi: 10.1109/TIA.2018.2835394.

[210] K. Xia, Y. Ye, J. Ni, Y. Wang, and P. Xu, "Model predictive control method of torque ripple reduction for BLDC motor," *IEEE Trans. Magn.*, vol. 56, no. 1, pp. 1–6, Jan. 2020, doi: 10.1109/TMAG.2019.2950953.

[211] M. Salehifar, M. Moreno-Eguilaz, G. Putrus, and P. Barras, "Simplified fault tolerant finite control set model predictive control of a five-phase inverter supplying BLDC motor in electric vehicle drive," *Electric Power Syst. Res.*, vol. 132, pp. 56–66, Mar. 2016, doi: 10.1016/j.epsr.2015.10.030.

[212] F. Naseri, E. Farjah, E. Schaltz, K. Lu, and N. Tashakor, "Predictive control of low-cost three-phase four-switch inverter-fed drives for brushless DC motor applications," *IEEE Trans. Circuits Syst. I, Reg. Papers*, vol. 68, no. 3, pp. 1308–1318, Mar. 2021, doi: 10.1109/TCSI.2020.3043468.

[213] M. S. Trivedi and R. Kumar Keshri, "Predictive deadbeat current control in stationary plane for PM BLDC motor drive," in *Proc. 43rd Annu. Conf. IEEE Ind. Electron. Soc.*, Beijing, China, Oct. 2017, pp. 6640–6645, doi: 10.1109/IECON.2017.8217159.

[214] A. G. de Castro, P. R. U. Guazzelli, S. T. C. A. D. Santos, C. M. R. de Oliveira, W. C. A. Pereira, and J. R. B. A. Monteiro, "Zero sequence power contribution on BLDC motor drives. Part II: An FCS-MPC current control of three-phase four-leg inverter based drive," in *Proc. 13th IEEE Int. Conf. Ind. Appl. (INDUSCON)*, Sao Paulo, Brazil, 2018, pp. 1024–1029, doi: 10.1109/INDUSCON.2018.8627310.

[215] M. H. Khooban, N. Vafamand, and T. Niknam, "T-S fuzzy model predictive speed control of electrical vehicles," *ISA Trans.*, vol. 64, pp. 231–240, 2016, doi: 10.1016/j.isatra.2016.04.019.

[216] R. S. Arashloo, M. Salehifar, J. L. R. Martinez, and V. Sala, "Fault-tolerant model predictive control of five-phase permanent magnet motors," in *Proc. 39th Annu. Conf. IEEE Ind. Electron. Society*, Vienna, Austria, 2013, pp. 2857–2862, doi: 10.1109/IECON.2013.6699584.

[217] S. M. Taher, A. H. Niasar, and S. A. Taher, "A new MPC-based approach for torque ripple reduction in BLDC motor drive," in *Proc. 12th Power Electron., Drive Syst., Technol. Conf. (PEDSTC)*, Tabriz, Iran, Feb. 2021, pp. 1–6, doi: 10.1109/PEDSTC52094.2021.9405871.

[218] A. Busch, M. Wielitzka, T. Ortmaier, and V. Kleyman, "Adaptive model predictive traction control for electric vehicles," in *Proc. 18th Eur. Control Conf. (ECC)*, Naples, Italy, Jun. 2019, pp. 1239–1244, doi: 10.23919/ECC.2019.8795687.

[219] N. Vafamand, M. M. Arefi, M. H. Khooban, T. Dragicevic, and F. Blaabjerg, "Nonlinear model predictive speed control of electric vehicles represented by linear parameter varying models with bias terms," *IEEE J. Emerg. Sel. Topics Power Electron.*, vol. 7, no. 3, pp. 2081–2089, Sep. 2019, doi: 10.1109/JESTPE.2018.2884346.

[220] M. A. Noyal Doss, S. Sekar Dash, and D. M. V. Marthandan, "A model predictive control to reduce torque ripple for brushless DC motor with inbuilt stator current control," *Universal J. Electr. Electron. Eng.*, vol. 1, no. 3, pp. 59–67, Oct. 2013, doi: 10.13189/ujeee.2013.010301.

[221] R. Jaiswal, A. Agarwal, R. Negi, and A. Vikram, "Design and development of experimental based phase modulated model predictive control for torque ripple reduction of MMC fed BLDC motor," *J. Eng. Res.*, vol. 70, p. 78, Aug. 2021, doi: 10.36909/jer.EMSME.13877.

[222] M. Gopinath, T. Yuvaraja, and S. Jeykumar, "Implementation of four quadrant operation of BLDC motor using model predictive controller," *Mater. Today: Proc.*, vol. 5, no. 1, pp. 1666–1672, 2018, doi: 10.1016/j.matpr.2017.11.261.

[223] A. G. Bartsch, J. R. Teixeira, J. de Oliveira, and M. S. M. Cavalca, "Procedures to design multi-model-based predictive controller applied to BLDC drive," *J. Control, Autom. Electr. Syst.*, vol. 30, no. 6, pp. 994–1006, Dec. 2019, doi: 10.1007/s40313-019-00521-7.

[224] J. Sashindran and N. R. Jayasree, *Performance of Sliding Mode Controller for Minimizing Commutation Torque Ripple in Permanent Magnet Brushless DC Motor*.

[225] P. Ramreddy and G. J. Rao, "Modelling and implementation for sliding mode control of BLDC motor drive," *Int. Adv. Res. J. Sci., Eng. Technol.*, 2020.

[226] J. J. Rath, S. Saha, and H. P. Ikkurti, "Sliding mode scheme for speed and current control of brushless DC (BLDC) motor," in *Proc. IEEE-Int. Conf. Adv. Eng., Sci. Manage. (ICAESM)*, Nagapattinam, India, 2012, pp. 450–455.

[227] S. Ghogare, G. Stebner, and S. Chaudhari, "Speed control for brushless DC motor driven vehicle using disturbance observer," in *Proc. 6th Int. Conf. Converg. Technol. (I2CT)*, Maharashtra, India, Apr. 2021, pp. 1–6, doi: 10.1109/I2CT51068.2021.9418168.

[228] Z. Alqarni, "Higher order sliding mode control for speed control of BLDC motor," in *Proc. IEEE 13th Annu. Comput. Commun. Workshop Conf. (CCWC)*, Las Vegas, NV, USA, Mar. 2023, pp. 0212–0217, doi: 10.1109/CCWC57344.2023.10099280.

[229] K. M. A. Prasad and U. Nair, "An intelligent fuzzy sliding mode controller for a BLDC motor," in *Proc. Int. Conf. Innov. Mech. Ind. Appl. (ICIMIA)*, Bengaluru, India, Feb. 2017, pp. 274–278, doi: 10.1109/ICIMIA.2017.7975618.

[230] S. B. Murali and P. M. Rao, "Adaptive sliding mode control of BLDC motor using cuckoo search algorithm," in *Proc. 2nd Int. Conf. Inventive Syst. Control (ICISC)*, Coimbatore, India, Jan. 2018, pp. 989–993, doi: 10.1109/ICISC.2018.8398950.

[231] A. T. Hafez, A. A. Sarhan, and S. Givigi, "Brushless DC motor speed control based on advanced sliding mode control (SMC) techniques," in *Proc. IEEE Int. Syst. Conf. (SysCon)*, Orlando, FL, USA, Apr. 2019, pp. 1–6, doi: 10.1109/SYSCON.2019.8836754.

[232] P. Shah, P. Ubare, D. Ingole, and D. Sonawane, ‘‘Performance improvement of BLDC motor speed control using sliding mode control and observer,’’ in *Proc. Int. Symp. Asian Control Assoc. Intell. Robot. Ind. Autom. (IRIA)*, Goa, India, Sep. 2021, pp. 247–252, doi: 10.1109/IRIA53009.2021.9588766.

[233] J. Mehmood, M. Abid, M. S. Khan, and A. Q. Khan, ‘‘Design of sliding mode control for a brushless DC motor,’’ in *Proc. IEEE 23rd Int. Multitopic Conf. (INMIC)*, Bahawalpur, Pakistan, 2020, pp. 1–5, doi: 10.1109/INMIC50486.2020.9318215.

[234] M. S. Boroujeni, G. A. Markadeh, J. Soltani, and F. Blaabjerg, ‘‘Torque ripple reduction of brushless DC motor with harmonic current injection based on integral terminal sliding mode control,’’ *IET Electric Power Appl.*, vol. 12, no. 1, pp. 25–36, Jan. 2018, doi: 10.1049/iet-epa.2017.0070.

[235] H. Hung-Khong and C. Seng-Chi, ‘‘Simulation and implementation of a sliding mode control for a brushless DC motor with RBFNN and disturbance observer,’’ in *Proc. Int. Autom. Control Conf. (CACS)*, Keelung, Taiwan, Nov. 2019, pp. 1–6, doi: 10.1109/CACS47674.2019.9024362.

[236] D. Potnuru and Y. S. Kumar, ‘‘Sliding mode observer and controller for performance improvement of brushless DC motor,’’ *Int. J. Eng. Technol.*, vol. 9, no. 2, pp. 812–820, Apr. 2017, doi: 10.21817/ijet/2017/v9i2/170902087.

[237] N. Fu, J. Deng, S. Wang, and H. Yu, ‘‘Model predictive current control with sliding mode speed control for brushless DC motor,’’ in *Proc. IEEE 9th Int. Power Electron. Motion Control Conf. (IPEMC-ECCE Asia)*, Nanjing, China, Dec. 2020, pp. 2234–2238, doi: 10.1109/IPEMC-ECCEAsia48364.2020.9367634.

[238] M. A. Begh and H. G. Herzog, ‘‘Comparison of field-oriented control and direct torque control,’’ Tech. Univ. Munich, Munich, Germany, Tech. Rep., 2018, doi: 10.13140/RG.2.2.21677.59360/1.

[239] D. Casadei, F. Profumo, G. Serra, and A. Tani, ‘‘FOC and DTC: Two viable schemes for induction motors torque control,’’ *IEEE Trans. Power Electron.*, vol. 17, no. 5, pp. 779–787, Sep. 2002, doi: 10.1109/TPEL.2002.802183.

[240] F. Wang, Z. Zhang, X. Mei, J. Rodríguez, and R. Kennel, ‘‘Advanced control strategies of induction machine: Field oriented control, direct torque control and model predictive control,’’ *Energies*, vol. 11, no. 1, p. 120, Jan. 2018, doi: 10.3390/en11010120.

[241] L. Yunfei and Z. Chengning, ‘‘A comparative experimental analysis of PMSM between deadbeat prediction current control and field-oriented control,’’ *Energy Proc.*, vol. 158, pp. 2488–2493, Feb. 2019, doi: 10.1016/j.egypro.2019.01.382.

[242] M. Azab, ‘‘Comparative study of BLDC motor drives with different approaches: FCS-model predictive control and hysteresis current control,’’ *World Electric Vehicle J.*, vol. 13, no. 7, p. 112, Jun. 2022, doi: 10.3390/wevj13070112.

[243] V. S. Bondre and A. G. Thosar, ‘‘Study of control techniques for torque ripple reduction in BLDC motor,’’ in *Proc. Innov. Power Adv. Comput.*, 2017, pp. 1–6.

[244] Y. Zhang, H. Liu, Z. Zhang, Y. Luo, Q. Guo, and S. Liao, ‘‘Cloud computing-based real-time global optimization of battery aging and energy consumption for plug-in hybrid electric vehicles,’’ *J. Power Sources*, vol. 479, Dec. 2020, Art. no. 229069, doi: 10.1016/j.jpowsour.2020.229069.

[245] J. Yuan and L. Yang, ‘‘Predictive energy management strategy for connected 48 V hybrid electric vehicles,’’ *Energy*, vol. 187, Nov. 2019, Art. no. 115952, doi: 10.1016/j.energy.2019.115952.

[246] X. Zhu, H. Zhang, B. Yang, and G. Zhang, ‘‘Cloud-based shaft torque estimation for electric vehicle equipped with integrated motor-transmission system,’’ *Mech. Syst. Signal Process.*, vol. 99, pp. 647–660, Jan. 2018, doi: 10.1016/j.ymssp.2017.07.006.

[247] H. A. Raja, H. Raval, T. Vaimann, A. Kallaste, A. Rassõlkin, and A. Belahcen, ‘‘Cost-efficient real-time condition monitoring and fault diagnostics system for BLDC motor using IoT and machine learning,’’ in *Proc. Int. Conf. Diag. Electr. Eng. (Diagnostika)*, Pilsen, Czech Republic, Sep. 2022, pp. 1–4, doi: 10.1109/Diagnostika55131.2022.9905102.

N. PRABHU received the M.E. degree from the PSG College of Technology, Anna University, Chennai, India, in 2011. He is currently pursuing the Ph.D. degree with the Vellore Institute of Technology (VIT), Vellore, Tamil Nadu. His Ph.D. research focuses mainly on control system development for electric motors used in electric vehicles. His research interest includes advanced control strategies for torque ripple mitigation of various electric motors.

R. THIRUMALAIVASAN (Senior Member, IEEE) received the B.E. degree in electrical and electronics engineering from Madras University, Chennai, India, in 1999, the M.Tech. degree from the College of Engineering, Anna University, Guindy, Chennai, India, in 2002, and the Ph.D. degree from the Department of Electrical Engineering, Jawaharlal Nehru Technological University, Hyderabad, India, in 2014. He was a Postdoctoral Fellow with the Engineering Systems Design Pillar, SUTD, Singapore, from 2015 to 2016. He is currently a Professor with the School of Electrical Engineering, Vellore Institute of Technology, Vellore, India. His research interests include electric vehicles, FACTS, HVdc, wind energy conversion systems, real-time digital simulation of power electronics, and power systems.

BRAGADESHWARAN ASHOK received the Ph.D. degree from the School of Mechanical Engineering, Vellore Institute of Technology (VIT), Vellore, in 2017. He is currently an Associate Professor with the Department of Automotive Technology, School of Mechanical Engineering, VIT. His research work is aimed at motor control algorithm development for electric vehicle applications. His research interests include automotive engineering, electric and hybrid vehicle powertrain calibration, IC engines, and automotive electronics. Recently, he has been awarded as ‘‘World’s Top 2% Scientists’’ by a study conducted from researchers at Stanford University.